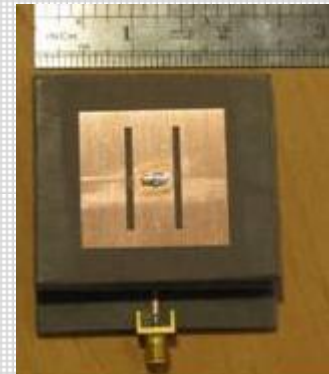
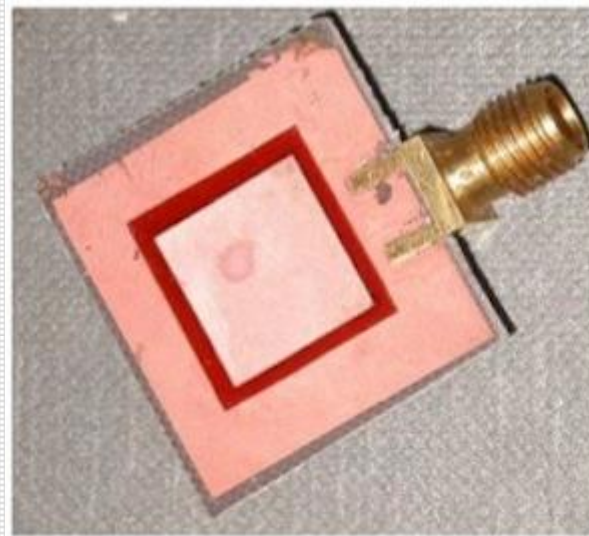
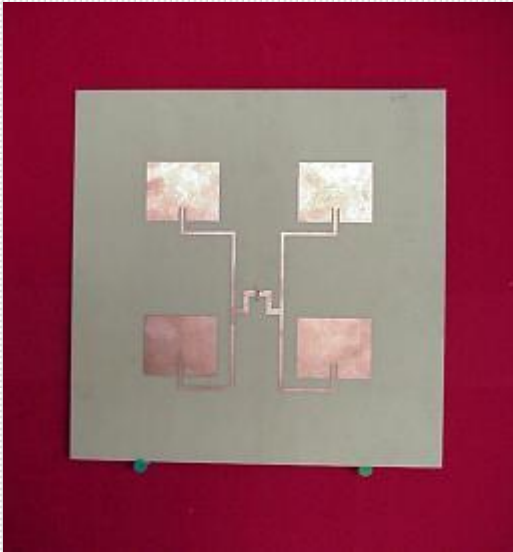


MICROSTRIP (PATCH) ANTENNAS



- one of the most useful constructions at microwave frequencies
- usually for $f > 1$ GHz
- consists of a metal “patch” on top of a grounded dielectric substrate
- the patch may be in a variety of shapes, but rectangular and circular are the most common.
- the patch may be positive or negative

- Invented by Bob Munson in 1972 (but earlier work by Dechamps goes back to 1953).
- Became popular starting in the 1970s.

G. Deschamps and W. Sichak, "Microstrip Microwave Antennas," Proc. of Third Symp. on USAF Antenna Research and Development Program, October 18–22, 1953.

R. E. Munson, "Microstrip Phased Array Antennas," *Proc. of Twenty-Second Symp. on USAF Antenna Research and Development Program*, October 1972.

R. E. Munson, "Conformal Microstrip Antennas and Microstrip Phased Arrays," *IEEE Trans. Antennas Propagat.*, vol. AP-22, no. 1 (January 1974): 74–78.

Advantages of Microstrip Antennas

- Low profile (can even be “conformal”)
- Easy to fabricate (use etching and photolithography) or even sharp blade
- Easy to feed (coaxial cable, microstrip line, etc.)
- Easy to use in an array or incorporate with other microstrip circuit elements
- Patterns are somewhat hemispherical, with a moderate directivity (about 6-8 dB is typical)

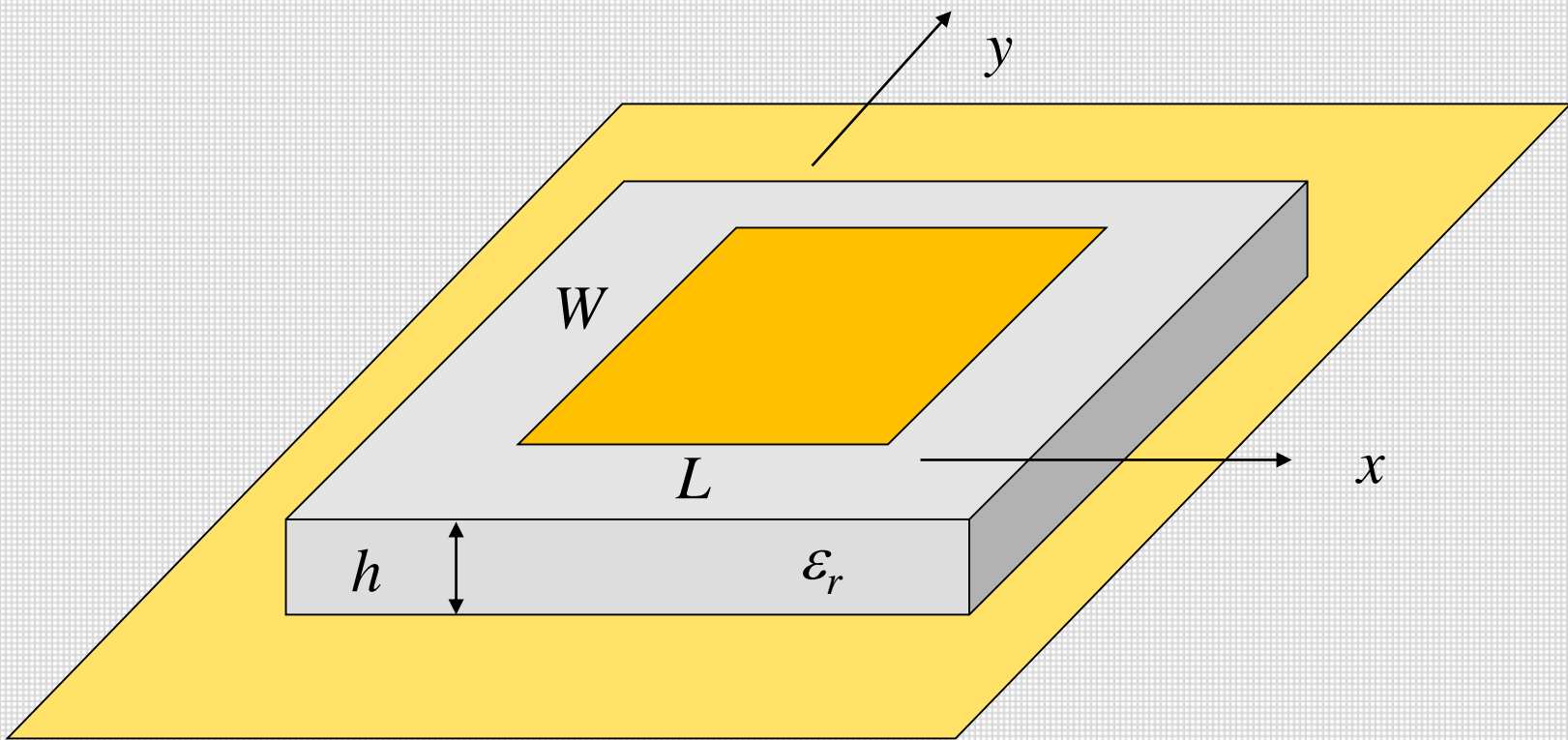
Disadvantages of Microstrip Antennas

- Low bandwidth (but can be improved by a variety of techniques). Bandwidths of a few percent are typical. Bandwidth is roughly proportional to the substrate thickness.
- Efficiency may be lower than with other antennas. Efficiency is limited by conductor and dielectric losses and by surface-wave loss

Conductor and dielectric losses become more severe for thinner substrates.

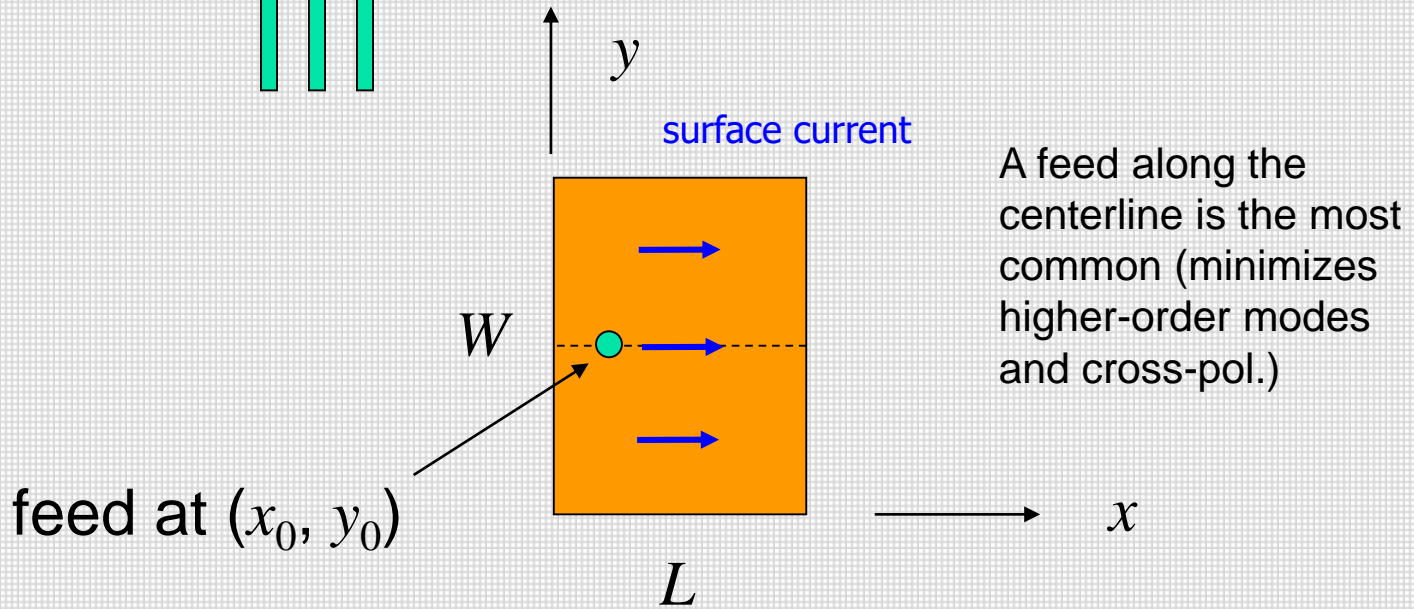
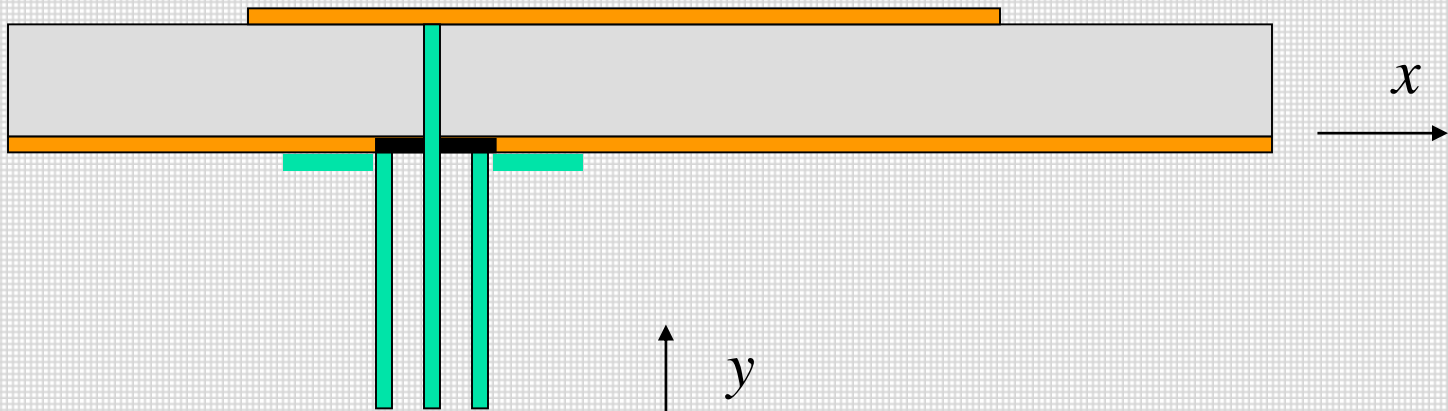
Surface-wave losses become more severe for thicker substrates (unless air or foam is used).

Typical geometry



L is the resonant dimension. The width W is usually chosen to be larger than L (to get higher bandwidth). However, usually $W < 2L$. $W = 1.5L$ is typical.

View showing coaxial feed



Basic operational principles

- ❑ The patch acts approximately as a **resonant cavity** (short circuit (PEC) walls on top and bottom, open-circuit (PMC) walls on the sides).
- ❑ In a cavity, only certain modes are allowed to exist, at different resonant frequencies.
- ❑ If the antenna is excited at a **resonance frequency**, a strong field is set up inside the cavity, and a strong current on the (bottom) surface of the patch. This produces significant radiation (a good antenna).

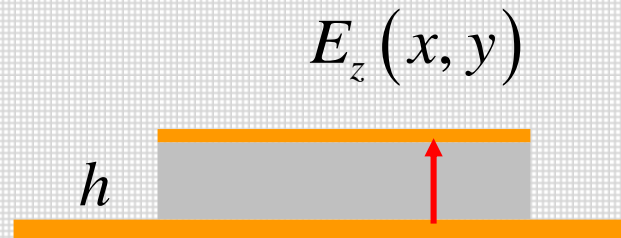
As the substrate thickness gets smaller the patch current radiates less, due to image cancellation. However, the Q of the resonant mode also increases, making the patch currents stronger at resonance. These two effects cancel, allowing the patch to radiate well even for small substrate thicknesses.

Thin Substrate Approximation

On patch and ground plane, $\underline{E}_t = \underline{0} \quad \longrightarrow \quad \underline{E} = \hat{\underline{z}} E_z(x, y)$

Inside the patch cavity, because of the thin substrate, the electric field vector is approximately independent of z .

Hence $\underline{E} \approx \hat{\underline{z}} E_z(x, y)$



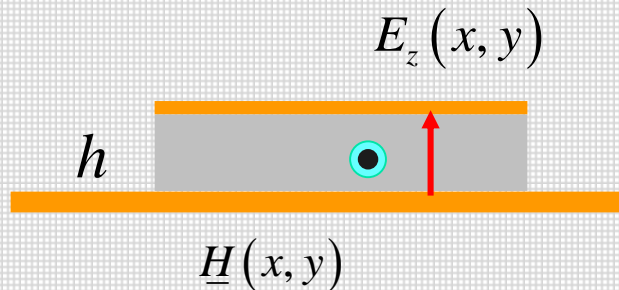
Thin Substrate Approximation

Magnetic field inside patch cavity:

$$\begin{aligned}\underline{H} &= -\frac{1}{j\omega\mu} \nabla \times \underline{E} \\ &= -\frac{1}{j\omega\mu} \nabla \times (\hat{z} E_z(x, y)) \\ &= -\frac{1}{j\omega\mu} (-\hat{z} \times \nabla E_z(x, y))\end{aligned}$$

$$\underline{H}(x, y) = \frac{1}{j\omega\mu} (\hat{z} \times \nabla E_z(x, y))$$

Note: The magnetic field is purely horizontal.
(The mode is TM_z .)



Magnetic Wall Approximation

On edges of patch,

$$\underline{J}_s \cdot \underline{\hat{n}} = 0$$

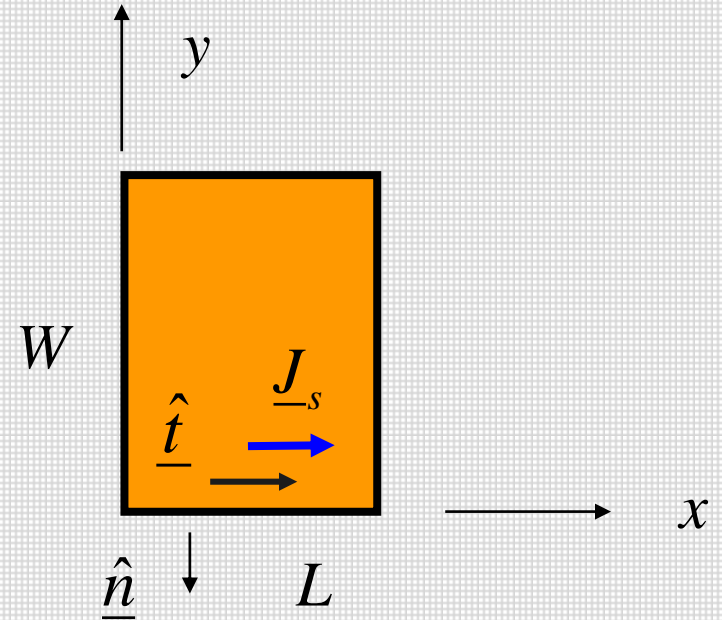
(\underline{J}_s is the sum of the top and bottom surface currents.)

Also, on bottom surface of patch conductor we have

$$\underline{J}_s^{bot} = (-\underline{\hat{z}} \times \underline{H}) \approx 0$$

Hence,

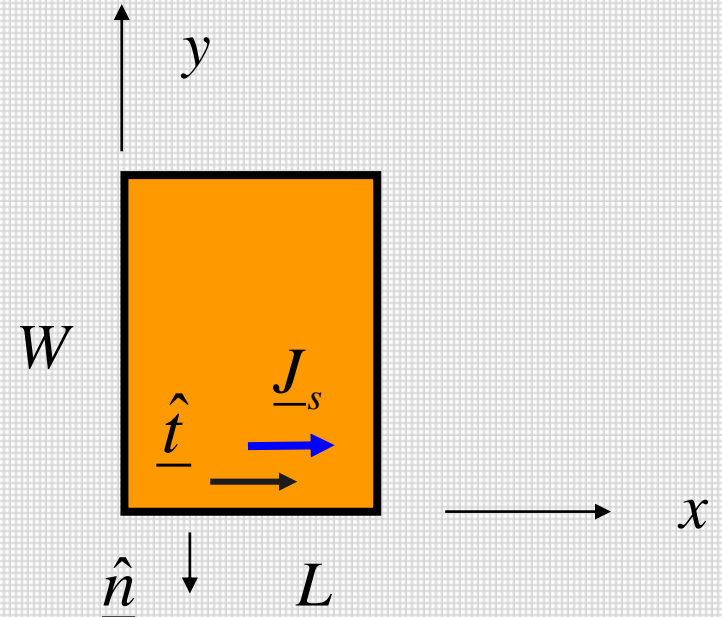
$$\underline{H}_t = \underline{0}$$



$$\underline{H} = \underline{\hat{n}} H_n$$

Since the magnetic field is approximately independent of z , we have an approximate PMC condition on the entire vertical edge.

$$\underline{H}_t = \underline{0} \quad (\text{PMC})$$



PMC

$$\underline{\hat{n}} \times \underline{H}(x, y) = \underline{0}$$

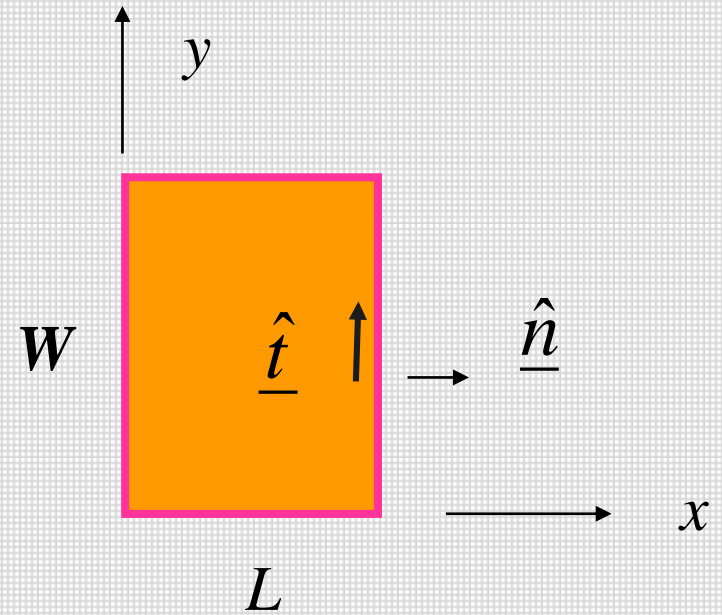
$$\underline{H}(x, y) = \frac{1}{j\omega\mu} (\underline{\hat{z}} \times \nabla E_z(x, y))$$

Hence,

$$\underline{\hat{n}} \times (\underline{\hat{z}} \times \nabla E_z(x, y)) = \underline{0}$$

$$\underline{\hat{z}} (\underline{\hat{n}} \cdot \nabla E_z(x, y)) = \underline{0}$$

$$\frac{\partial E_z}{\partial n} = 0$$



$$\underline{\hat{n}} \times (\underline{\hat{z}} \times \nabla E_z(x, y)) = \underline{\hat{z}} (\underline{\hat{n}} \cdot \nabla E_z(x, y)) - \nabla E_z(x, y) (\underline{\hat{n}} \cdot \underline{\hat{z}})$$



PMC

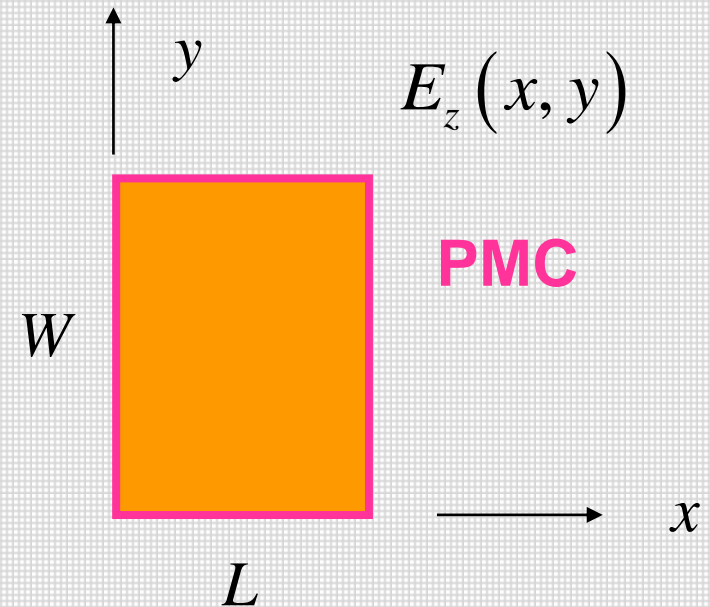
Resonance Frequencies

$$\nabla^2 E_z + k^2 E_z = 0$$

From separation of variables:

$$E_z = \cos\left(\frac{m\pi x}{L}\right) \cos\left(\frac{n\pi y}{W}\right)$$

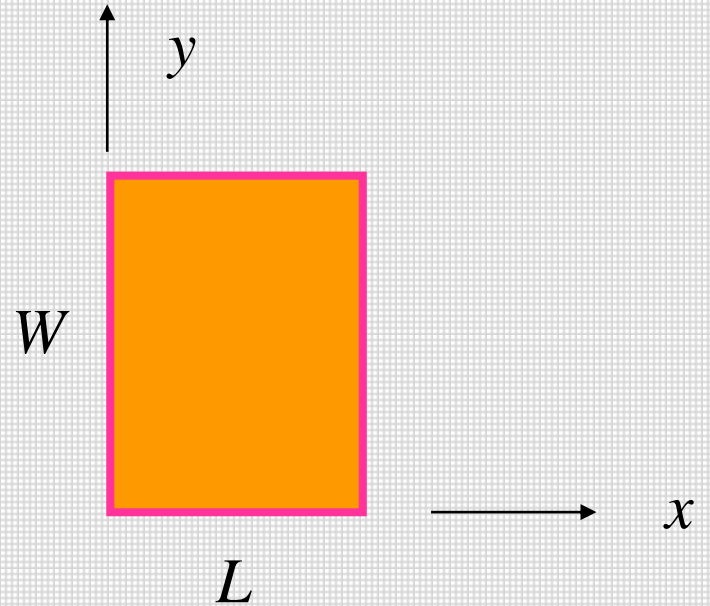
(TM_{mn} mode)



$$\left[-\left(\frac{m\pi}{L}\right)^2 - \left(\frac{n\pi}{W}\right)^2 + k^2 \right] E_z = 0$$

Hence
$$\left[-\left(\frac{m\pi}{L}\right)^2 - \left(\frac{n\pi}{W}\right)^2 + k^2 \right] = 0$$

$$k^2 = \left(\frac{m\pi}{L} \right)^2 + \left(\frac{n\pi}{W} \right)^2$$



Recall that

$$k = \omega \sqrt{\mu_0 \epsilon_0} \sqrt{\epsilon_r}$$

$$\omega = 2\pi f$$

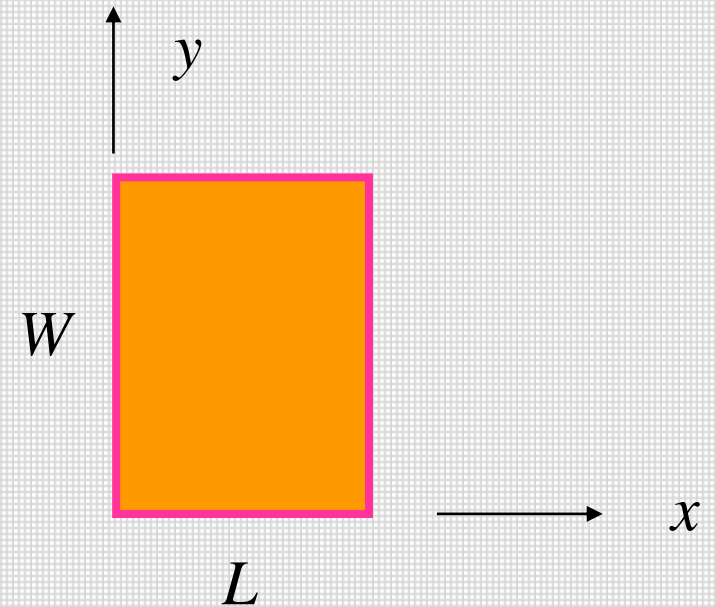
Hence

$$f = \frac{c}{2\pi \sqrt{\epsilon_r}} \sqrt{\left(\frac{m\pi}{L} \right)^2 + \left(\frac{n\pi}{W} \right)^2}$$

$$c = 1 / \sqrt{\mu_0 \epsilon_0}$$

Hence $f = f_{mn}$

(resonance frequency of
(m, n) mode)



$$f_{mn} = \frac{c}{2\pi\sqrt{\epsilon_r}} \sqrt{\left(\frac{m\pi}{L}\right)^2 + \left(\frac{n\pi}{W}\right)^2}$$

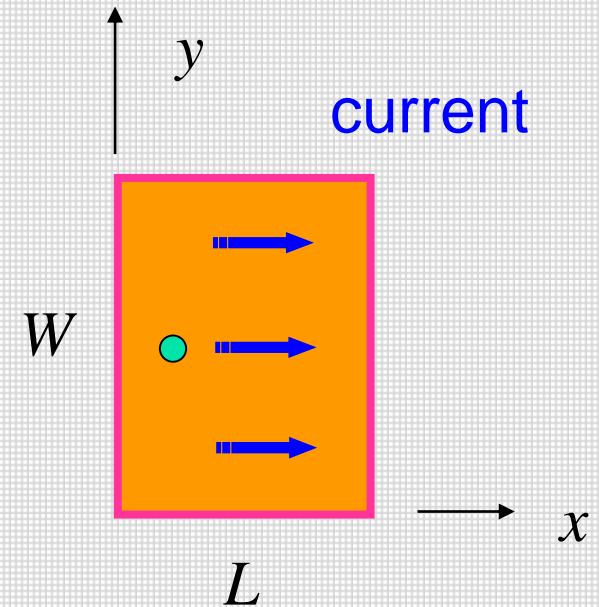
(1,0) Mode

This mode is most often used because the radiation pattern has a **broadside beam**.

$$E_z = \cos\left(\frac{\pi x}{L}\right)$$

$$f_{10} = \frac{c}{2\sqrt{\epsilon_r}} \left(\frac{1}{L}\right)$$

$$\underline{J}_s = \hat{x} \left(\frac{-1}{j\omega\mu_0}\right) \left(\frac{\pi}{L}\right) \sin\left(\frac{\pi x}{L}\right)$$



This mode acts as a wide microstrip line (width W) that has a resonant length of 0.5 guided wavelengths in the x direction.

Basic Properties of Microstrip Antennas

Resonance Frequency

The resonance frequency is controlled by the patch length L and the substrate permittivity.

Approximately, (assuming PMC walls)

$$k^2 = \left(\frac{m\pi}{L} \right)^2 + \left(\frac{n\pi}{W} \right)^2$$

Note: This is equivalent to saying that the length L is one-half of a wavelength in the dielectric:

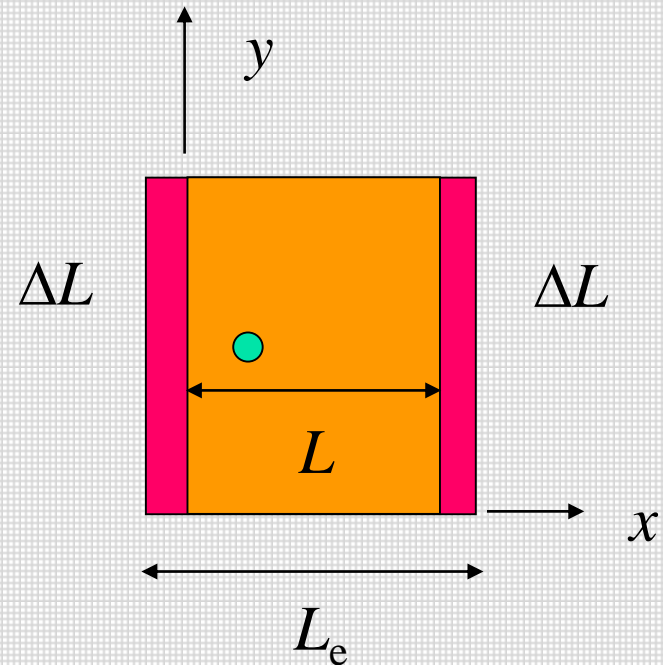
$$(1,0) \text{ mode: } kL = \pi \quad \longrightarrow \quad L = \lambda_d / 2 = \frac{\lambda_0 / 2}{\sqrt{\epsilon_r}}$$

Note: A higher substrate permittivity allows for a smaller antenna (miniaturization) – but lower bandwidth.

The calculation can be improved by adding a “fringing length extension” ΔL to each edge of the patch to get an “effective length” L_e .

$$L_e = L + 2\Delta L$$

$$f_{10} = \frac{c}{2\sqrt{\epsilon_r}} \left(\frac{1}{L_e} \right)$$



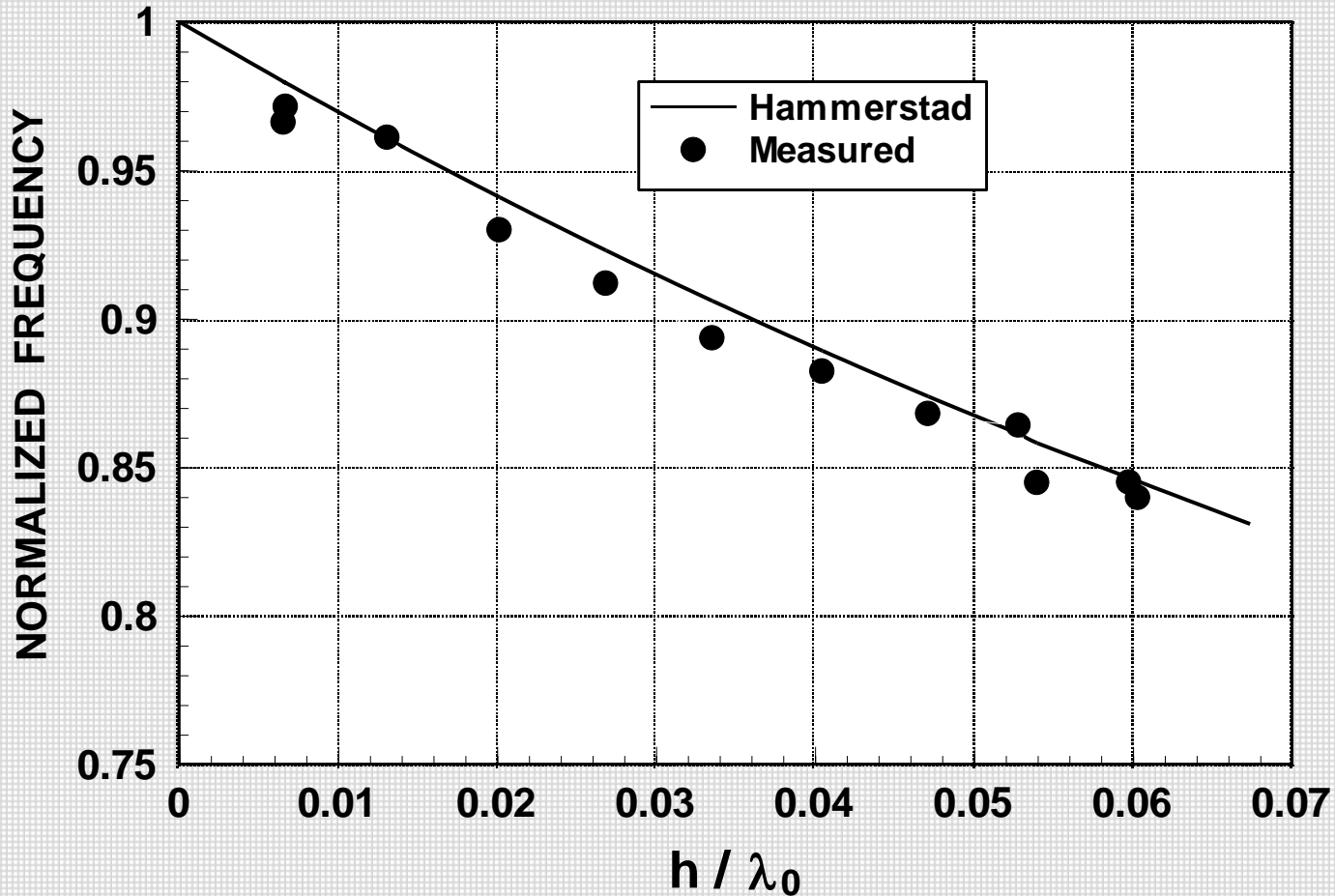
Hammerstad formula:

$$\Delta L / h = 0.412 \left[\frac{\left(\epsilon_r^{eff} + 0.3 \right) \left(\frac{W}{h} + 0.264 \right)}{\left(\epsilon_r^{eff} - 0.258 \right) \left(\frac{W}{h} + 0.8 \right)} \right]$$

$$\epsilon_r^{eff} = \frac{\epsilon_r + 1}{2} + \left(\frac{\epsilon_r - 1}{2} \right) \left[1 + 12 \left(\frac{h}{W} \right) \right]^{-1/2}$$

usually $\Delta L \approx 0.5 h$

Results: Resonance frequency



$$\epsilon_r = 2.2$$

$$W/L = 1.5$$

The resonance frequency has been normalized by the zero-order value (without fringing):

$$f_N = f / f_0$$

Bandwidth: Substrate effects

- The bandwidth is directly proportional to substrate thickness h .
- However, if h is greater than about $0.05 \lambda_0$, the probe inductance (for a coaxial feed) becomes large enough so that matching is difficult.
- The bandwidth is inversely proportional to ϵ_r (a foam substrate gives a high bandwidth).

Bandwidth: geometry effect

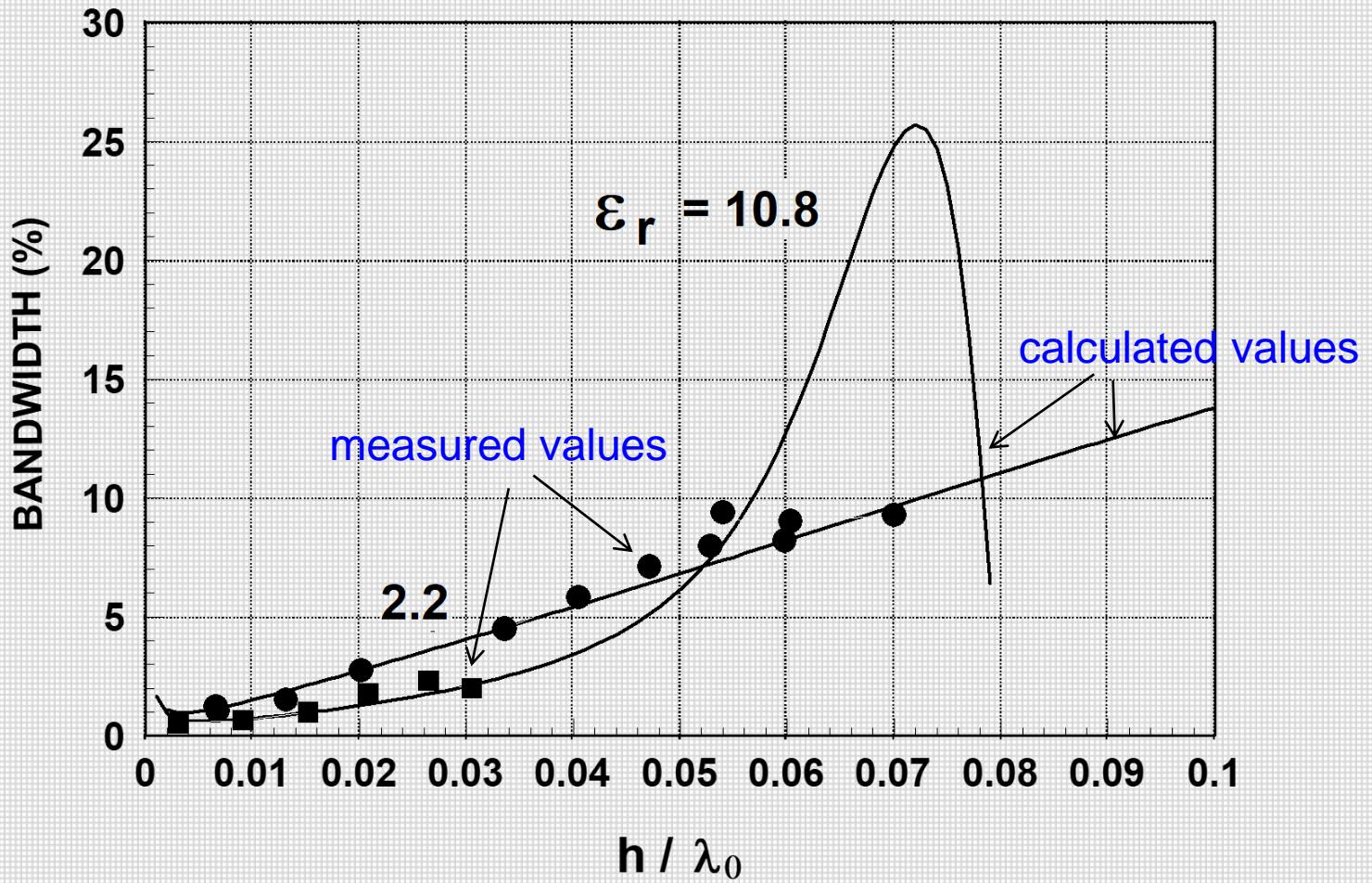
- The bandwidth is directly proportional to the width W .

Normally $W < 2L$ because of geometry constraints and to avoid (0, 2) mode:

$W = 1.5 L$ is typical.

Typical results

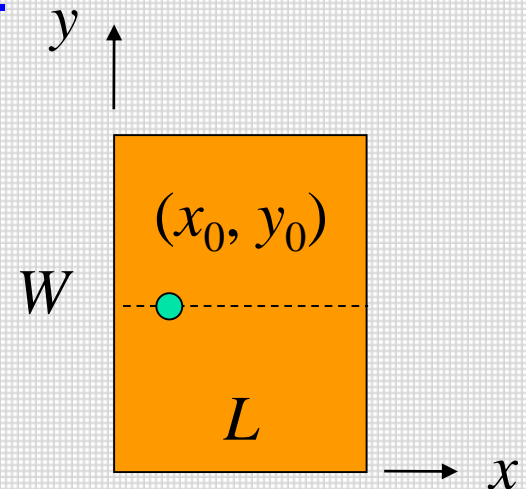
- For a typical substrate thickness ($h / \lambda_0 = 0.02$), and a typical substrate permittivity ($\epsilon_r = 2.2$) the bandwidth is about 3%.
- By using a thick foam substrate, bandwidth of about 10% can be achieved.
- By using special feeding techniques (aperture coupling) and stacked patches, bandwidths of 100% have been achieved.



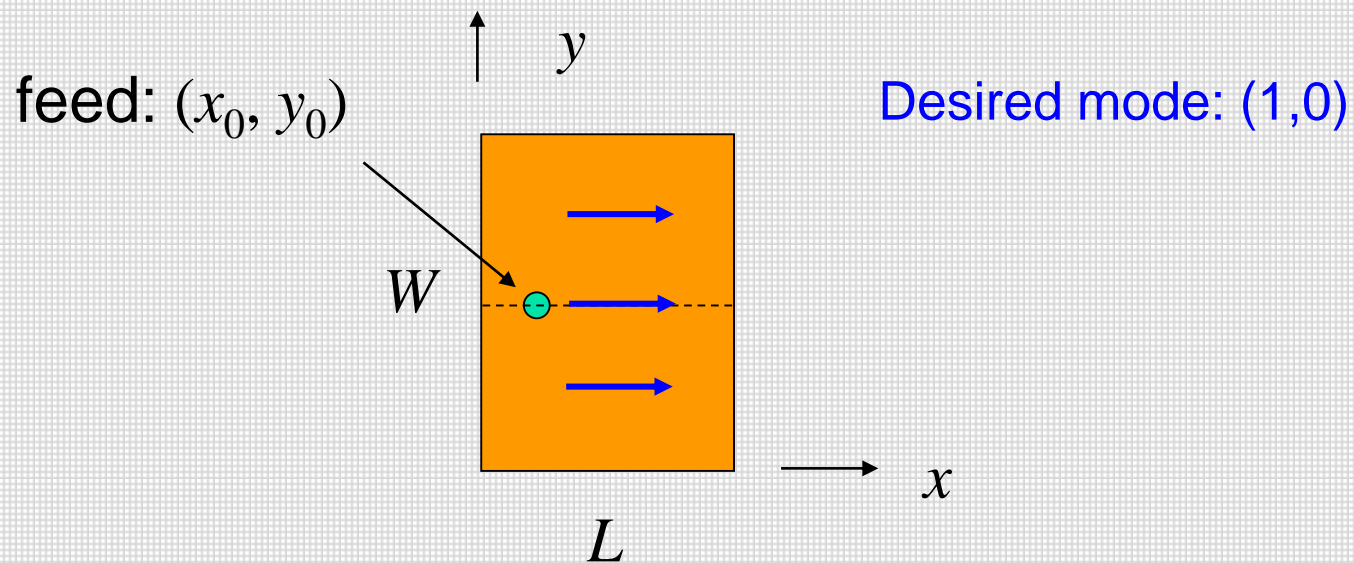
$\epsilon_r = 2.2$ or 10.8 $W/L = 1.5$

Resonant Input Impedance

- The resonant input impedance is almost independent of the substrate thickness h (the variation is mainly due to dielectric and conductor loss)
- The resonant input impedance is proportional to ϵ_r .
- The resonant input impedance is directly controlled by the location of the feed point. (maximum at edges $x = 0$ or $x = L$, zero at center of patch.



Note: The patch is usually fed along the **centerline** ($y_0 = W / 2$) to maintain symmetry and thus minimize excitation of undesirable modes (which cause cross-pol).

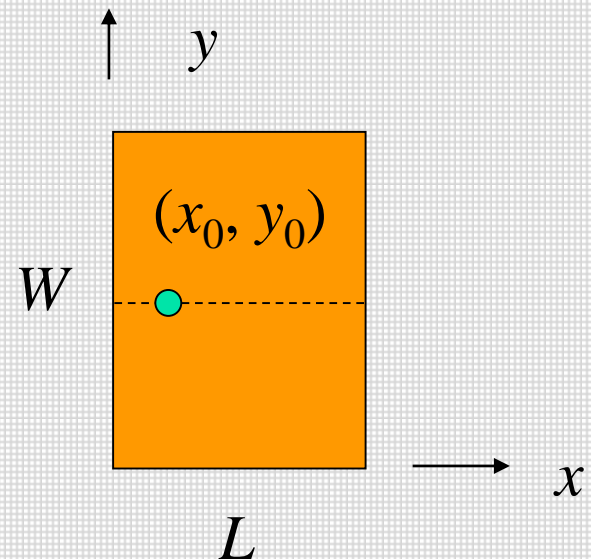


For a given mode, it can be shown that the resonant input resistance is proportional to the square of the cavity-mode field at the feed point.

$$R_{in} \propto E_z^2(x_0, y_0)$$

For (1,0) mode:

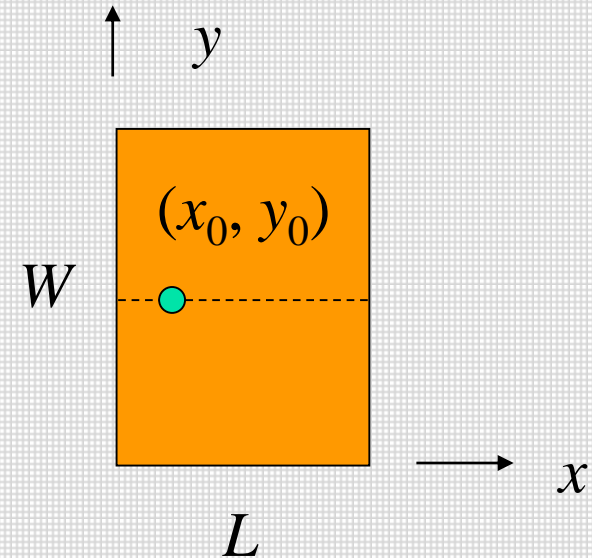
$$R_{in} \propto \cos^2\left(\frac{\pi x_0}{L}\right)$$



Resonant Input Resistance (cont.)

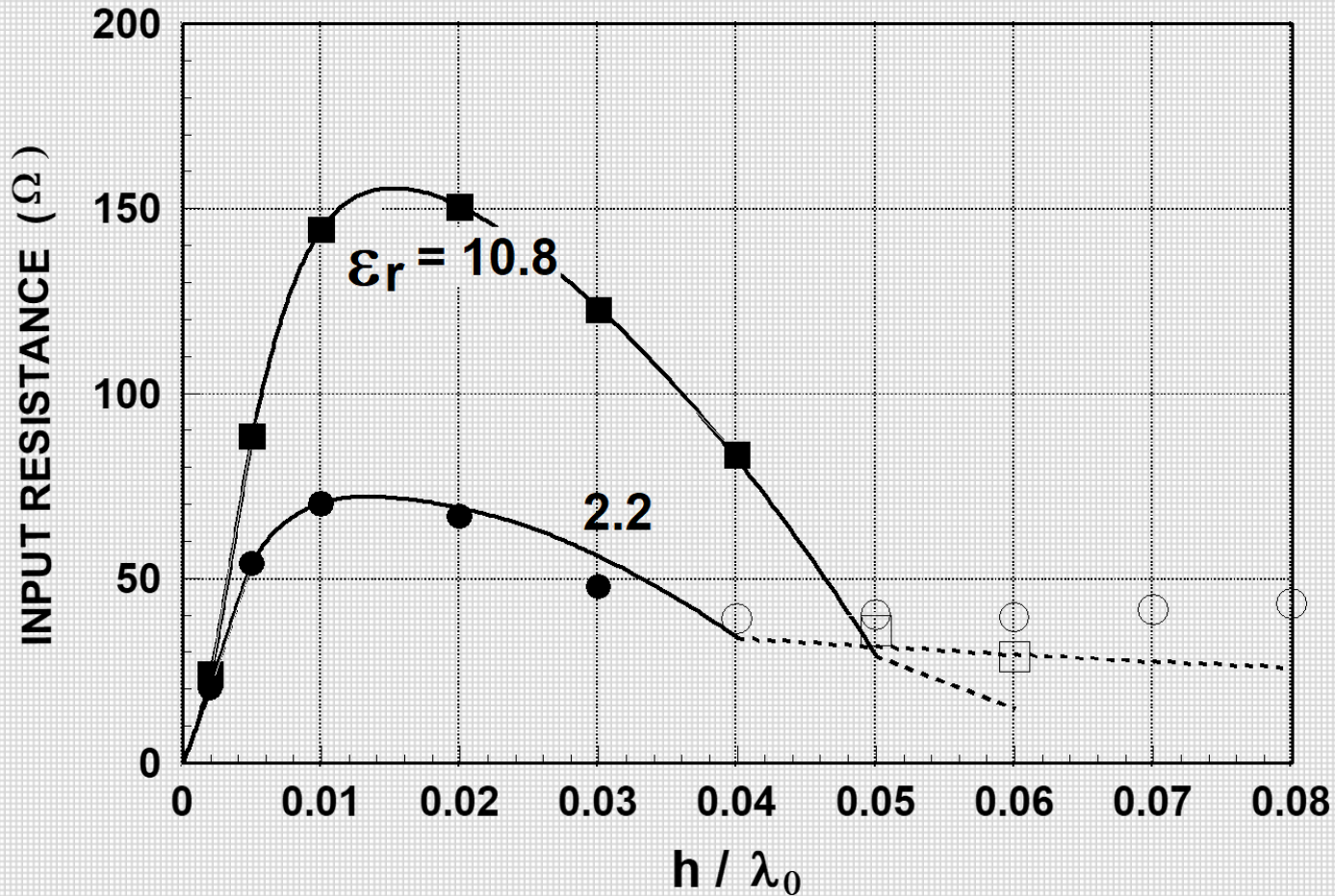
Hence, for (1,0) mode:

$$R_{in} = R_{edge} \cos^2 \left(\frac{\pi x_0}{L} \right)$$



The value of R_{edge} depends strongly on the substrate permittivity. For a typical patch, it may be about 100-200 Ohms.

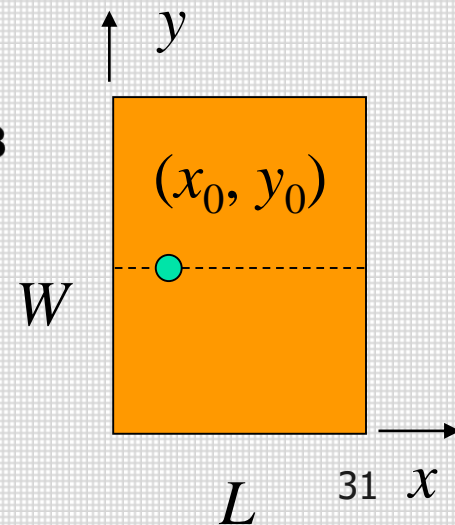
Results: Resonant input resistance



$$\epsilon_r = 2.2 \text{ or } 10.8$$

$$W/L = 1.5 \quad y_0 = W/2$$

$$x_0 = L/4$$

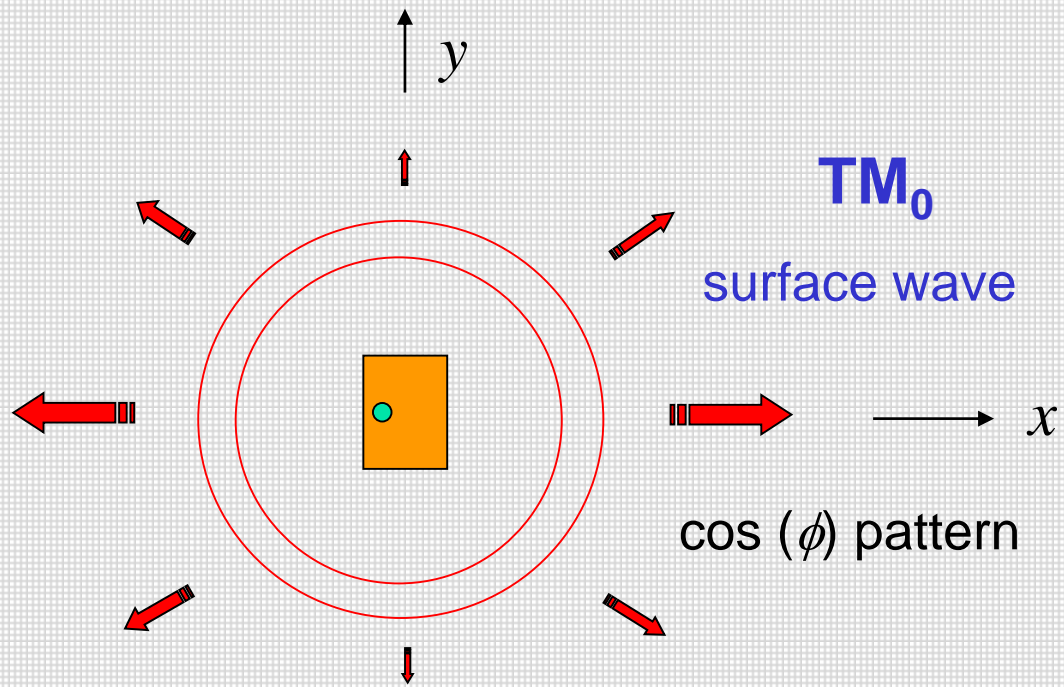


Radiation Efficiency

- Radiation efficiency is the ratio of power radiated into space, to the total input power.

$$e_r = \frac{P_r}{P_{tot}}$$

- The radiation efficiency is less than 100% due to
 - conductor loss
 - dielectric loss
 - surface-wave power



Hence,

$$e_r = \frac{P_r}{P_{tot}} = \frac{P_r}{P_r + (P_c + P_d + P_{sw})}$$

P_r = radiated power

P_c = power dissipated by conductors

P_{tot} = total input power

P_d = power dissipated by dielectric

P_{sw} = power launched into surface wave

- Conductor and dielectric loss is more important for thinner substrates.
- Conductor loss increases with frequency (proportional to $f^{1/2}$) due to the skin effect. Conductor loss is usually more important than dielectric loss.

$$R_s = \frac{1}{\sigma\delta}$$

$$\delta = \sqrt{\frac{2}{\omega\mu\sigma}}$$

R_s is the surface resistance of the metal. The skin depth of the metal is δ .

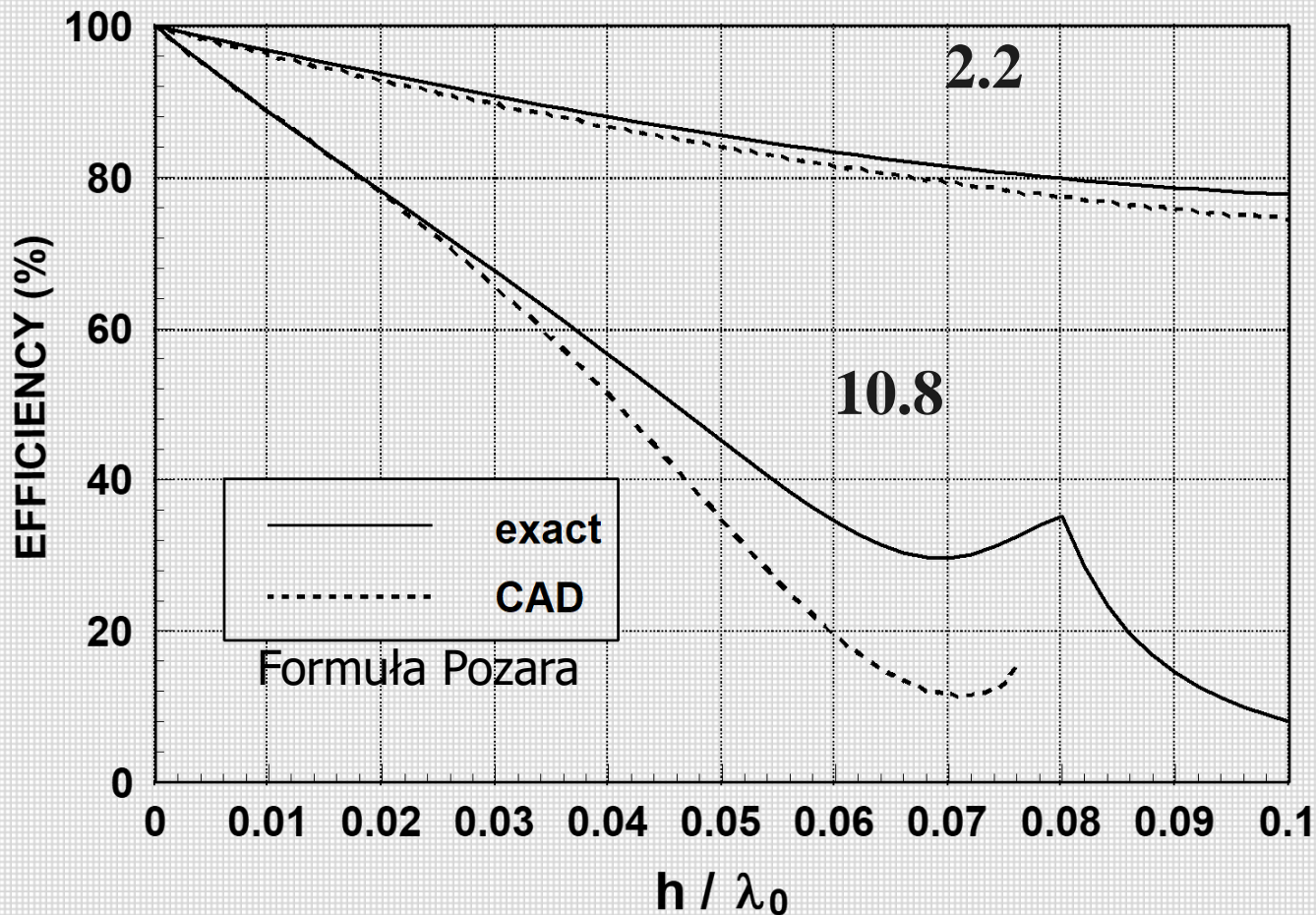
- Surface-wave power is more important for thicker substrates or for higher substrate permittivities. (The surface-wave power can be minimized by using a foam substrate.)

- For a **foam substrate**, higher radiation efficiency is obtained by making the substrate thicker (minimizing the conductor and dielectric losses).

The thicker the better!

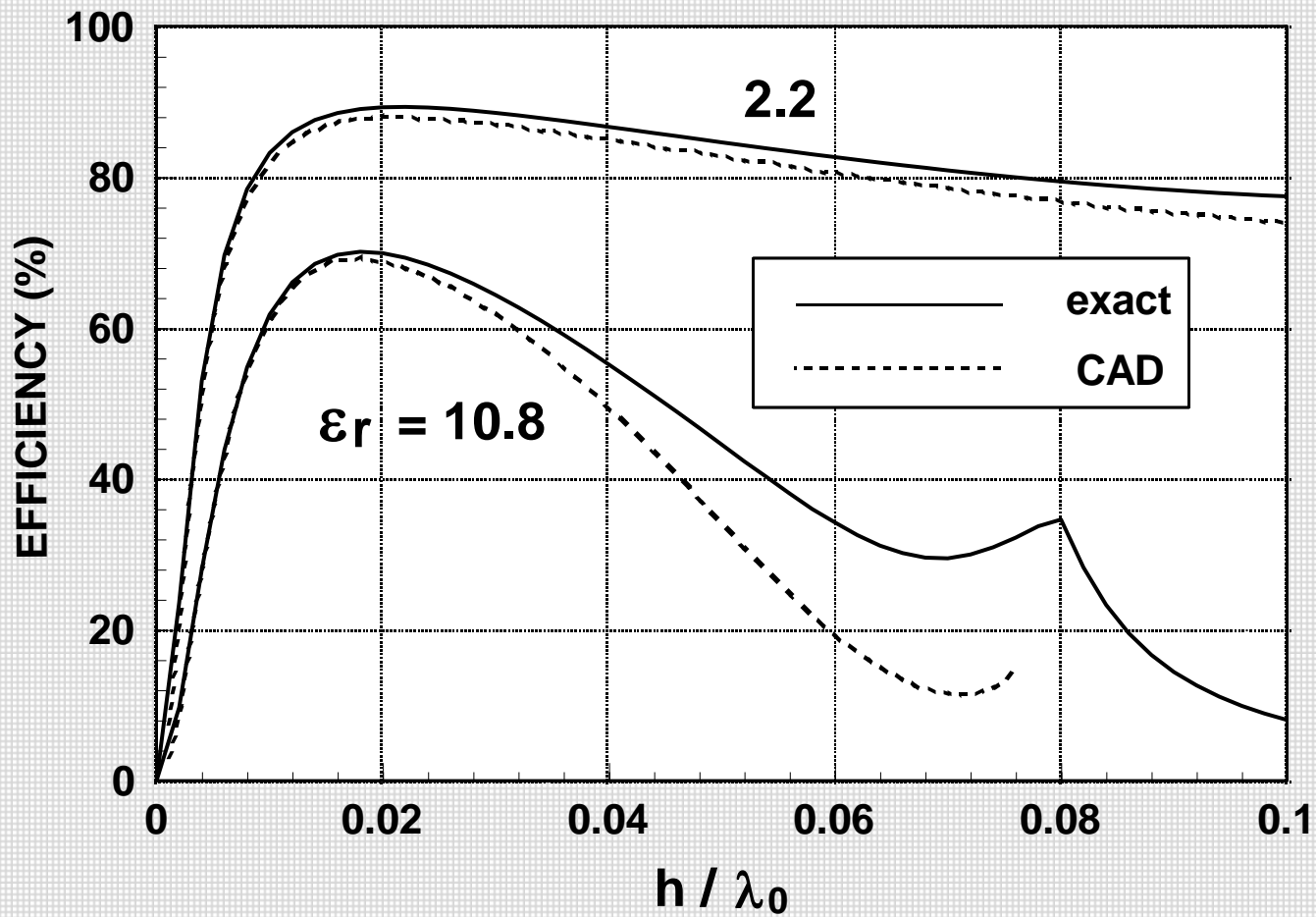
- For a **typical substrate** such as $\epsilon_r = 2.2$, the radiation efficiency is maximum for $h / \lambda_0 \approx 0.02$.

Conductor and dielectric losses are neglected



$$\epsilon_r = 2.2 \text{ lub } 10.8 \quad W/L = 1.5$$

Accounting for all losses



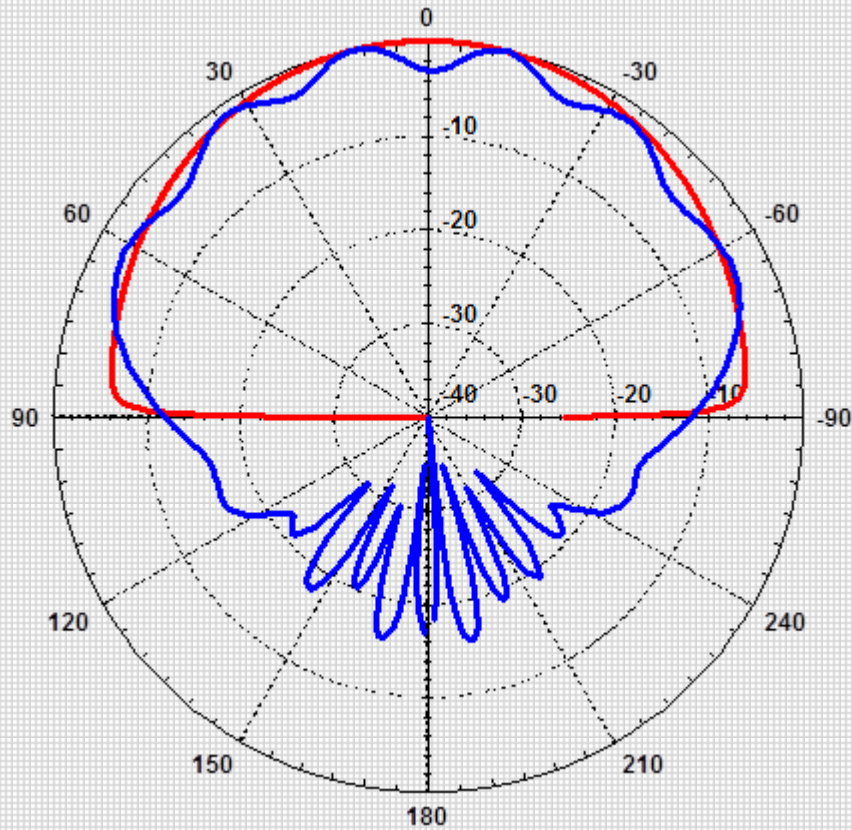
$\epsilon_r = 2.2$ or 10.8 $W/L = 1.5$

Radiation Patterns

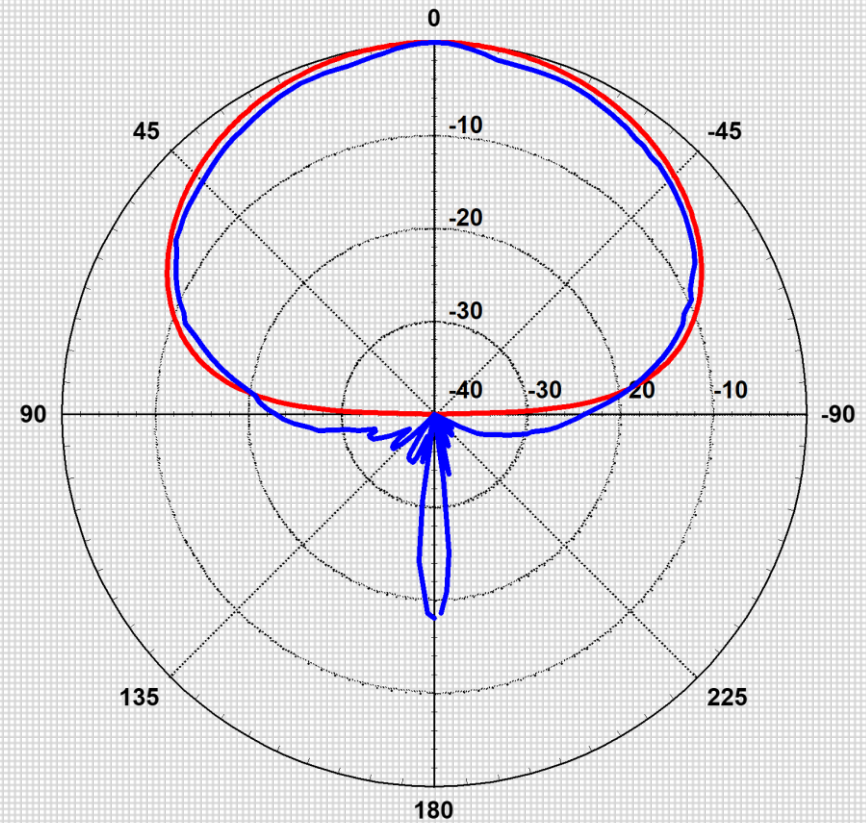
- The E-plane pattern is typically broader than the H-plane pattern.
- The truncation of the ground plane will cause edge diffraction, which tends to degrade the pattern by introducing rippling in the forward direction and back-radiation

Pattern distortion is more severe in the E-plane, due to the angle dependence of the vertical polarization E_θ and the SW pattern. Both vary as $\cos(\phi)$.

E-plane pattern



H-plane pattern



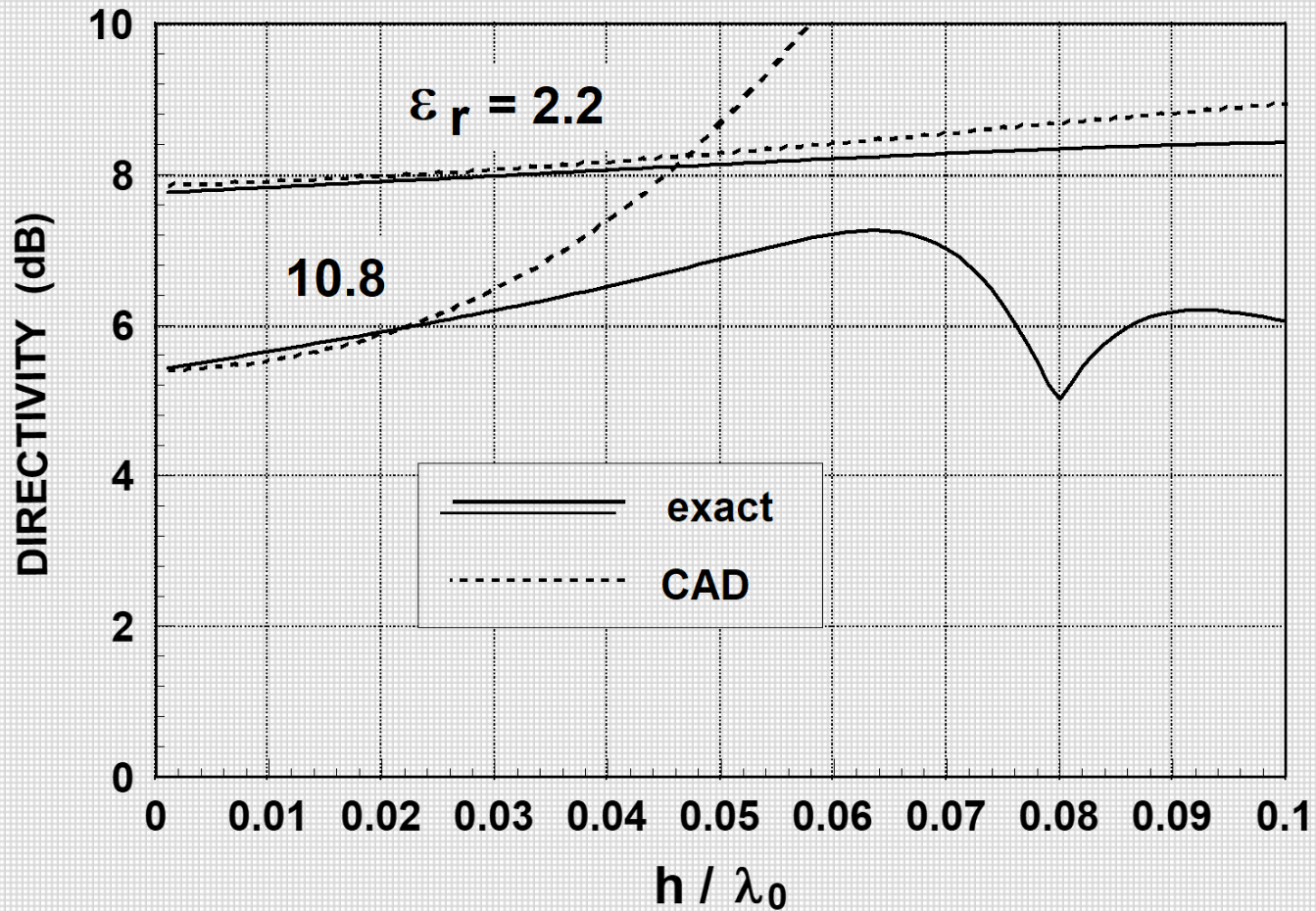
Red: infinite substrate and ground plane

Blue: 1 m² ground plane

Directivity

- The directivity is fairly insensitive to the substrate thickness.
- The directivity is higher for lower permittivity, because the patch is larger.

Directivity

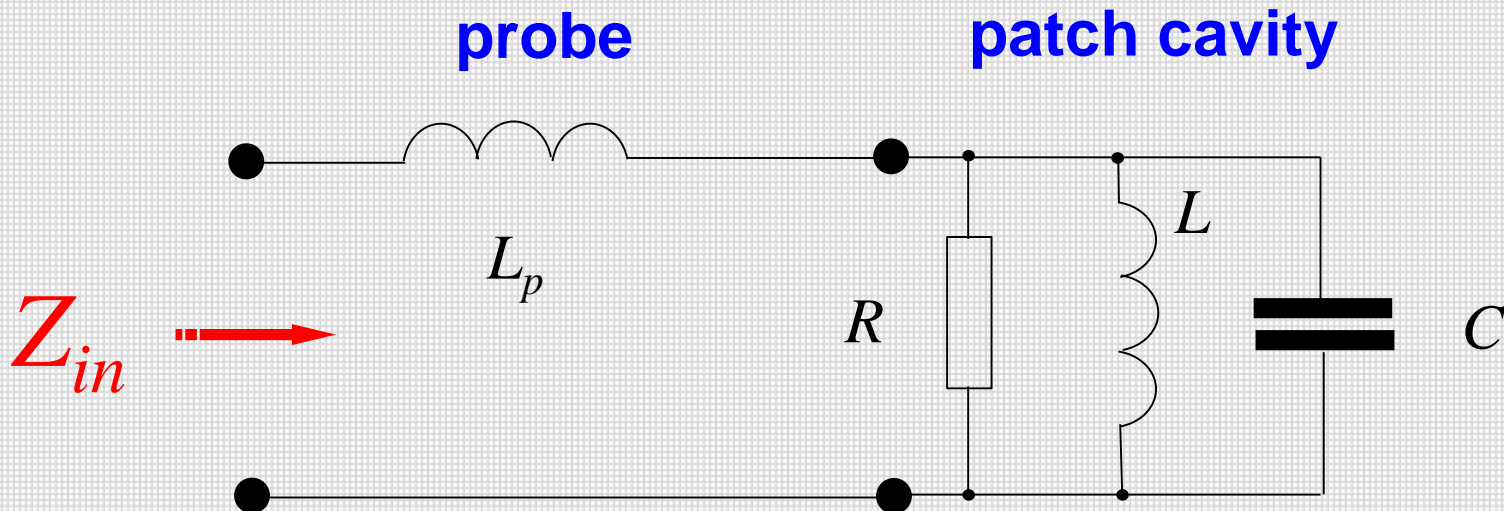


$\epsilon_r = 2.2$ or 10.8

$W / L = 1.5$

Approximate CAD Model for Z_{in}

- Near the resonance frequency, the patch cavity can be approximately modeled as an RLC circuit.
- A probe inductance L_p is added in series, to account for the “probe inductance” of a probe feed.



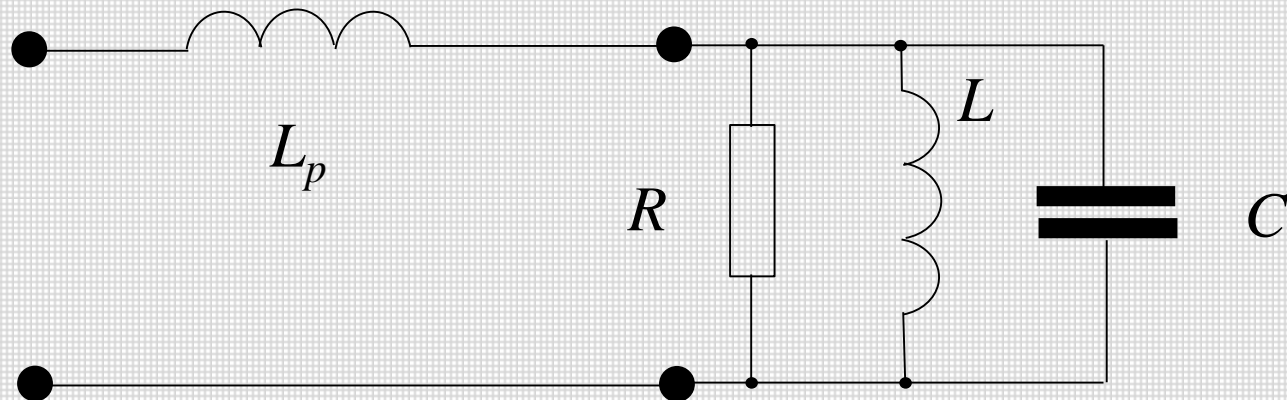
$$Z_{in} \approx j\omega L_p + \frac{R}{1 + j2Q(f/f_0 - 1)}$$

$$Q = \frac{R}{\omega_0 L}$$

$$BW = \frac{1}{\sqrt{2} Q}$$

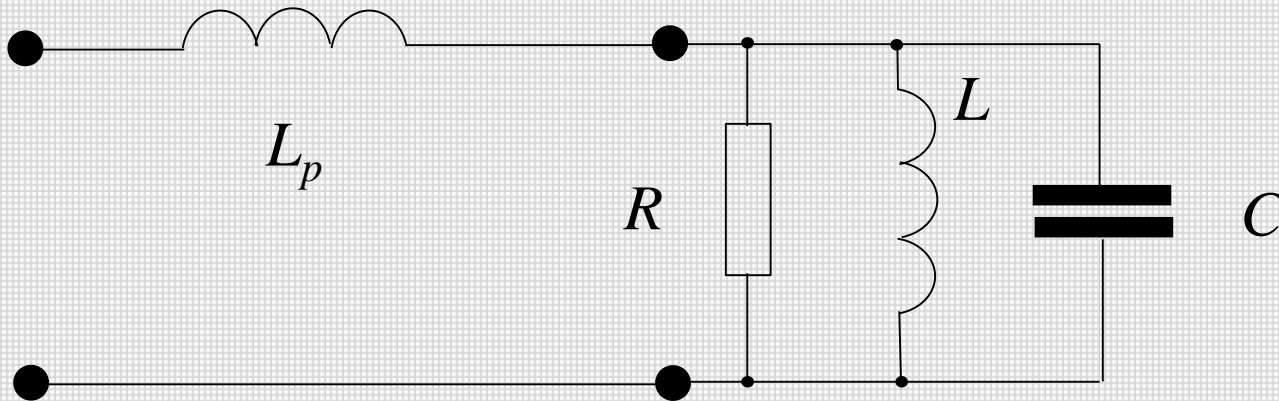
BW jest definiowany
poprzez $SWR < 2.0$

$$\omega_0 = 2\pi f_0 = \frac{1}{\sqrt{LC}}$$

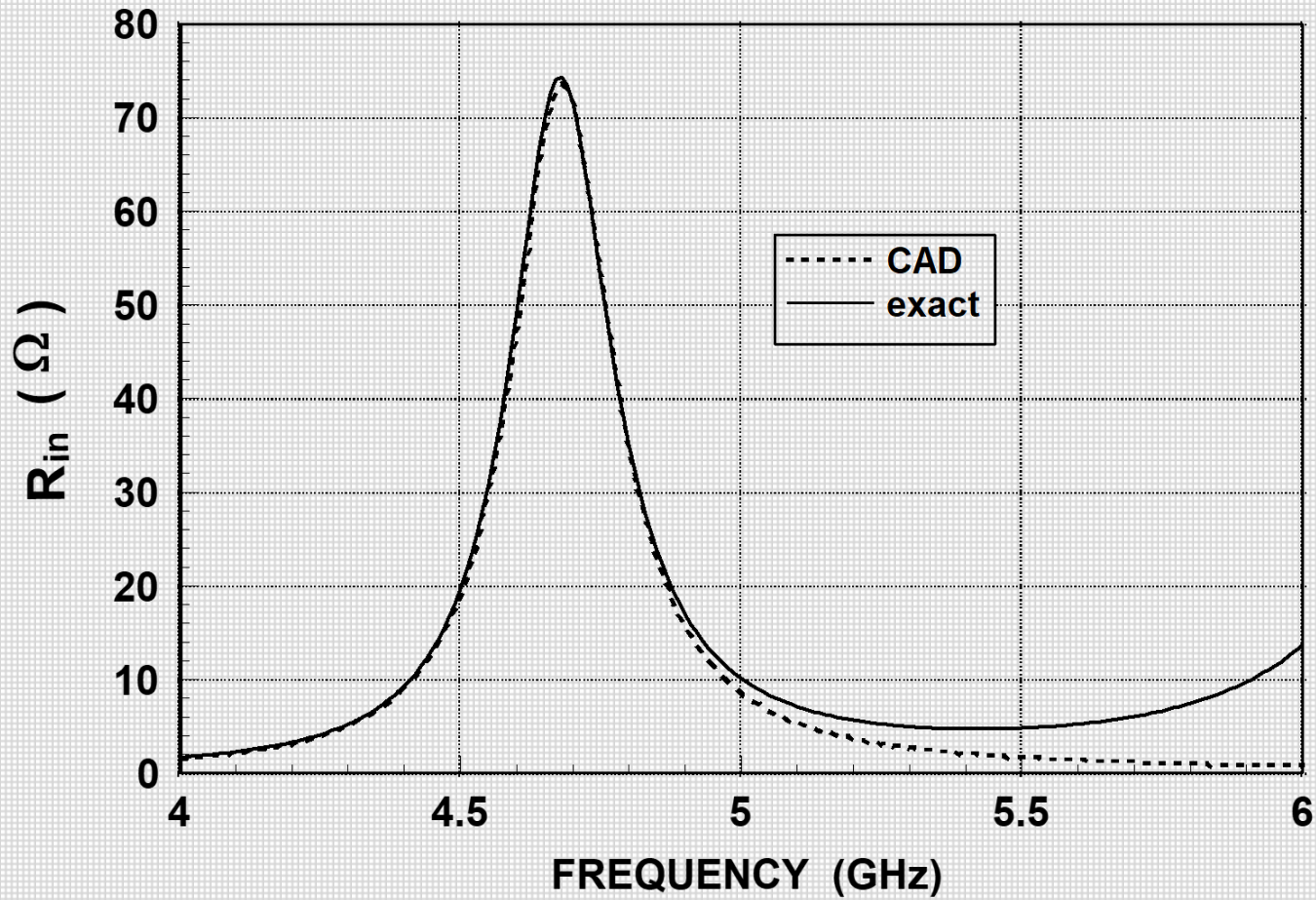


$$R = R_{in \max}$$

$R_{in \max}$ is the input resistance at the resonance of the patch cavity (the frequency that maximizes R_{in}).



Input resistance vs. frequency



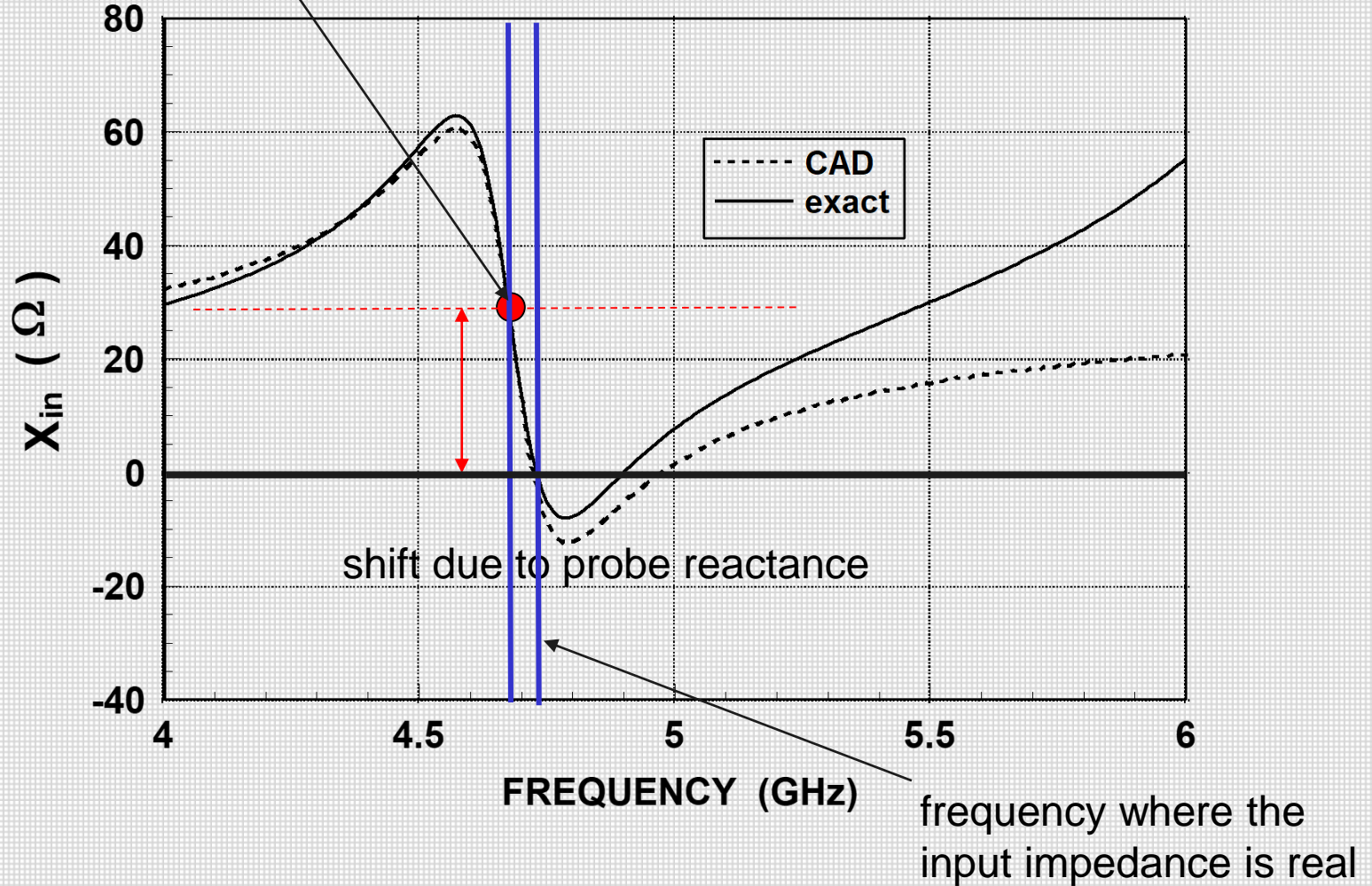
$$\epsilon_r = 2.2$$

$$W/L = 1.5$$

$$L = 3.0 \text{ cm}$$

Input reactance vs. frequency

frequency where the input resistance is maximum (f_0)



$$\epsilon_r = 2.2$$

$$W/L = 1.5$$

$$L = 3.0 \text{ cm}$$

Approximate formula for feed (probe) reactance (in Ohms)

a = probe radius h = probe height

$$X_f = \frac{\eta_0}{2\pi} (k_0 h) \left[-\gamma + \ln \left(\frac{2}{\sqrt{\epsilon_r} (k_0 a)} \right) \right]$$

This is based on an infinite parallel-plate model.

$$X_f = \omega L_p$$

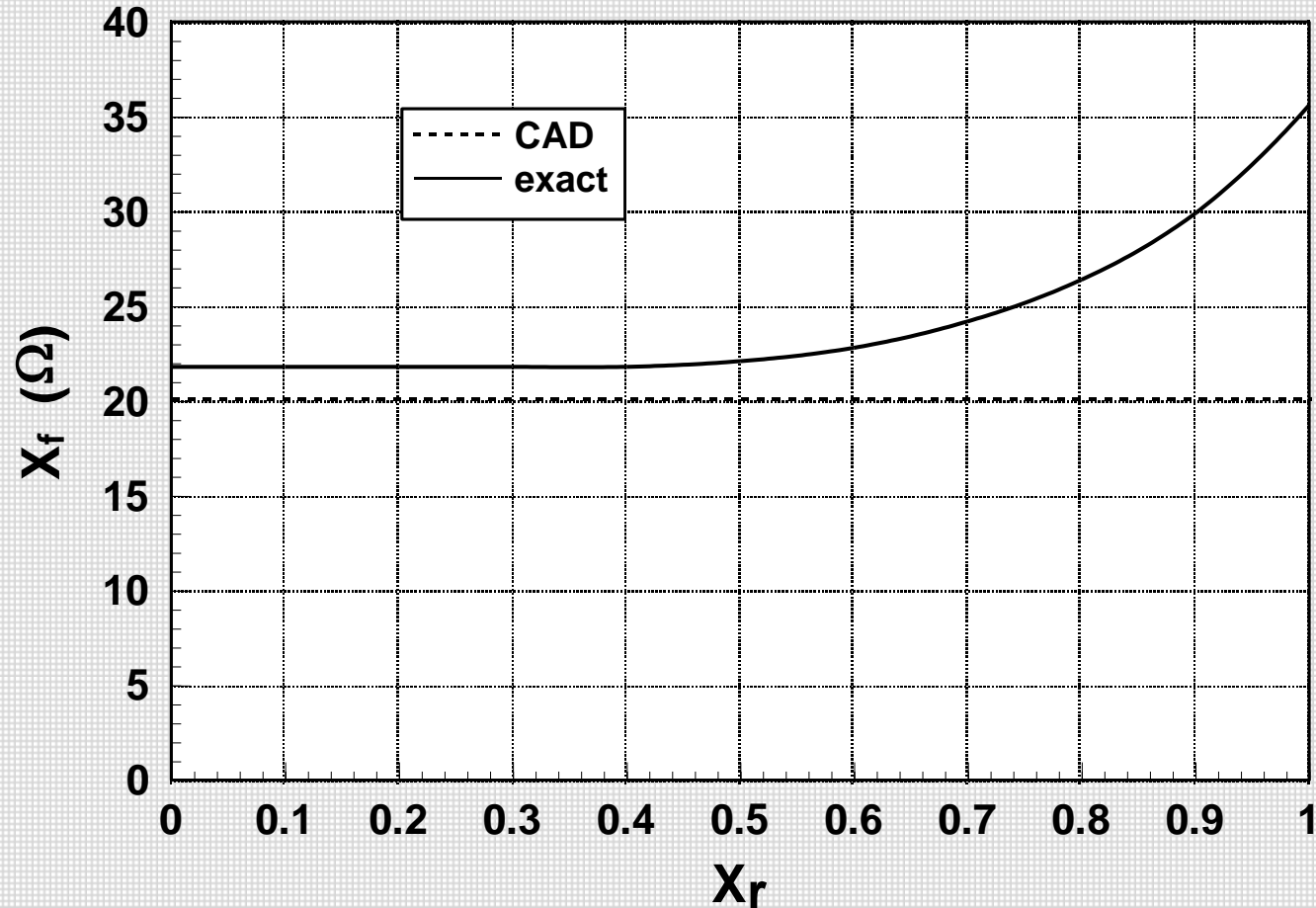
$\gamma \doteq 0.577216$ (Euler's constant)

$$\eta_0 = \sqrt{\mu_0 / \epsilon_0} = 376.73 \Omega$$

- Feed (probe) reactance increases proportionally with substrate thickness h .
- Feed reactance increases for smaller probe radius.

$$X_f = \frac{\eta_0}{2\pi} (k_0 h) \left[-\gamma + \ln \left(\frac{2}{\sqrt{\epsilon_r} (k_0 a)} \right) \right]$$

Probe reactance ($X_f = X_p = \omega L_p$)



$$\epsilon_r = 2.2$$

$$W/L = 1.5$$

$$h = 0.0254 \lambda_0$$

$$a = 0.5 \text{ mm}$$

$$X_r = 2 (x_0 / L) - 1$$

X_r is zero at the center of the patch, and is 1.0 at the patch edge

Important CAD Formulas

Radiation Efficiency

$$e_r = \frac{e_r^{hed}}{1 + e_r^{hed} \left[\ell_d + \left(\frac{R_s}{\pi \eta_0} \right) \left(\frac{1}{h / \lambda_0} \right) \right] \left[\left(\frac{3}{16} \right) \left(\frac{\epsilon_r}{p c_1} \right) \left(\frac{L}{W} \right) \left(\frac{1}{h / \lambda_0} \right) \right]}$$

where

$\ell_d = \tan \delta =$ loss tangent of substrate

$R_s =$ surface resistance of metal $= \frac{1}{\sigma \delta} = \sqrt{\frac{\omega \mu}{2 \sigma}}$

“hed” refers to a unit-amplitude horizontal electric dipole

$$e_r^{hed} = \frac{P_{sp}^{hed}}{P_{sp}^{hed} + P_{sw}^{hed}} = \frac{1}{1 + \frac{P_{sw}^{hed}}{P_{sp}^{hed}}}$$

where

$$P_{sp}^{hed} = \frac{1}{\lambda_0^2} (k_0 h)^2 (80\pi^2 c_1)$$

$$P_{sw}^{hed} = \frac{1}{\lambda_0^2} (k_0 h)^3 \left[60\pi^3 c_1 \left(1 - \frac{1}{\epsilon_r} \right)^3 \right]$$

Hence we have

$$e_r^{hed} = \frac{1}{1 + \frac{3}{4} \pi (k_0 h) \left(\frac{1}{c_1} \right) \left(1 - \frac{1}{\epsilon_r} \right)^3}$$

Physically, this term is the radiation efficiency of a horizontal electric dipole (hed) on top of the substrate.

The constants are defined as

$$c_1 = 1 - \frac{1}{\varepsilon_r} + \frac{2/5}{\varepsilon_r^2}$$

$$p = 1 + \frac{a_2}{10} (k_0 W)^2 + (a_2^2 + 2a_4) \left(\frac{3}{560} \right) (k_0 W)^4 + c_2 \left(\frac{1}{5} \right) (k_0 L)^2 \\ + a_2 c_2 \left(\frac{1}{70} \right) (k_0 W)^2 (k_0 L)^2$$

$$c_2 = -0.0914153$$

$$a_2 = -0.16605$$

$$a_4 = 0.00761$$

Improved formula (Pozar)

$$e_r^{hed} = \frac{1}{1 + \frac{P_{sw}^{hed}}{P_{sp}^{hed}}} \quad P_{sp}^{hed} = \frac{1}{\lambda_0^2} (k_0 h)^2 (80\pi^2 c_1)$$

$$P_{sw}^{hed} = \frac{\eta_0 k_0^2}{4} \frac{\epsilon_r (x_0^2 - 1)^{3/2}}{\epsilon_r (1 + x_1) + (k_0 h) \sqrt{x_0^2 - 1} (1 + \epsilon_r^2 x_1)}$$

$$x_1 = \frac{x_0^2 - 1}{\epsilon_r - x_0^2} \quad x_0 = 1 + \frac{-\epsilon_r^2 + \alpha_0 \alpha_1 + \epsilon_r \sqrt{\epsilon_r^2 - 2\alpha_0 \alpha_1 + \alpha_0^2}}{\epsilon_r^2 - \alpha_1^2}$$

Improved formula (cont.)

$$\alpha_0 = s \tan \left[(k_0 h) s \right]$$

$$\alpha_1 = -\frac{1}{s} \left[\tan \left[(k_0 h) s \right] + \frac{(k_0 h) s}{\cos^2 \left[(k_0 h) s \right]} \right]$$

$$s = \sqrt{\epsilon_r - 1}$$

Bandwidth

$$BW = \frac{1}{\sqrt{2}} \left[\ell_d + \left(\frac{R_s}{\pi \eta_0} \right) \left(\frac{1}{h / \lambda_0} \right) + \left(\frac{16}{3} \right) \left(\frac{p c_1}{\epsilon_r} \right) \left(\frac{h}{\lambda_0} \right) \left(\frac{W}{L} \right) \left(\frac{1}{e_r^{hed}} \right) \right]$$

BW is defined from the frequency limits f_1 and f_2 at which $SWR = 2.0$

$$BW = \frac{f_2 - f_1}{f_0} \quad (\text{multiply by 100 if you want to get \%})$$

Resonant Input Resistance (probe-feed)

$$R = R_{edge} \cos^2 \left(\frac{\pi x_0}{L} \right)$$

$$R_{edge} = \frac{\left(\frac{4}{\pi} \right) (\eta_0) \left(\frac{L}{W} \right) \left(\frac{h}{\lambda_0} \right)}{\ell_d + \left(\frac{R_s}{\pi \eta_0} \right) \left(\frac{1}{h/\lambda_0} \right) + \left(\frac{16}{3} \right) \left(\frac{p c_1}{\epsilon_r} \right) \left(\frac{W}{L} \right) \left(\frac{h}{\lambda_0} \right) \left(\frac{1}{e_r^{hed}} \right)}$$

Directivity

$$D = \left(\frac{3}{pc_1} \right) \left[\frac{\epsilon_r}{\epsilon_r + \tan^2(k_1 h)} \right] (\text{tanc}^2(k_1 h))$$

where

$$\text{tanc}(x) \equiv \tan(x) / x$$

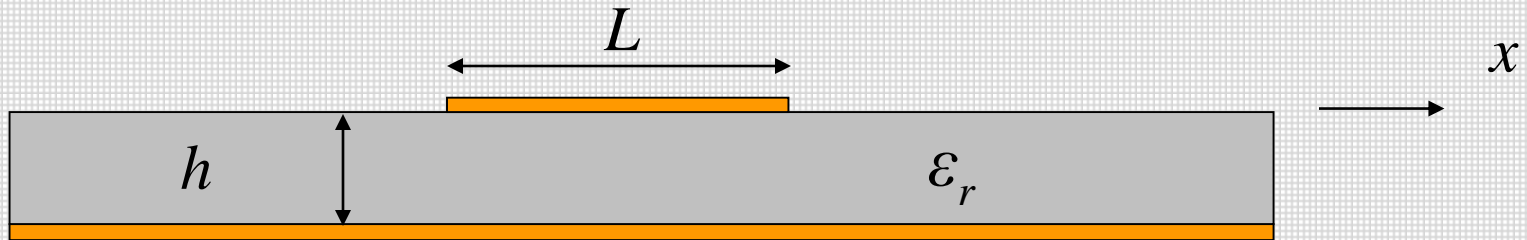
For thin substrates:

$$D \approx \frac{3}{p c_1}$$

The directivity is essentially independent of the substrate thickness.

Radiation Patterns

(based on electric current model)

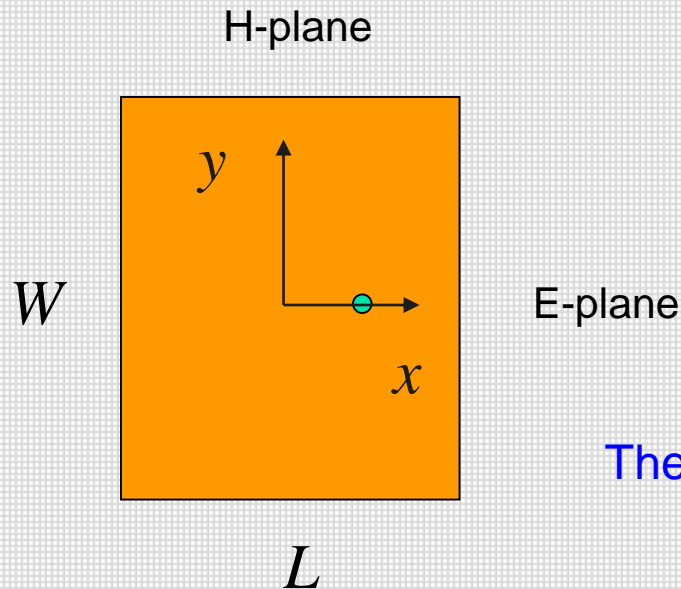


infinite GP and substrate

The origin is at the center of the patch.

(1,0) mode

$$\underline{J}_s = \underline{\hat{x}} \cos\left(\frac{\pi x}{L}\right)$$



The probe is on the x axis.

The far-field pattern can be determined by reciprocity.

$$E_i(r, \theta, \phi) = E_i^{hex}(r, \theta, \phi) \left(\frac{\pi WL}{2} \right) \left[\frac{\sin\left(\frac{k_y W}{2}\right)}{\frac{k_y W}{2}} \right] \left[\frac{\cos\left(\frac{k_x L}{2}\right)}{\left(\frac{\pi}{2}\right)^2 - \left(\frac{k_x L}{2}\right)^2} \right]$$

$$i = \theta \text{ or } \phi$$

$$k_x = k_0 \sin \theta \cos \phi$$

$$k_y = k_0 \sin \theta \sin \phi$$

The “hex” pattern is for a horizontal electric dipole in the x direction, sitting on top of the substrate.

$$E_{\phi}^{hex} (r, \theta, \phi) = -E_0 \sin \phi F(\theta)$$

$$E_{\theta}^{hex} (r, \theta, \phi) = E_0 \cos \phi G(\theta)$$

where $E_0 = \left(\frac{-j\omega \mu_0}{4\pi r} \right) e^{-jk_0 r}$

$$F(\theta) = 1 + \Gamma^{TE}(\theta) = \frac{2 \tan(k_0 h N(\theta))}{\tan(k_0 h N(\theta)) - j N(\theta) \sec \theta}$$

$$G(\theta) = \cos \theta (1 + \Gamma^{TM}(\theta)) = \frac{2 \tan(k_0 h N(\theta)) \cos \theta}{\tan(k_0 h N(\theta)) - j \frac{\epsilon_r}{N(\theta)} \cos \theta}$$

$$N(\theta) = \sqrt{\epsilon_r - \sin^2(\theta)}$$

Antennas with circular polarization

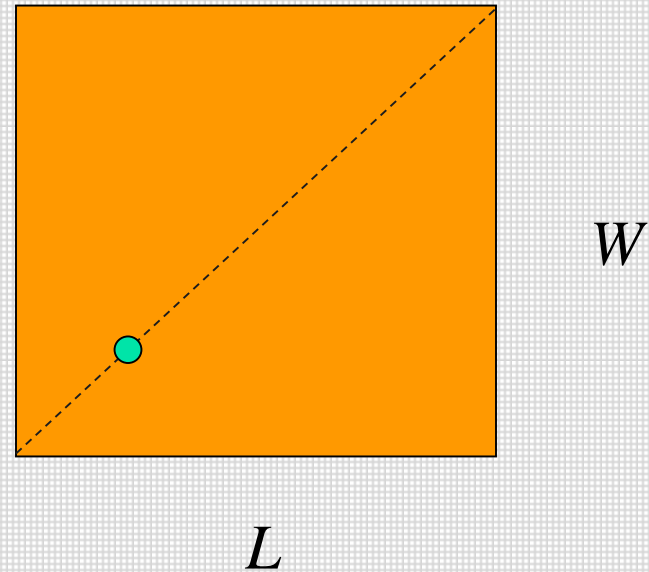
Three main techniques:

- 1) Single feed with “nearly degenerate” eigenmodes (compact but narrow CP bandwidth).
- 2) Dual feed with delay line or 90° hybrid phase shifter (broader CP bandwidth but uses more space).
- 3) Synchronous subarray technique (produces high-quality CP due to cancellation effect, but requires more space).

Single Feed

The feed is on the diagonal.
The patch is **nearly** (but not exactly) square.

$$L \approx W$$



Basic principle: the two modes are excited with equal amplitude, but with a $\pm 45^\circ$ phase.

Design equations:

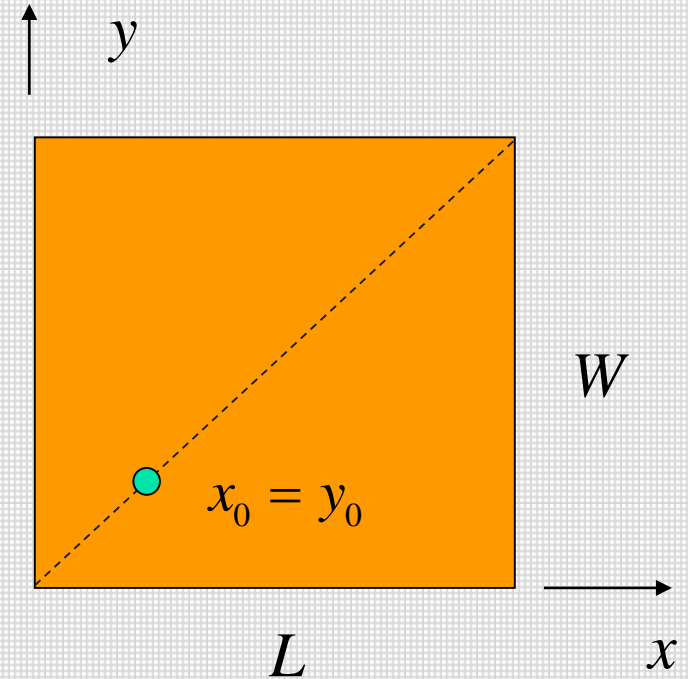
$f_0 = f_{CP}$ The resonance frequency (R_{in} is maximum) is the optimum CP frequency.

$$BW = \frac{1}{\sqrt{2Q}}$$

(SWR < 2)

$$\left. \begin{aligned} f_x &= f_0 \left(1 \mp \frac{1}{2Q} \right) \\ f_y &= f_0 \left(1 \pm \frac{1}{2Q} \right) \end{aligned} \right\}$$

Top sign for LHCP,
bottom sign for RHCP.



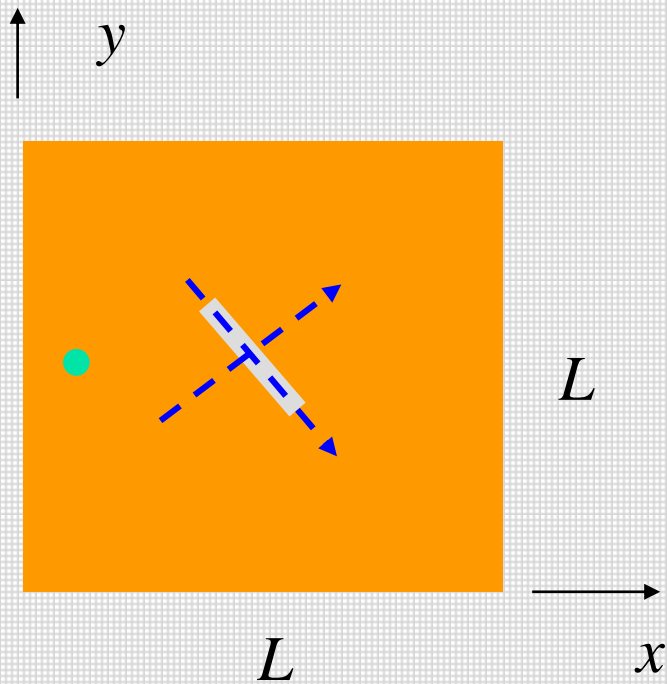
At resonance:

$$R_{in} = R_x = R_y$$

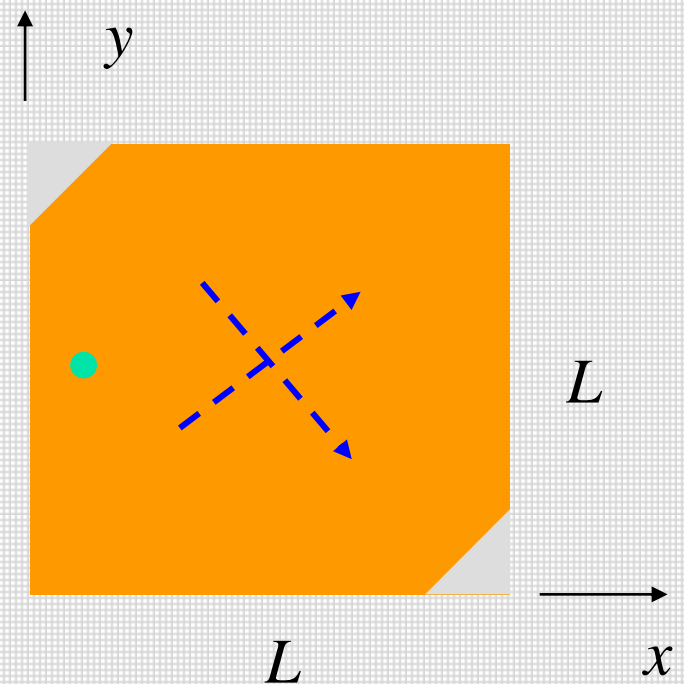
R_x and R_y are the resonant input resistances of the two LP (x and y) modes, for the same feed position as in the CP patch.

Other Variations

Note: Diagonal modes are used as degenerate modes



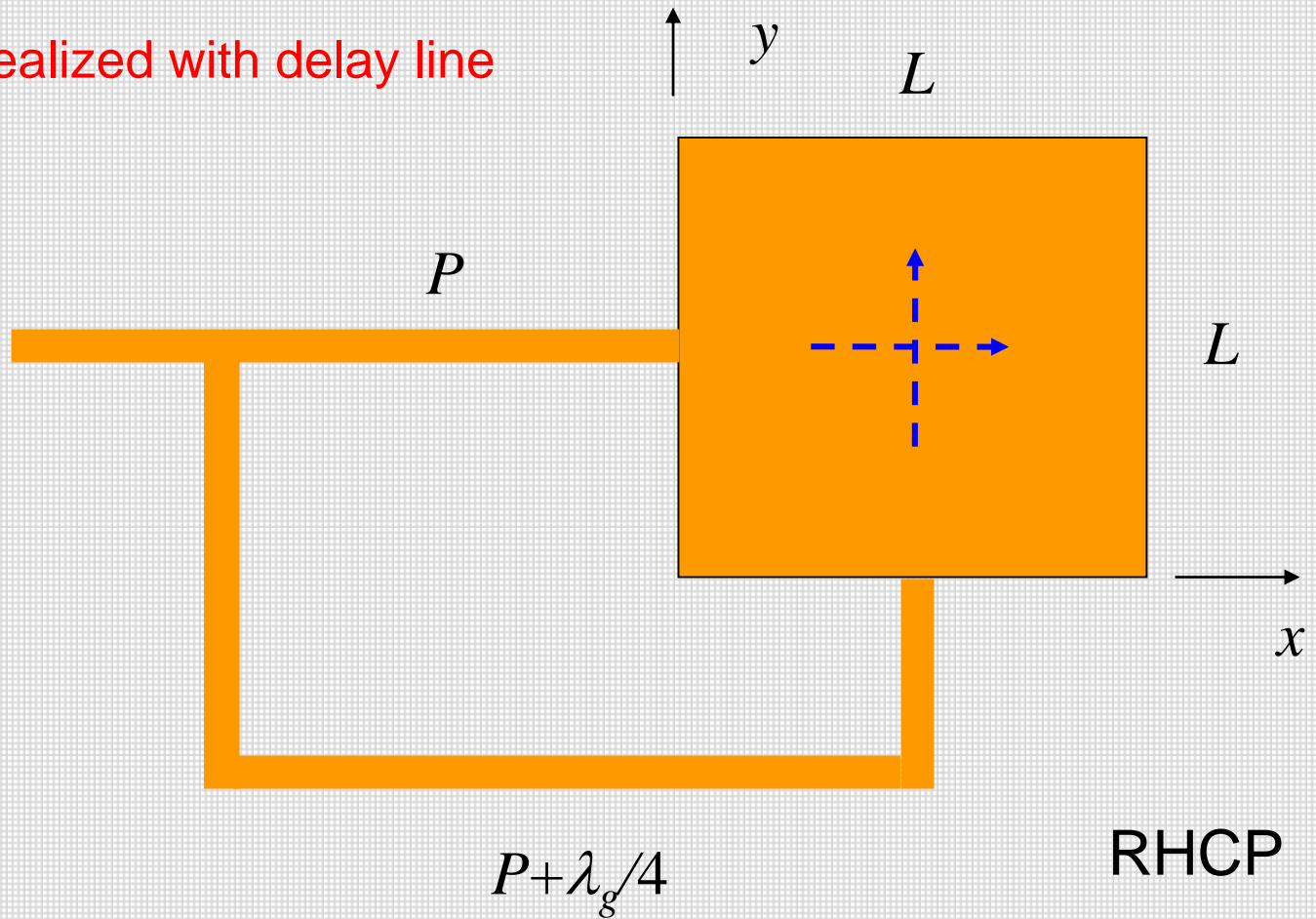
Patch with slot



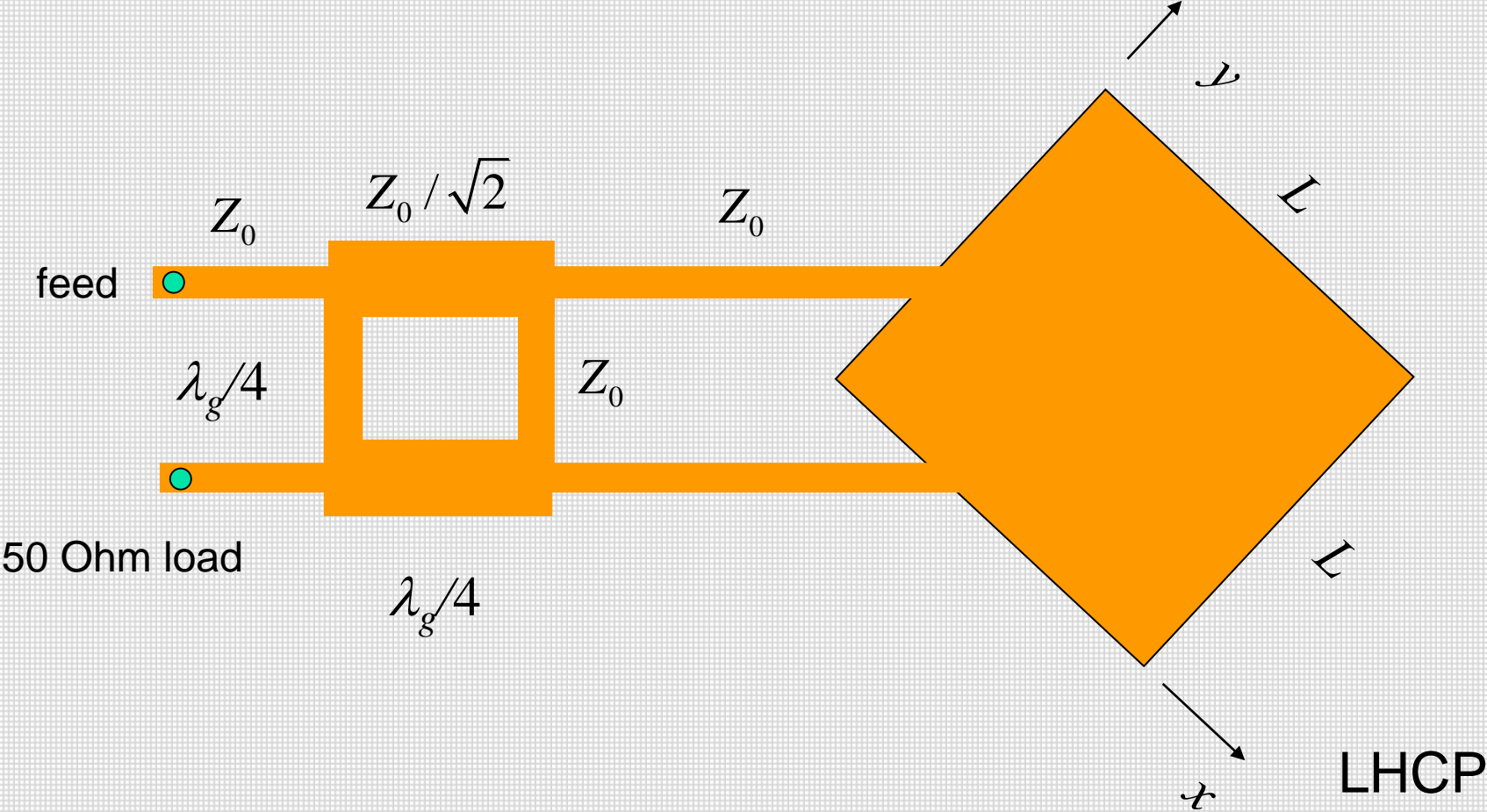
Patch with truncated corners

Dual Feed

Phase shift realized with delay line

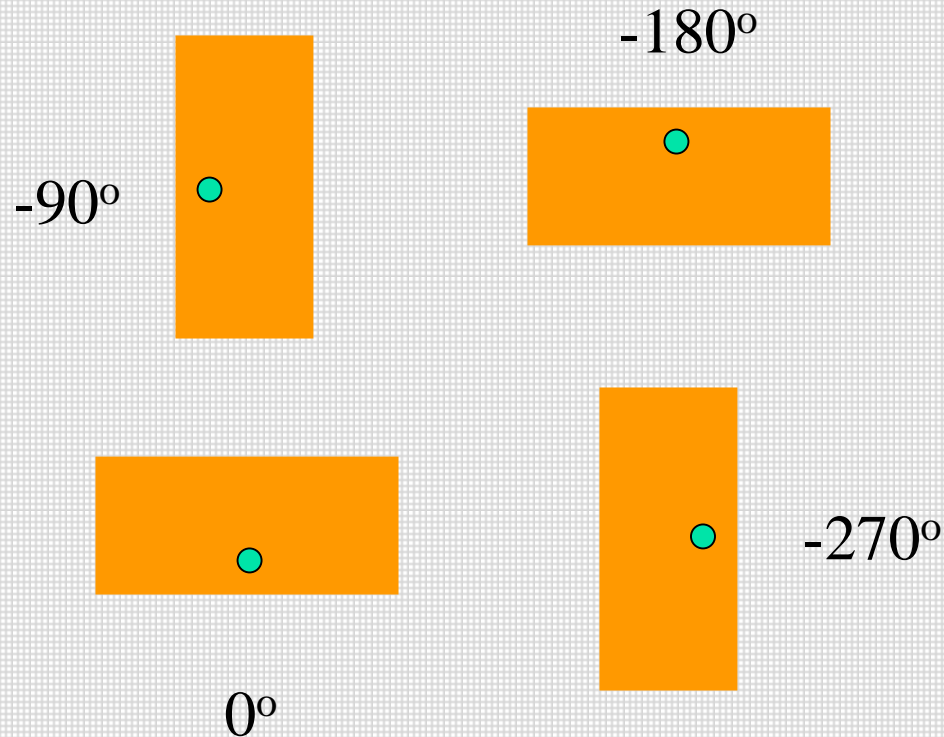


Phase shift realized with 90° hybrid (branchline coupler)



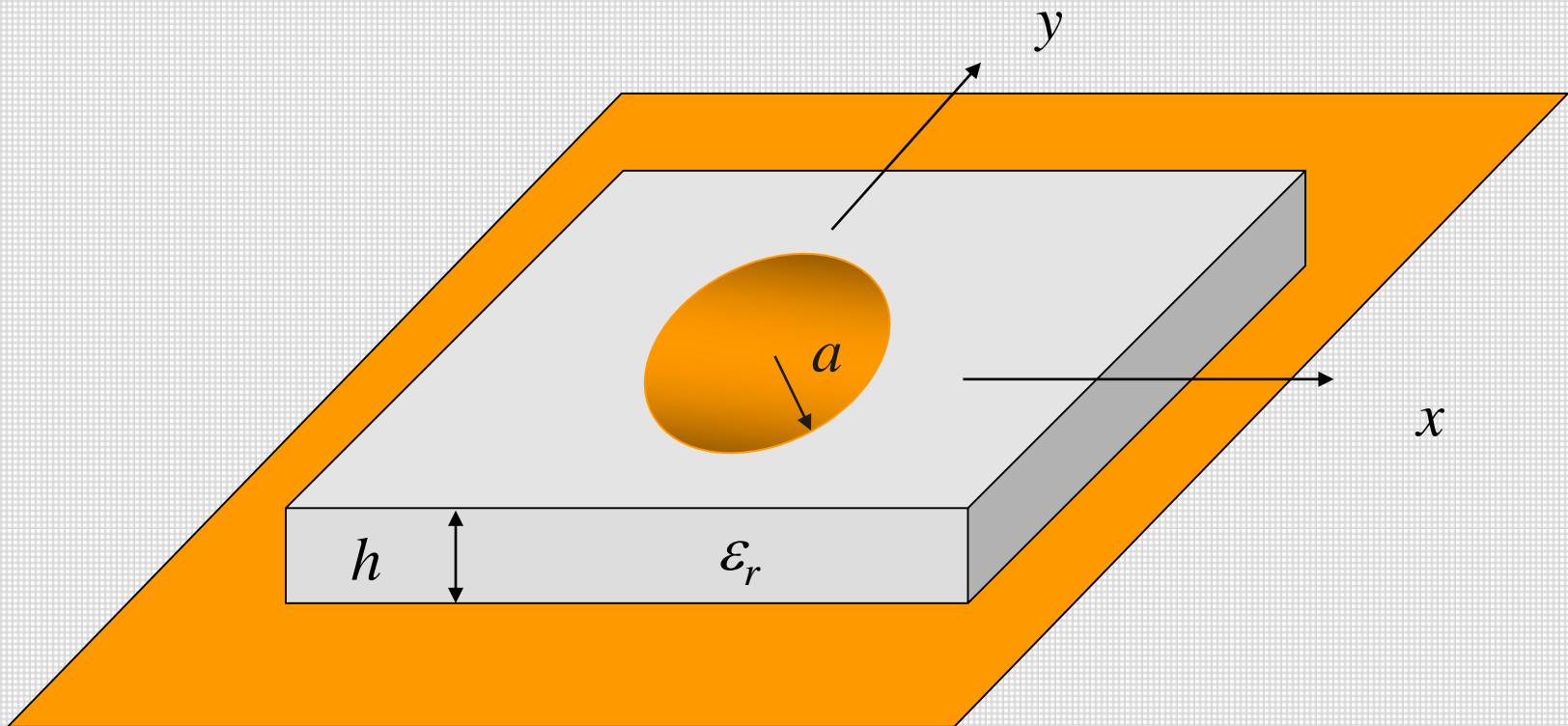
Synchronous Rotation

Elements are rotated in space and fed with phase shifts



Because of symmetry, radiation from higher-order modes (or probes) tends to be reduced, resulting in good cross-pol.

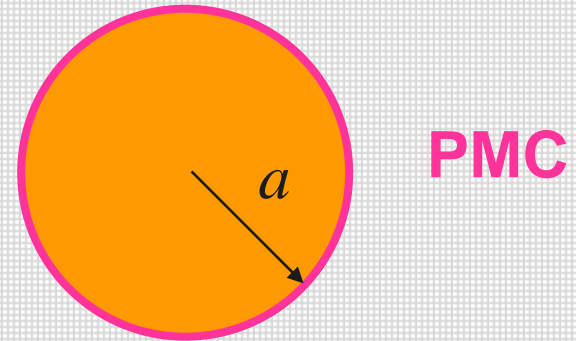
Circular Patch



Resonance Frequency

From separation of variables:

$$E_z = \cos(m\phi) J_m(k\rho)$$



J_m = Bessel function of first kind, order m .

$$\left. \frac{\partial E_z}{\partial \rho} \right|_{\rho=a} = 0 \quad \longrightarrow \quad J'_m(ka) = 0$$

$$ka = x'_{mn}$$

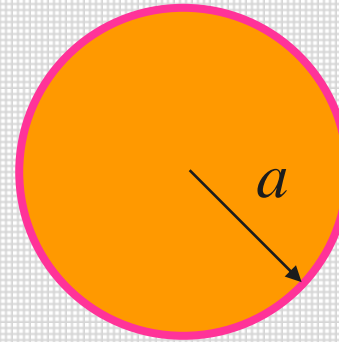
(nth root of J'_m Bessel function)

$$f_{mn} = \frac{c}{2\pi\sqrt{\epsilon_r}} x'_{mn}$$

Dominant mode: TM_{11}

$$f_{11} = \frac{c}{2\pi a\sqrt{\epsilon_r}} x'_{11}$$

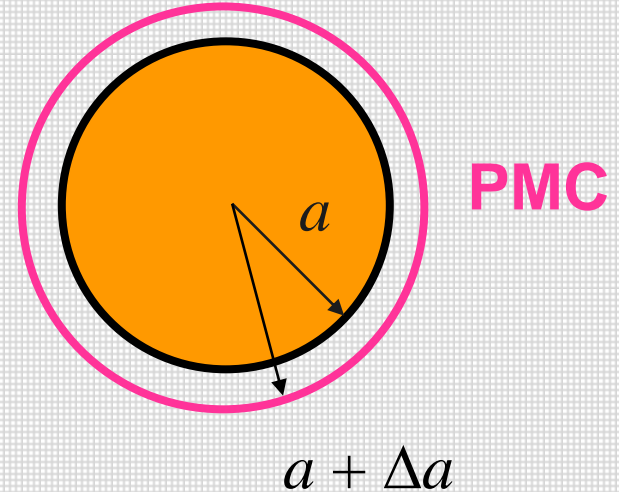
$$x'_{11} \approx 1.842$$



PMC

Fringing extension: $a_e = a + \Delta a$

$$f_{11} = \frac{c}{2\pi a_e \sqrt{\epsilon_r}} x'_{11}$$



“Long/Shen Formula”:

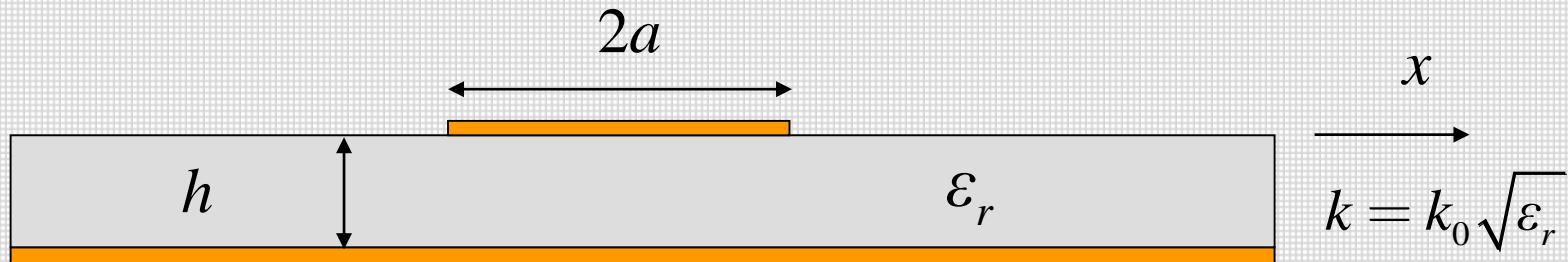
$$a_e = a \sqrt{1 + \frac{2h}{\pi a \epsilon_r} \left[\ln \left(\frac{\pi a}{2h} \right) + 1.7726 \right]}$$

or

$$\Delta a \approx \frac{h}{\pi \epsilon_r} \left[\ln \left(\frac{\pi a}{2h} \right) + 1.7726 \right]$$

Patterns

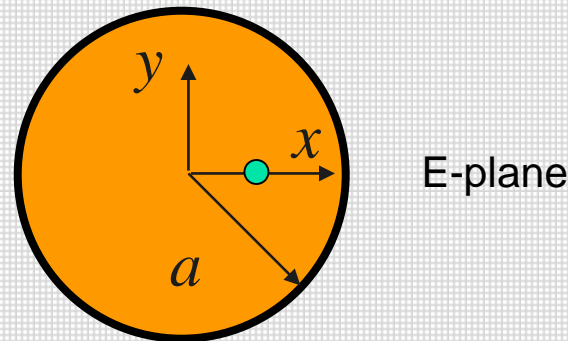
(based on magnetic current model)



infinite GP and substrate

H-plane

The origin is at the center of the patch.



The probe is on the x axis.

In patch cavity:

$$E_z(\rho, \phi) = \cos \phi \left(\frac{J_1(k\rho)}{J_1(ka)} \right) \left(\frac{1}{h} \right)$$

(The edge voltage has a maximum of one volt.)

$$E_{\theta}^R(r, \theta, \phi) = 2\pi a \frac{E_0}{\eta_0} \operatorname{tanc}(k_{z1}h) \cos\phi J_1'(k_0 a \sin\theta) Q(\theta)$$

$$E_{\phi}^R(r, \theta, \phi) = -2\pi a \frac{E_0}{\eta_0} \operatorname{tanc}(k_{z1}h) \sin\phi \left(\frac{J_1(k_0 a \sin\theta)}{k_0 a \sin\theta} \right) P(\theta)$$

where

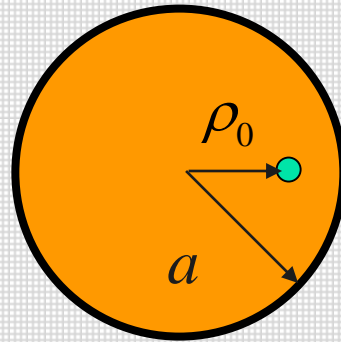
$$\operatorname{tanc} x = \tan x / x$$

$$P(\theta) = \cos\theta (1 - \Gamma^{TE}(\theta)) = \cos\theta \left[\frac{-2jN(\theta)}{\tan(k_0 h N(\theta)) - jN(\theta)\sec\theta} \right]$$

$$Q(\theta) = 1 - \Gamma^{TM}(\theta) = \frac{-2j \left(\frac{\epsilon_r}{N(\theta)} \right) \cos\theta}{\tan(k_0 h N(\theta)) - j \frac{\epsilon_r}{N(\theta)} \cos\theta}$$

$$N(\theta) = \sqrt{\epsilon_r - \sin^2(\theta)}$$

Input Resistance



$$R_{in} \approx R_{edge} \left[\frac{J_1^2(k\rho_0)}{J_1^2(ka)} \right]$$

$$R_{edge} = \left[\frac{1}{2P_{sp}} \right] e_r$$

e_r = radiation efficiency

where

$$P_{sp} = \frac{\pi}{8\eta_0} (k_0 a)^2 \int_0^{\pi/2} \text{tanc}^2(k_0 h N(\theta)) \cdot \left[|Q(\theta)|^2 J_1'^2(k_0 a \sin \theta) + |P(\theta)|^2 J_{inc}^2(k_0 a \sin \theta) \right] \sin \theta d\theta$$

$$J_{inc}(x) = J_1(x) / x$$

P_{sp} = power radiated into space by circular patch with maximum edge voltage of one volt.

CAD Formula:

$$P_{sp} = \frac{\pi}{8\eta_0} (k_0 a)^2 I_c$$

$$I_c = \frac{4}{3} p_c$$

$$p_c = \sum_{k=0}^6 (k_0 a)^{2k} e_{2k}$$

$$e_0 = 1$$

$$e_2 = -0.400000$$

$$e_4 = 0.0785710$$

$$e_6 = -7.27509 \times 10^{-3}$$

$$e_8 = 3.81786 \times 10^{-4}$$

$$e_{10} = -1.09839 \times 10^{-5}$$

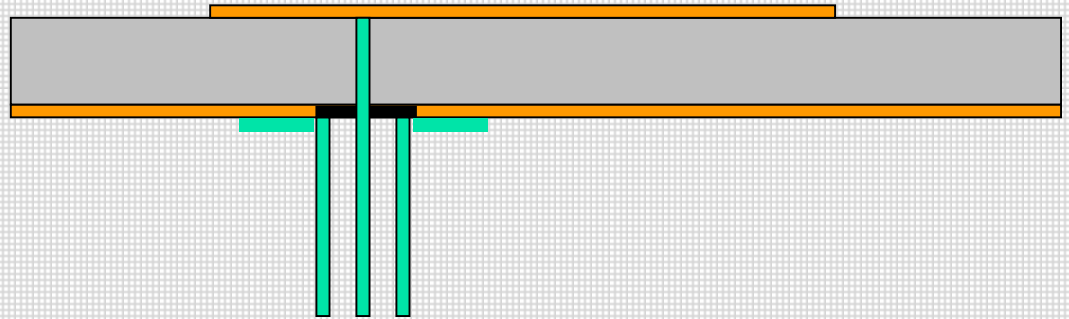
$$e_{12} = 1.47731 \times 10^{-7}$$

Feeding Methods

Coaxial Feed

Advantages:

- Simple
- Easy to obtain input match



$$R = R_{edge} \cos^2 \left(\frac{\pi x_0}{L} \right)$$

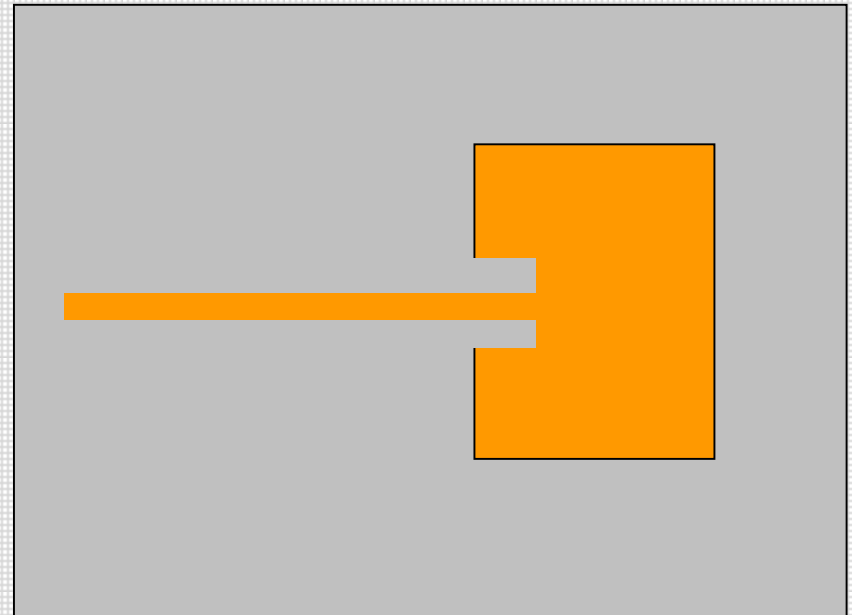
Disadvantages:

- Difficult to obtain input match for thicker substrates, due to probe inductance.
- Significant probe radiation for thicker substrates

Inset-Feed

Advantages:

- Simple
- Allows for planar feeding
- Easy to obtain input match

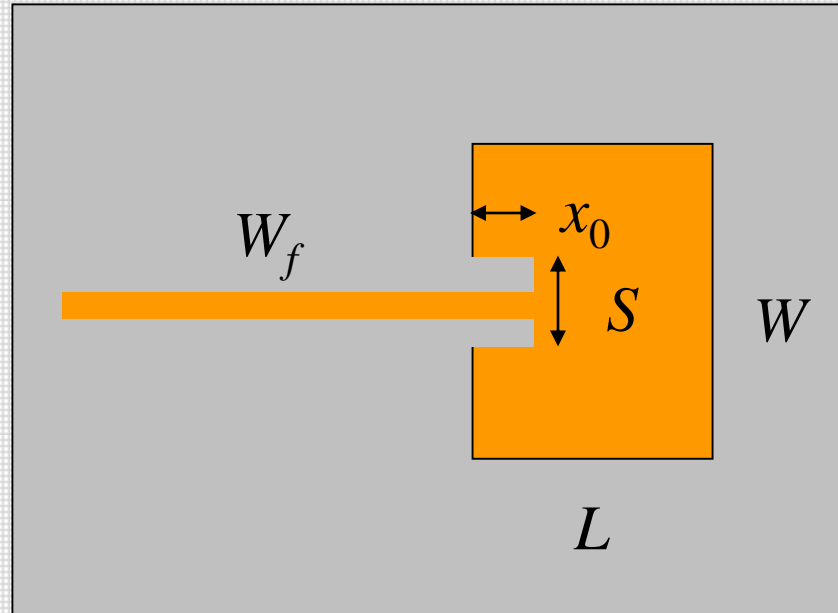


Disadvantages:

- Significant line radiation for thicker substrates
- For deep notches, pattern may show distortion.

Recent work has shown that the resonant input resistance varies as

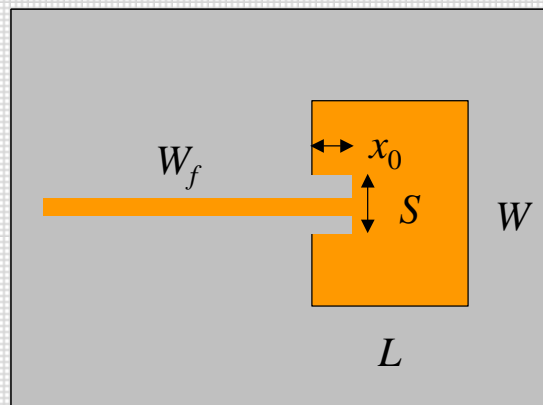
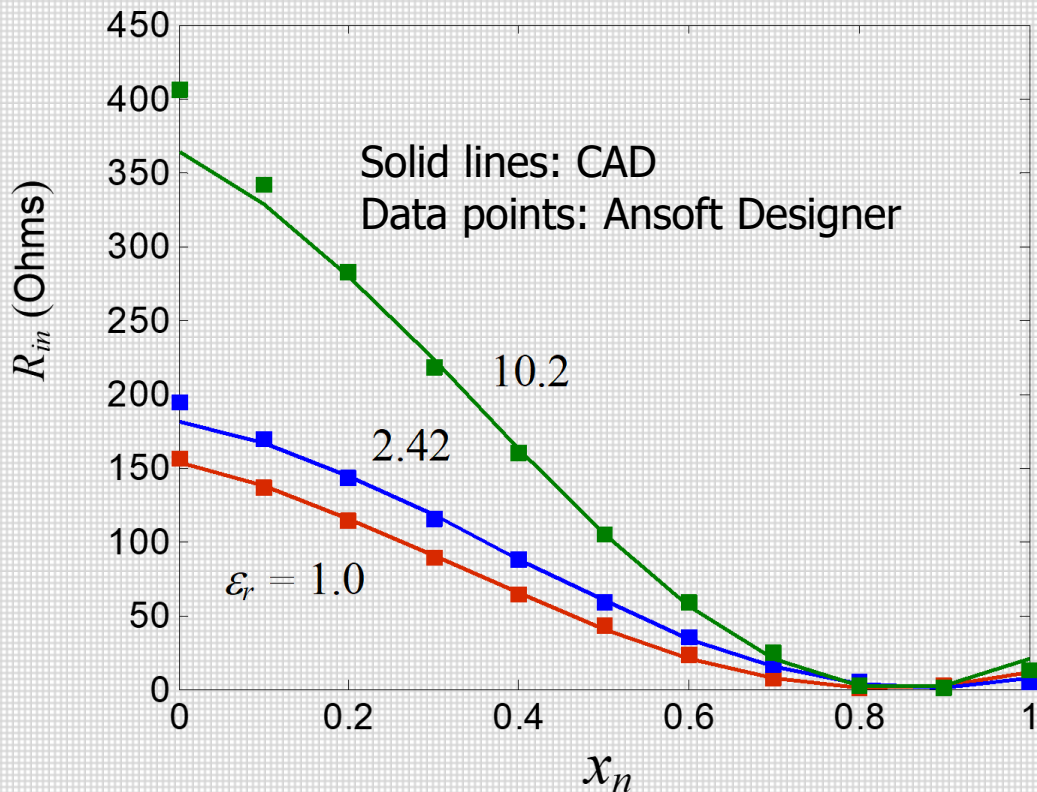
$$R_{in} = A \cos^2 \left(\frac{\pi}{2} \left(\frac{2x_0}{L} - B \right) \right)$$



The coefficients A and B depend on the notch width S but (to a good approximation) not on the line width W_f .

Y. Hu, D. R. Jackson, J. T. Williams, and S. A. Long, "Characterization of the Input Impedance of the Inset-Fed Rectangular Microstrip Antenna," *IEEE Trans. Antennas and Propagation*, Vol. 56, No. 10, pp. 3314-3318, Oct. 2008.

Results for a resonant patch fed on three different substrates.



$h = 0.254 \text{ cm}$
 $L / W = 1.5$
 $S / W_f = 3$

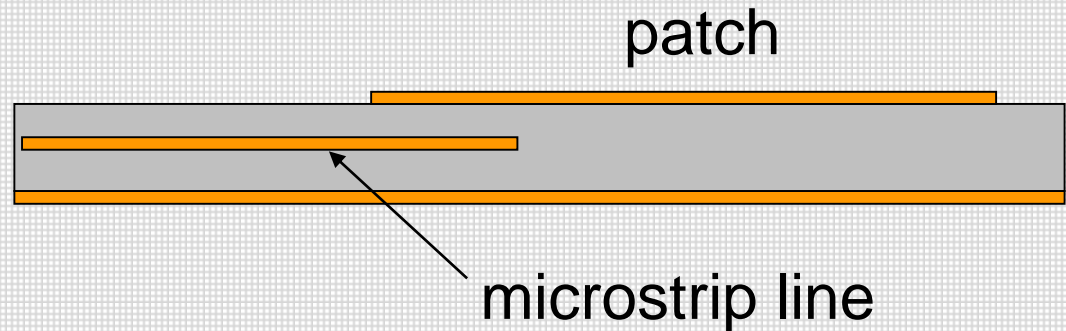
$$x_n = x_0 / (L/2)$$

$\epsilon_r = 1.00$ $W_f = 0.616 \text{ cm}$	$\epsilon_r = 2.42$ $W_f = 0.380 \text{ cm}$	$\epsilon_r = 10.2$ $W_f = 0.124 \text{ cm}$
---	---	---

Proximity (EMC) Coupling

Advantages:

- Allows for planar feeding
- Less line radiation compared to microstrip feed



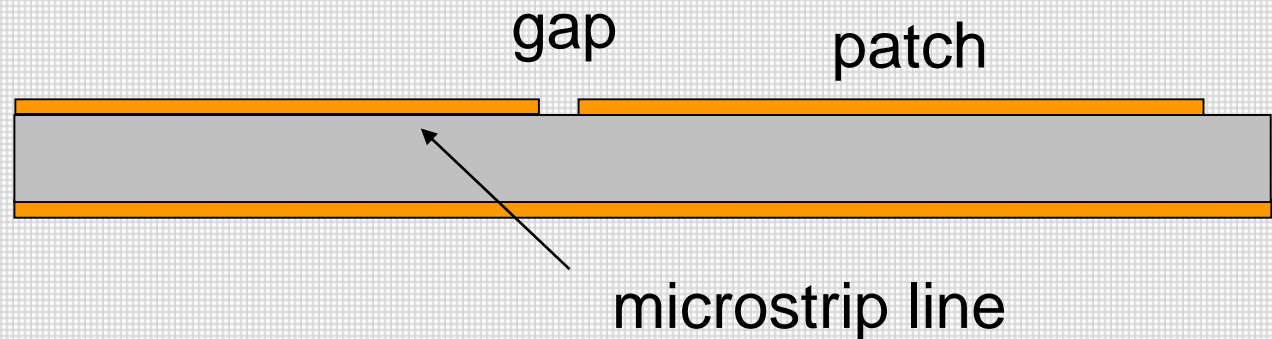
Disadvantages:

- Requires multilayer fabrication
- Alignment is important for input match

Gap Coupling

Advantages:

- Allows for planar feeding
- Can allow for a match with high edge impedances, where a notch might be too large



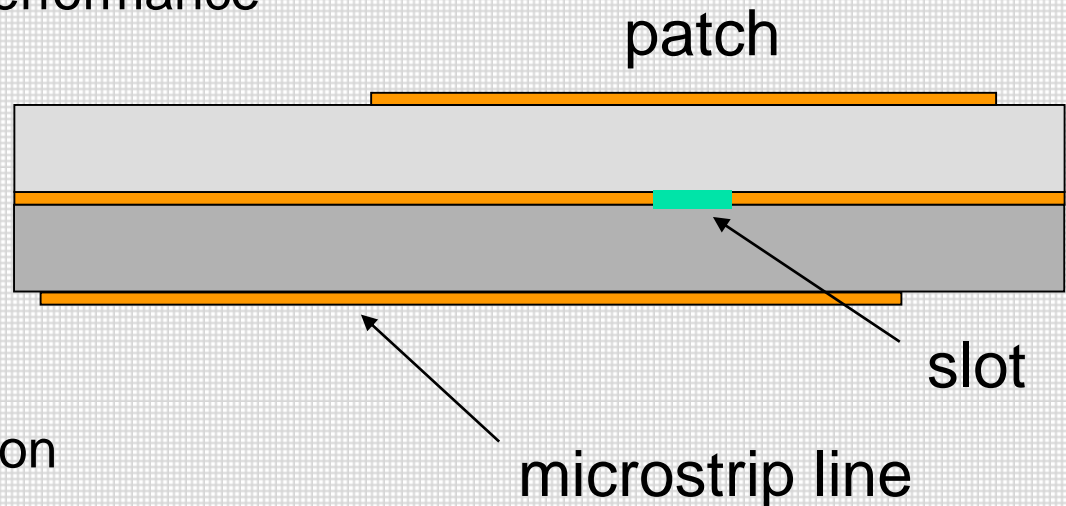
Disadvantages:

- Requires accurate gap fabrication
- Requires full-wave design

Aperture Coupled Patch (ACP)

Advantages:

- Allows for planar feeding
- Feed-line radiation is isolated from patch radiation
- Higher bandwidth, since probe inductance restriction is eliminated for the substrate thickness, and a double-resonance can be created.
- Allows for use of different substrates to optimize antenna and feed-circuit performance



Disadvantages:

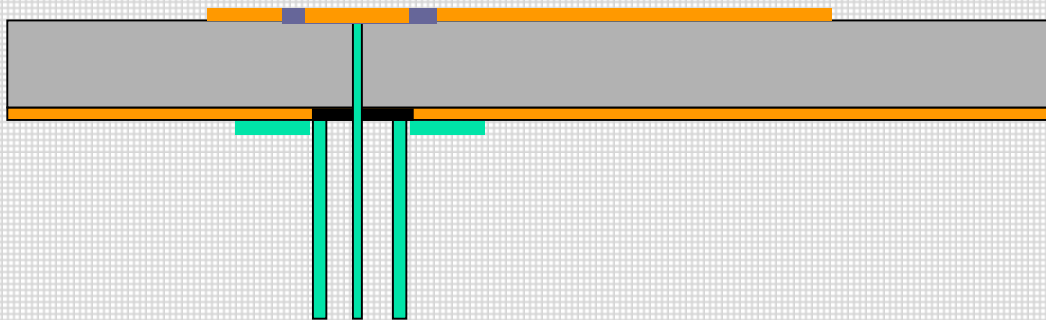
- Requires multilayer fabrication
- Alignment is important for input match

Improving Bandwidth: Probe Compensation

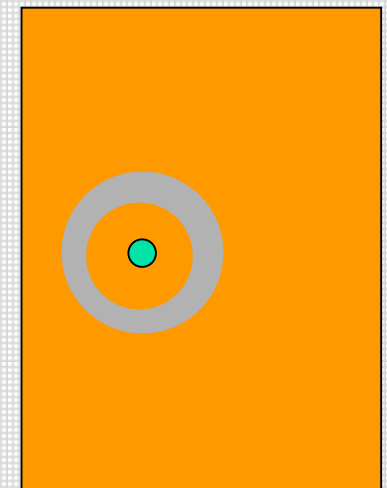
L-shaped probe:



Capacitive “top hat” on probe:



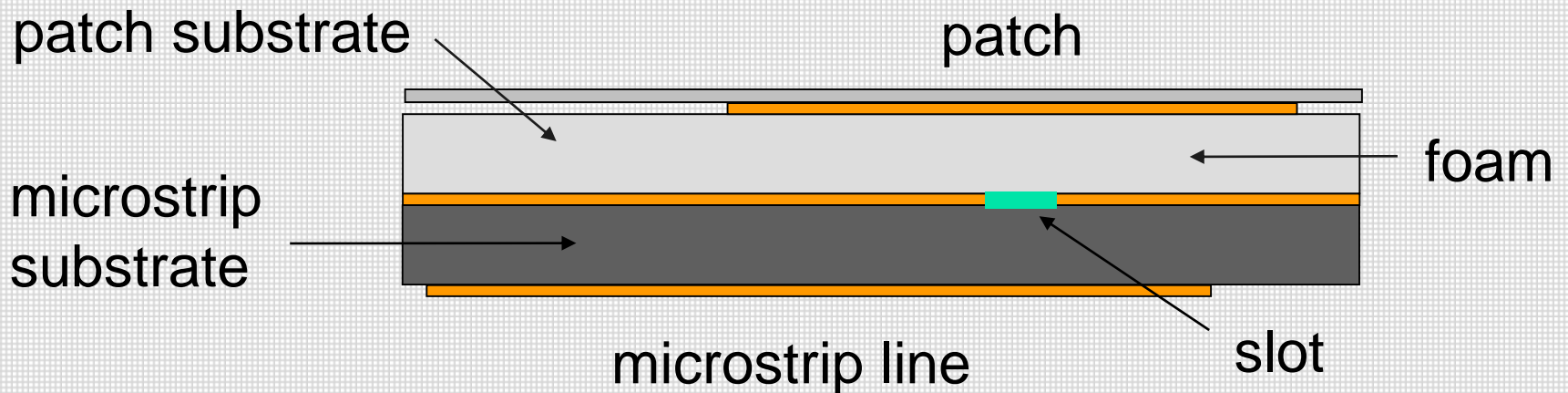
top view



SSFIP technology

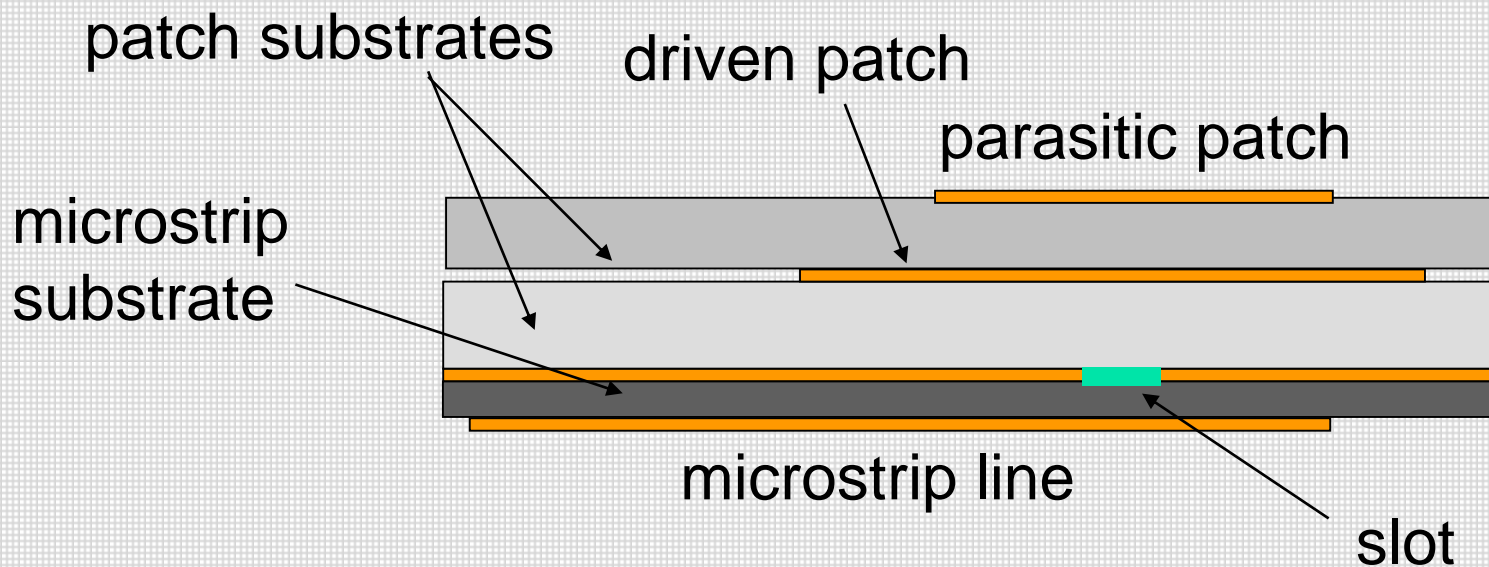
SSFIP: Strip Slot Foam Inverted Patch (a version of the ACP).

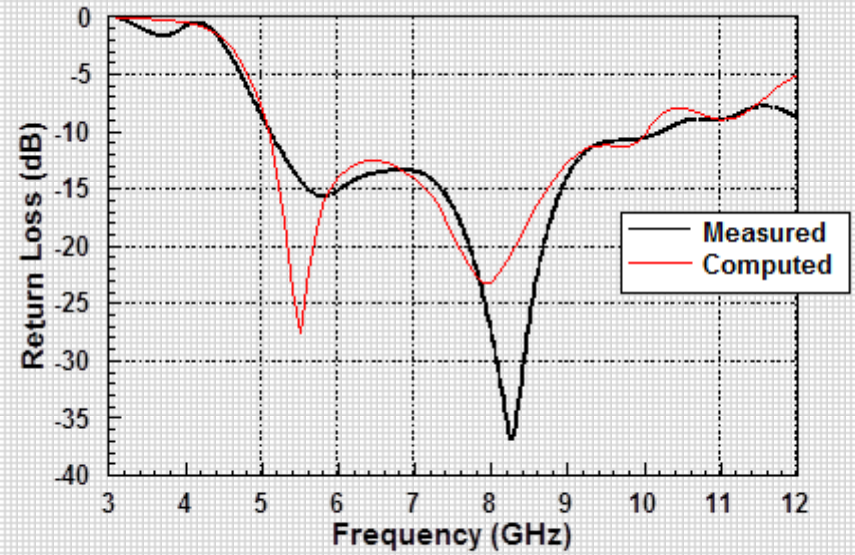
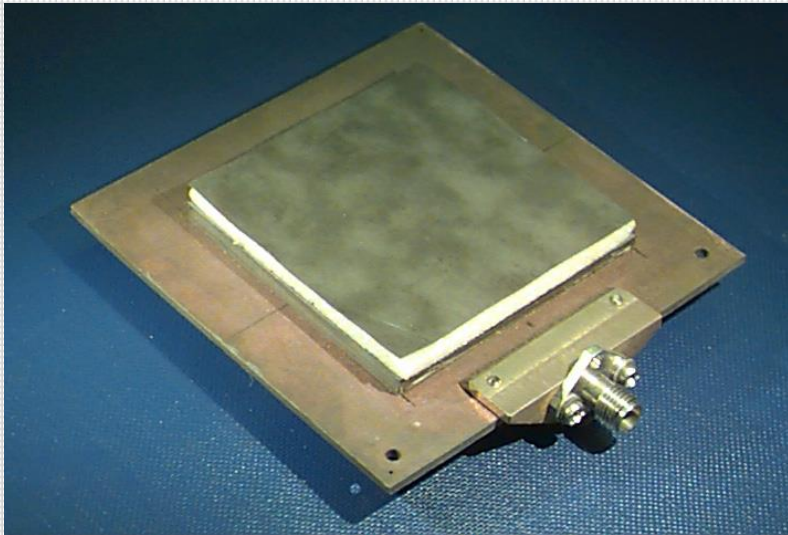
- Bandwidths greater than 25% have been achieved.
- Increased bandwidth is due to the thick foam substrate and also a dual-tuned resonance (patch+slot).



Stacked Patches

- Bandwidth increase is due to thick low-permittivity antenna substrates and a dual or triple-tuned resonance.
- Bandwidths of 25% have been achieved using a probe feed.
- Bandwidths of 100% have been achieved using an ACP feed.

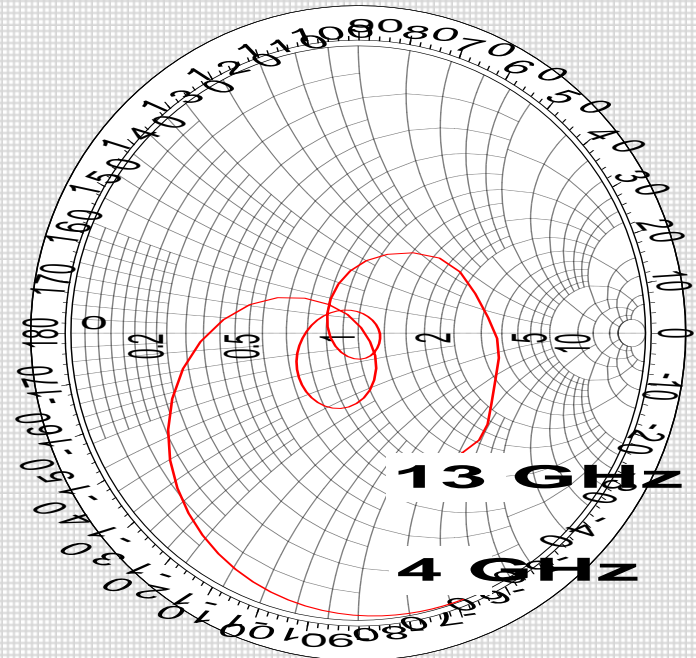




Stacked patch with ACP feed

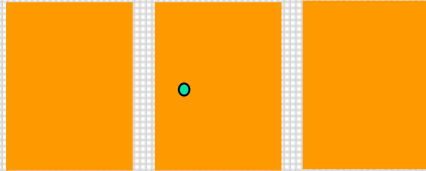
-10 dB S_{11} bandwidth is about 100%

Two extra loops are observed on the Smith chart.

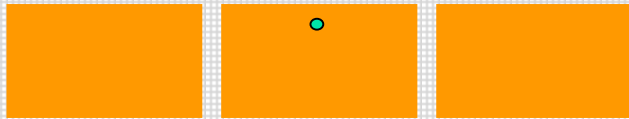


Parasitic Patches

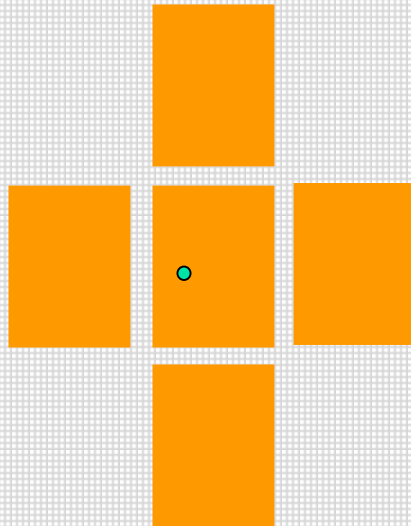
Most of this work was pioneered by K. C. Gupta.



Radiating Edges Gap Coupled
Microstrip Antennas
(REGCOMA).



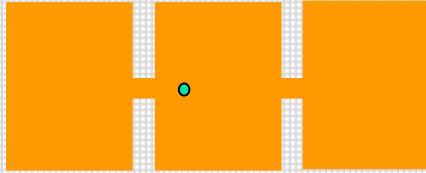
Non-Radiating Edges Gap
Coupled Microstrip Antennas
(NEGCOMA)



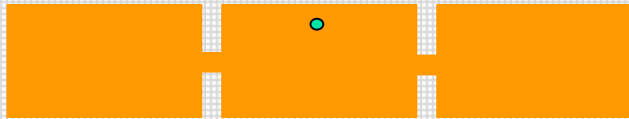
Four-Edges Gap Coupled
Microstrip Antennas
(FEGCOMA)

Bandwidth improvement factor:
REGCOMA: 3.0, NEGCOMA: 3.0, FEGCOMA: 5.0

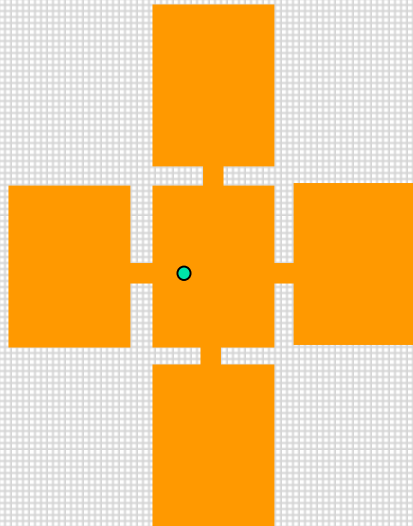
Direct-Coupled Patches



Radiating Edges Direct
Coupled Microstrip Antennas
(REDCOMA).



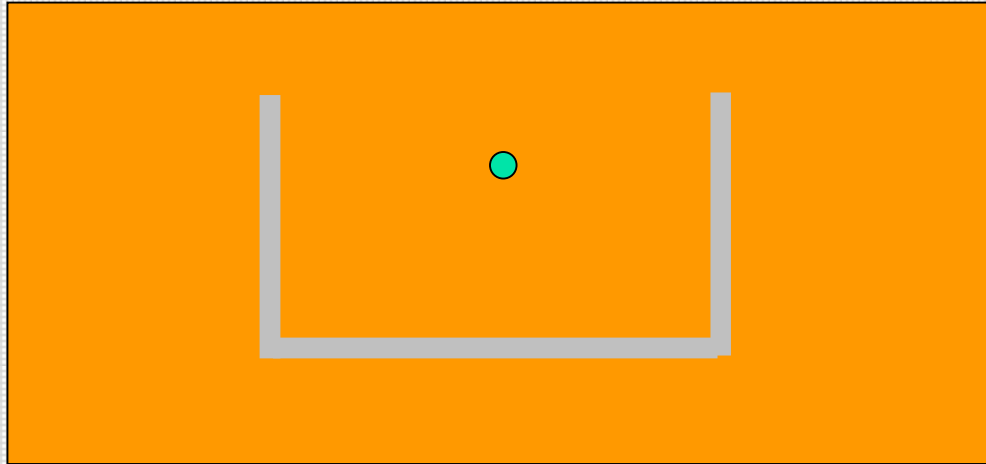
Non-Radiating Edges Direct
Coupled Microstrip Antennas
(NEDCOMA)



Four-Edges Direct Coupled
Microstrip Antennas
(FEDCOMA)

Bandwidth improvement factor:
REDCOMA: 5.0, NEDCOMA: 5.0, FEDCOMA: 7.0

U-shaped slot

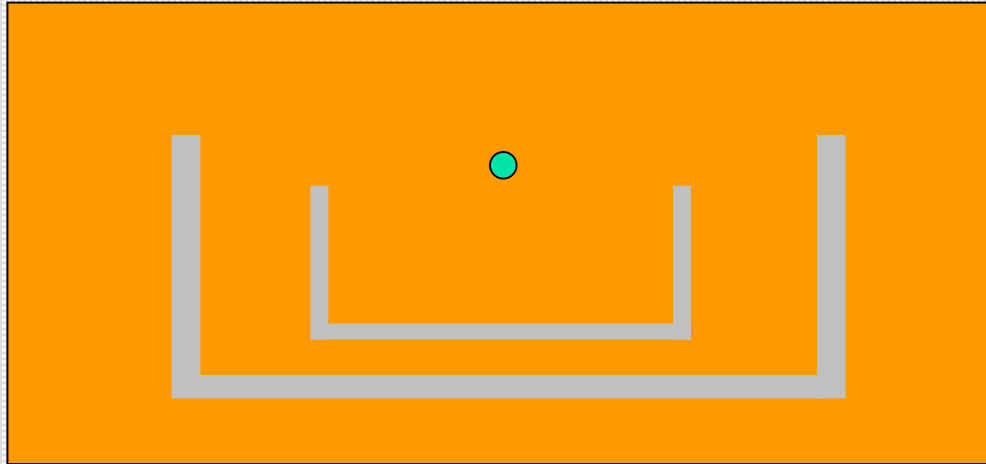


The introduction of a U-shaped slot can give a significant bandwidth (10%-40%).

(This is partly due to a double resonance effect.)

“Single Layer Single Patch Wideband Microstrip Antenna,” T. Huynh and K. F. Lee, Electronics Letters, Vol. 31, No. 16, pp. 1310-1312, 1986.

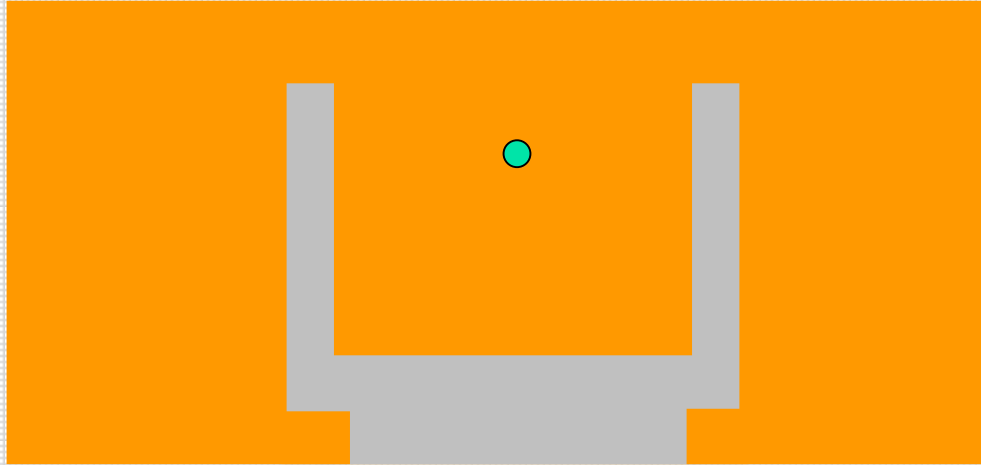
Double U-Slot



A 44% bandwidth was achieved.

“Double U-Slot Rectangular Patch Antenna,” Y. X. Guo, K. M. Luk, and Y. L. Chow, Electronics Letters, Vol. 34, No. 19, pp. 1805-1806, 1998.

E-Patch



A modification of the U-slot patch.

A bandwidth of 34% was achieved (40% using a capacitive “washer” to compensate for the probe inductance).

“A Novel E-shaped Broadband Microstrip Patch Antenna,” B. L. Ooi and Q. Shen, Microwave and Optical Technology Letters, Vol. 27, No. 5, pp. 348-352, 2000.

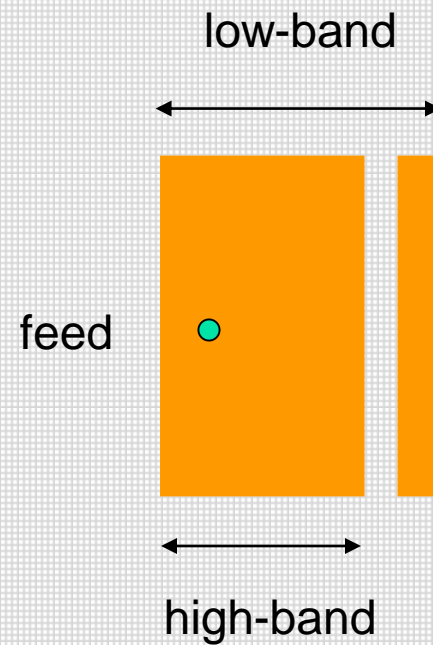
Multi-Band Antennas

A multi-band antenna is often more desirable than a broad-band antenna, if multiple narrow-band channels are to be covered.

General Principle:

Introduce multiple resonance paths into the antenna. (The same technique can be used to increase bandwidth via multiple resonances, if the resonances are closely spaced.)

Examples



Dual-Band E patch

Dual-Band Patch with Parasitic Strip

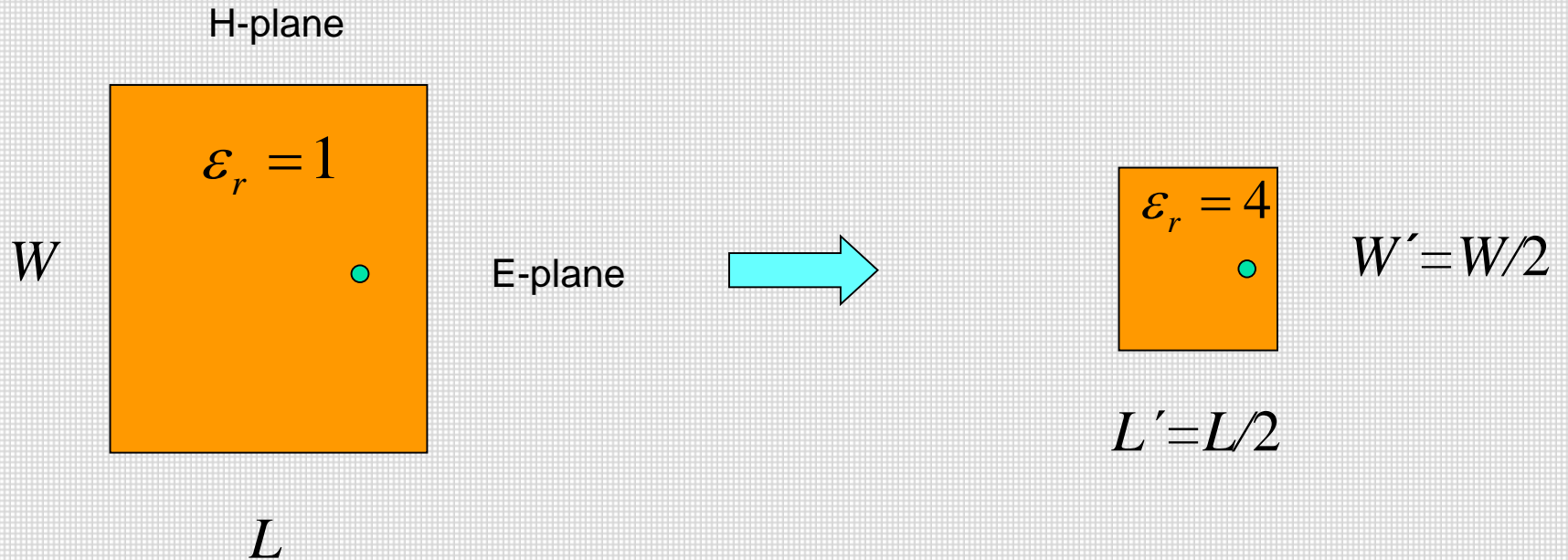
Miniaturization

- High Permittivity
- Quarter-Wave Patch
- planar inverted F antennas
- Capacitive Loading
- Slots
- Meandering

Note: Miniaturization usually comes at a price of reduced bandwidth.

General rule: The maximum obtainable bandwidth is proportional to the volume of the patch (based on the Chu limit.)

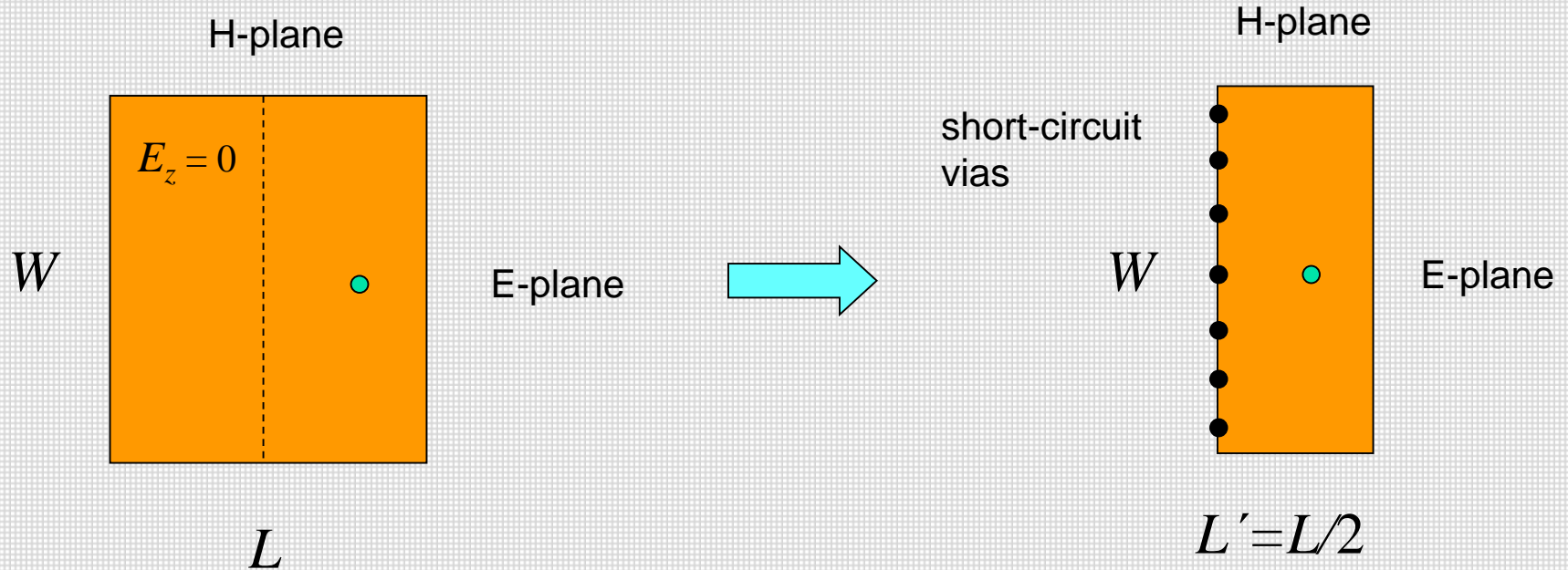
High Permittivity



It has about **one-fourth** the bandwidth of the regular patch.

(Bandwidth is inversely proportional to the permittivity.)

Quarter-Wave Patch

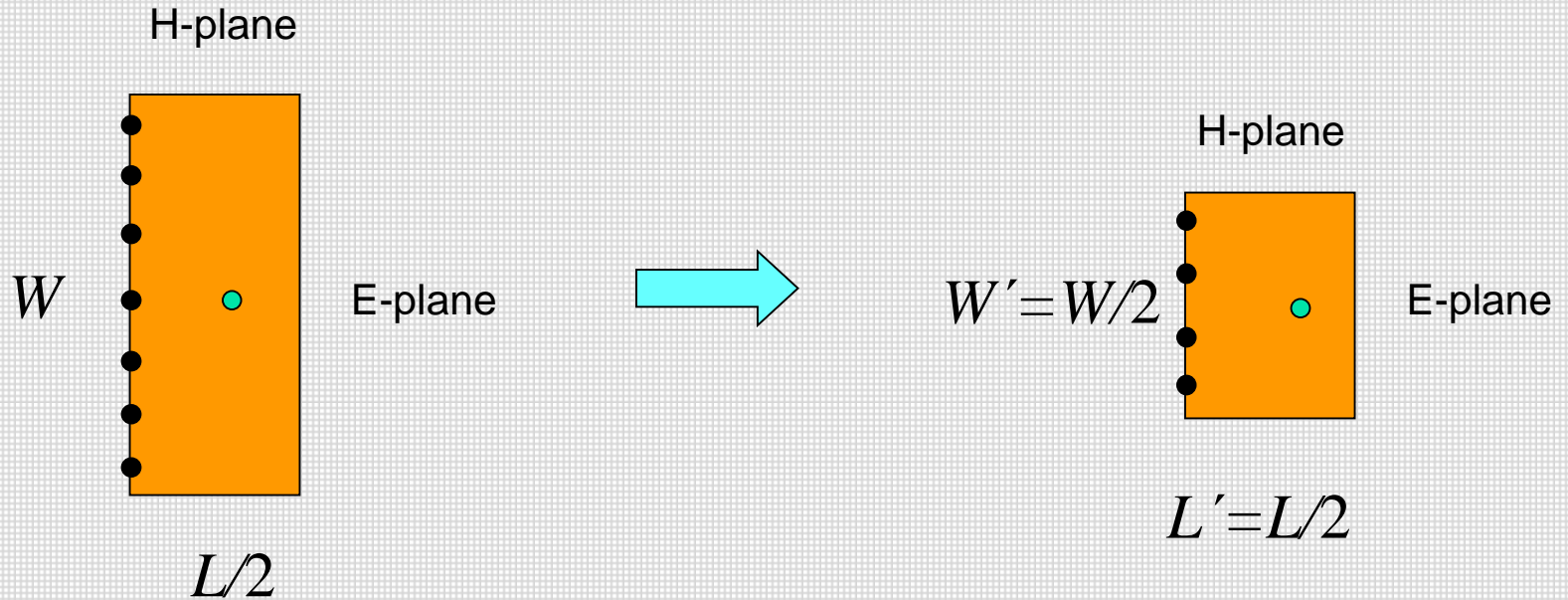


It has about **one-half** the bandwidth of the regular patch.

Neglecting losses:

$$Q = \omega_0 \frac{U_s}{P_r} \quad \left. \begin{array}{l} U_s \rightarrow U_s / 2 \\ P_r \rightarrow P_r / 4 \end{array} \right\} \Rightarrow Q \rightarrow 2Q$$

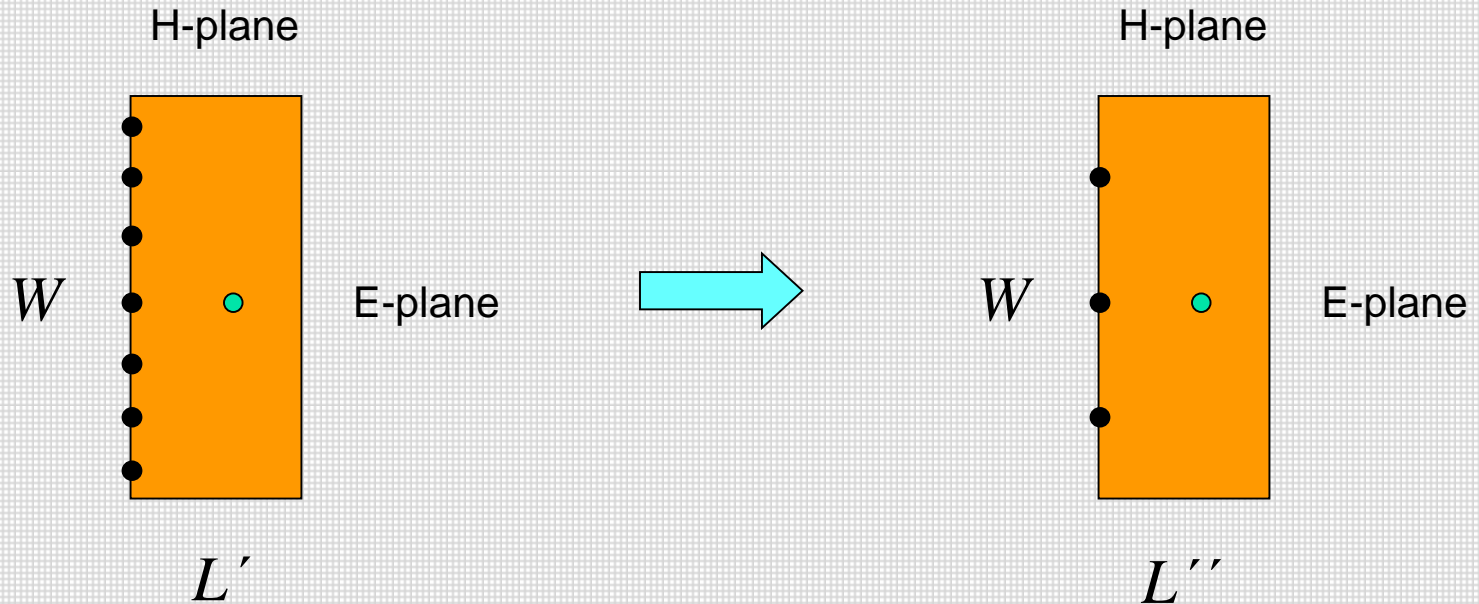
Smaller Quarter-Wave Patch



It has about **one-fourth** the bandwidth of the regular patch.

(Bandwidth is proportional to the patch width.)

Quarter-Wave Patch with Fewer Vias

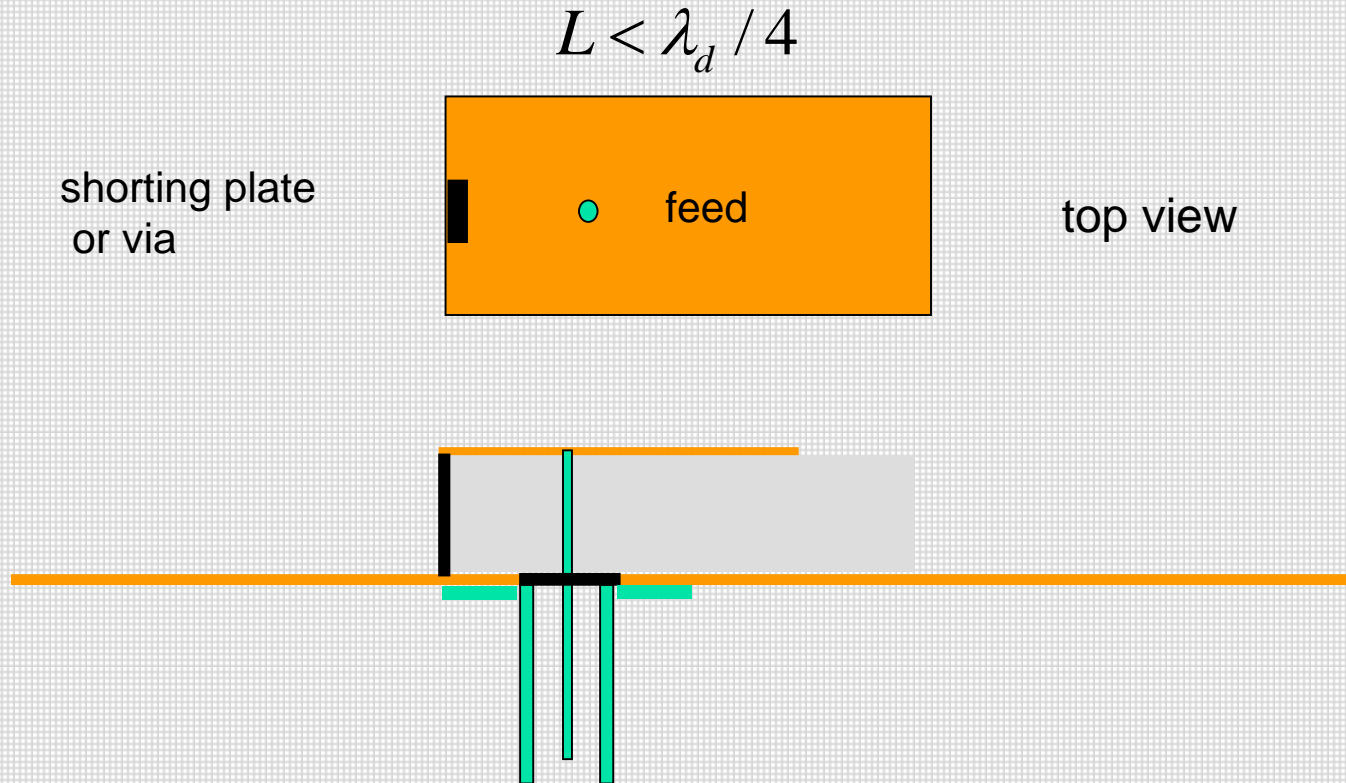


$$L'' < L'$$

Fewer vias actually gives more miniaturization!

(The edge has a larger inductive impedance.)

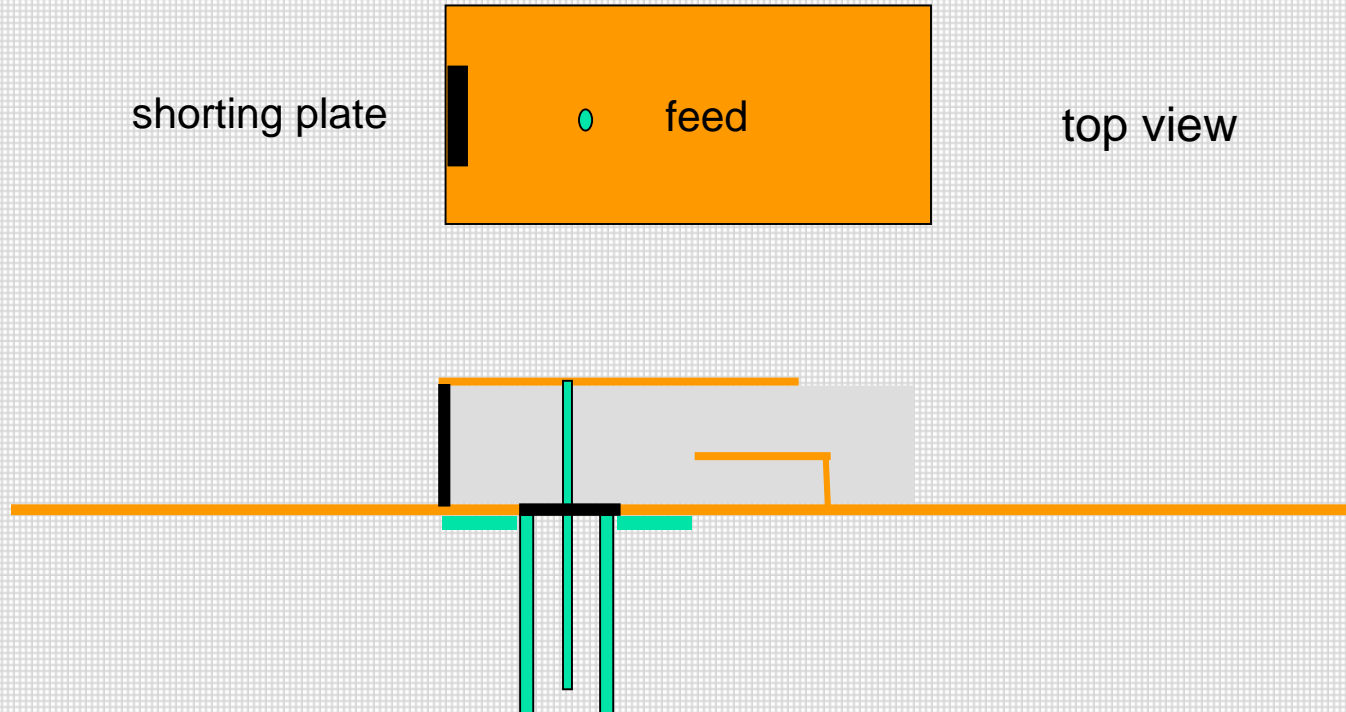
Planar Inverted F Antenna (PIFA)



A single shorting plate or via is used.

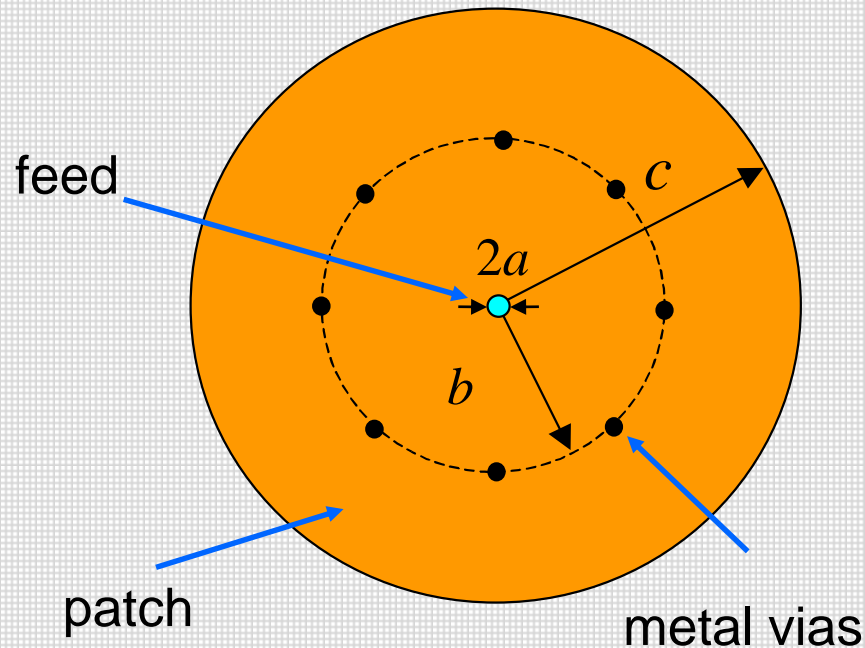
This antenna can be viewed as a limiting case of the quarter-wave patch, or as an LC resonator.

PIFA with Capacitive Loading



The capacitive loading allows for the length of the PIFA to be reduced.

Circular Patch Loaded with Vias

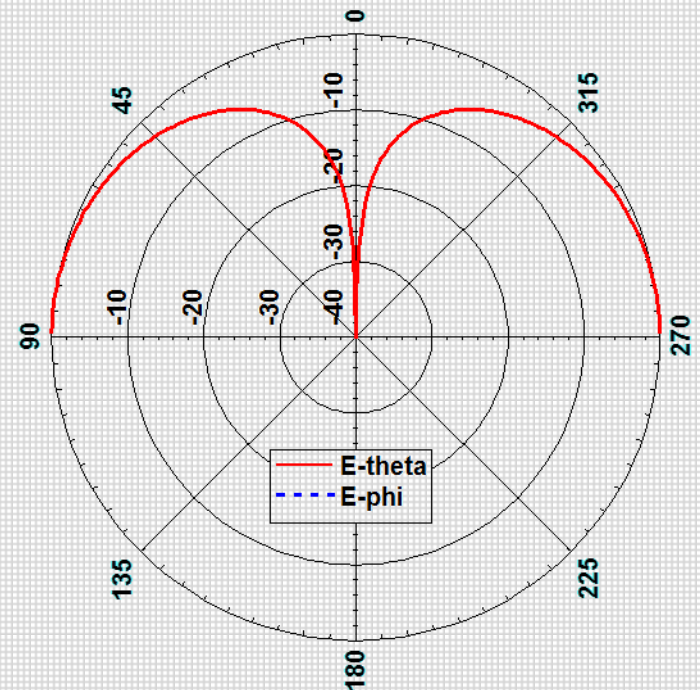
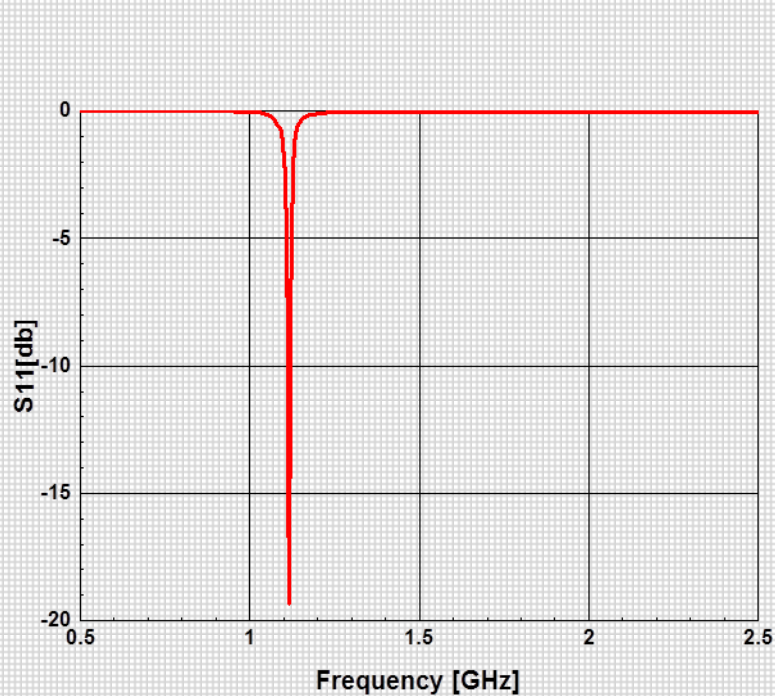


The patch has a monopole-like pattern

The patch operates in the $(0,0)$ mode, as an LC resonator

(Hao Xu Ph.D. dissertation, UH, 2006)

Circular Patch Loaded with 2 Vias

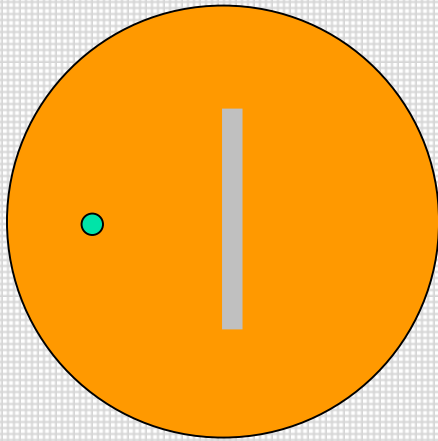


Unloaded: Resonance frequency = 5.32 GHz.

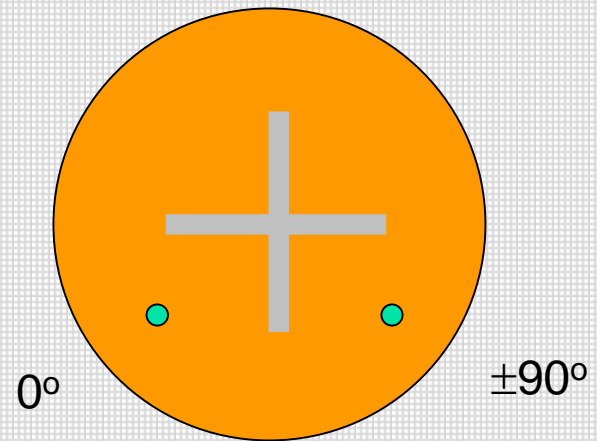
(miniaturization factor = 4.8)

Slotted Patch

Top view



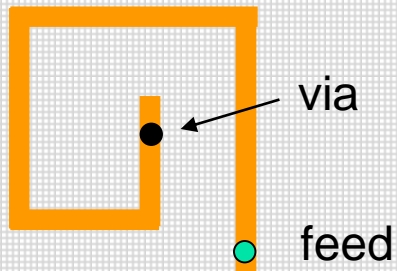
linear



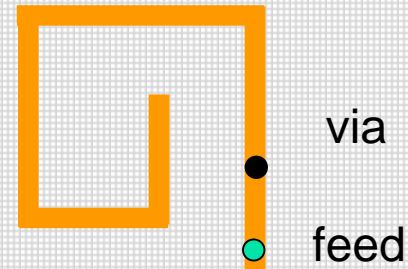
CP

The slot forces the current to flow through a longer path, increasing the effective dimensions of the patch.

Meandering



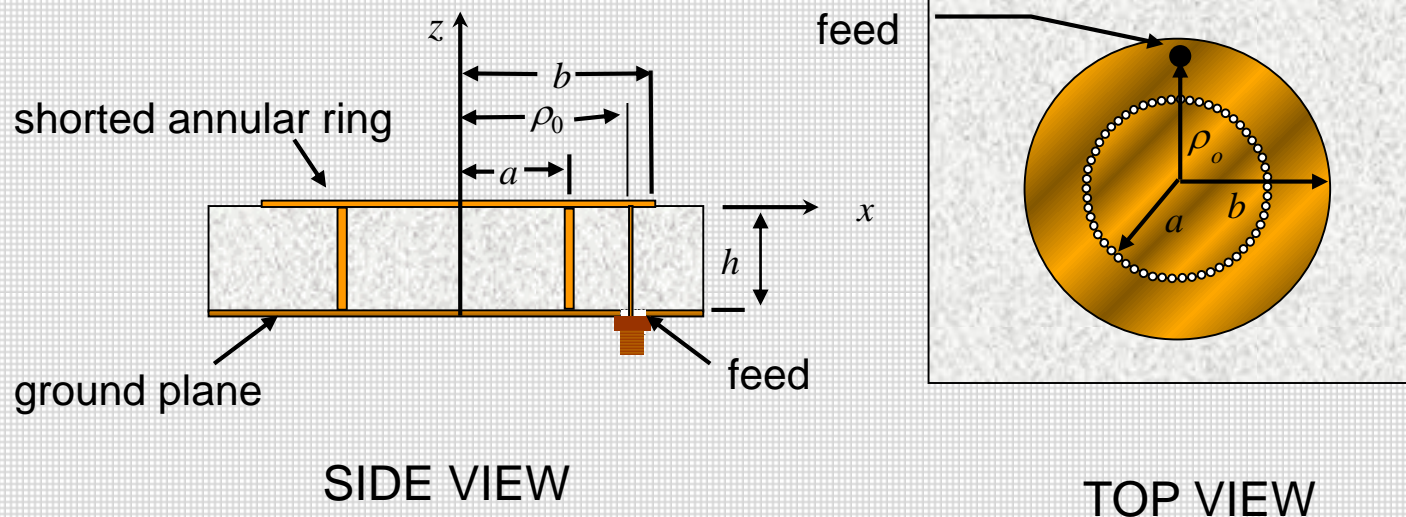
Meandered quarter-wave patch



Meandered PIFA
(Planar Inverted-F (type) Antenna)

Meandering forces the current to flow through a longer path, increasing the effective dimensions of the patch.

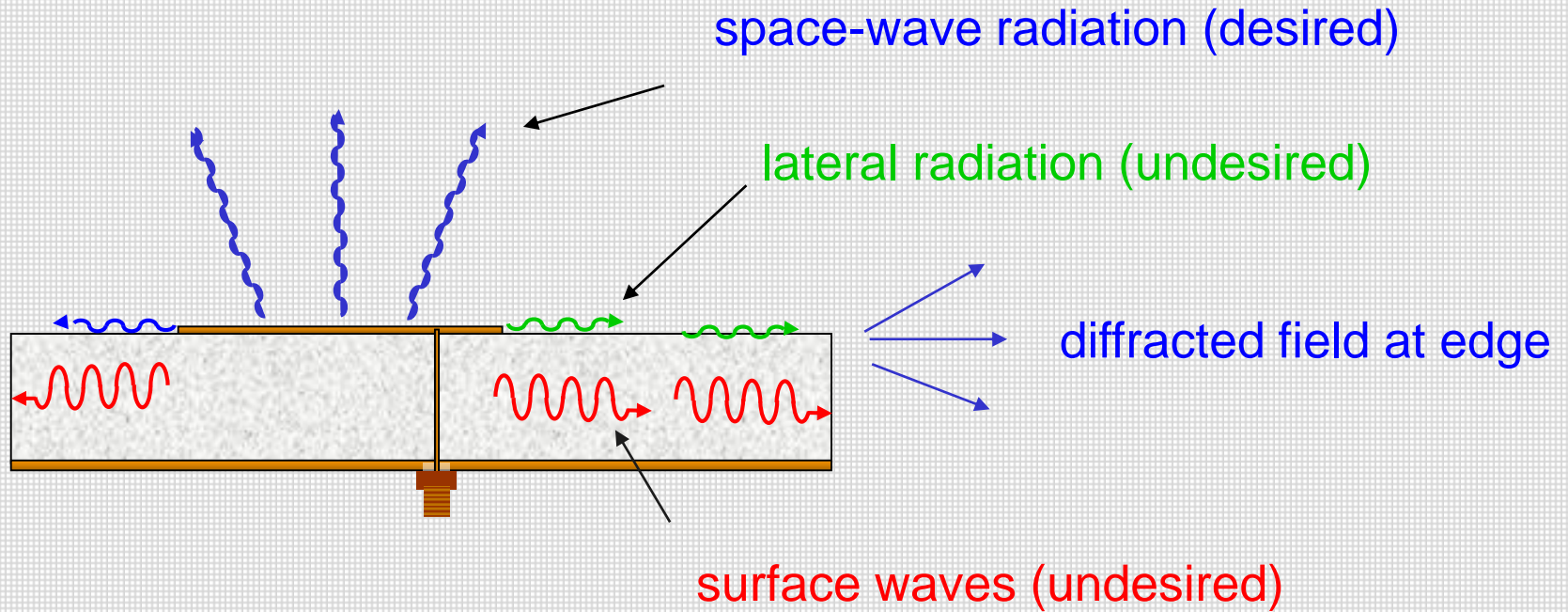
Reducing Surface-Wave Excitation and Lateral Radiation



Reduced Surface Wave (RSW) Antenna

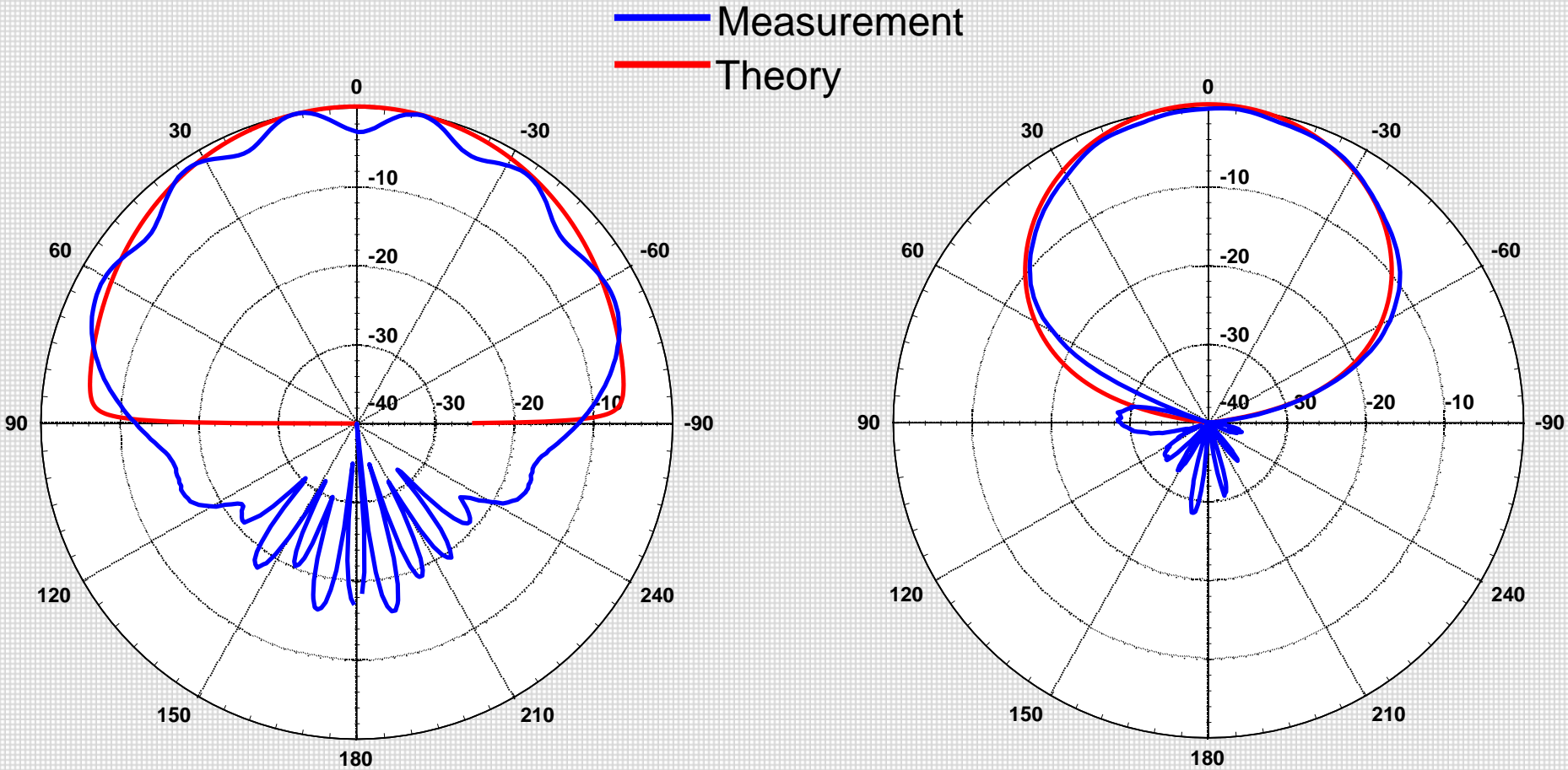
D. R. Jackson, J. T. Williams, A. K. Bhattacharyya, R. Smith, S. J. Buchheit, and S. A. Long, "Microstrip Patch Designs that do Not Excite Surface Waves," IEEE Trans. Antennas Propagat., vol. 41, No 8, pp. 1026-1037, August 1993.

Reducing surface-wave (RSW) excitation and lateral radiation reduces edge diffraction



E-plane Radiation Patterns

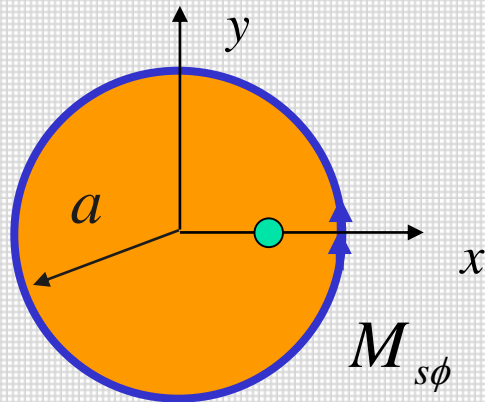
Measurements were taken on a 1 m diameter circular ground plane at 1.575 GHz.



conventional

RSW

Principle of surface waves reducing



TM₁₁ mode:

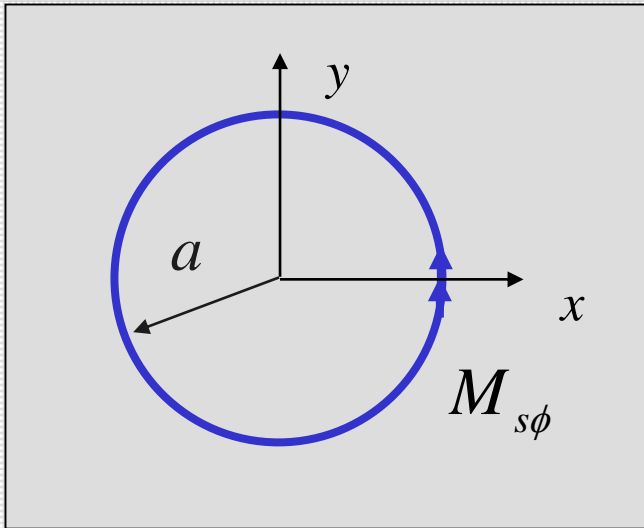
$$E_z(\rho, \phi) = V_0 \left(\frac{-1}{hJ_1(ka)} \right) \cos \phi J_1(k\rho)$$

At edge: $E_z = -\frac{V_0}{h} \cos \phi$

$$\underline{M}_s = -\underline{\hat{n}} \times \underline{E} = -\underline{\hat{\rho}} \times (\underline{\hat{z}} E_z)$$

$$M_{s\phi}(\phi) = E_z(a, \phi)$$

$$M_{s\phi} = -\frac{V_0}{h} \cos \phi$$



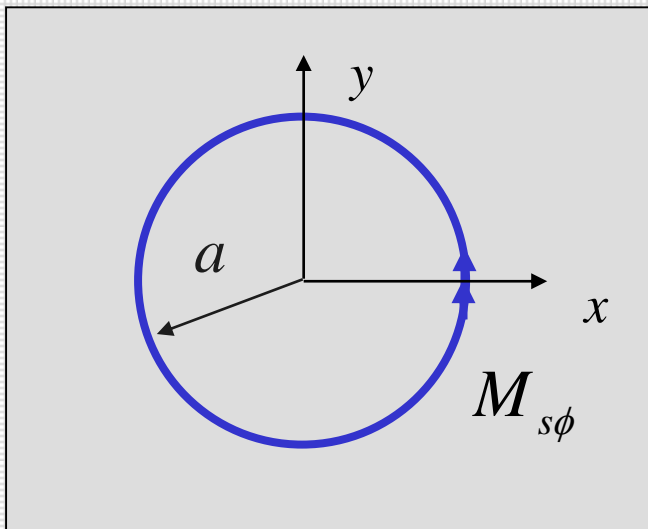
$$M_{s\phi} = -\frac{V_0}{h} \cos \phi$$

Surface-Wave Excitation: $E_z^{TM_0} = A_{TM_0} \cos \phi H_1^{(2)}(\beta_{TM_0} \rho) e^{-jk_{z0}z}$

$(z > h)$

$$A_{TM_0} = AJ_1'(\beta_{TM_0} a)$$

Set $J_1'(\beta_{TM_0} a) = 0$



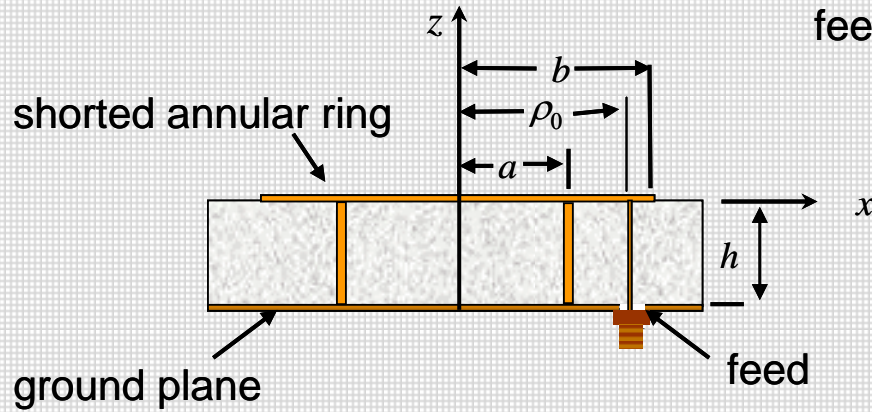
$$\beta_{TM_0} a = x'_{1n}$$

For TM_{11} mode: $x'_{11} \approx 1.842$

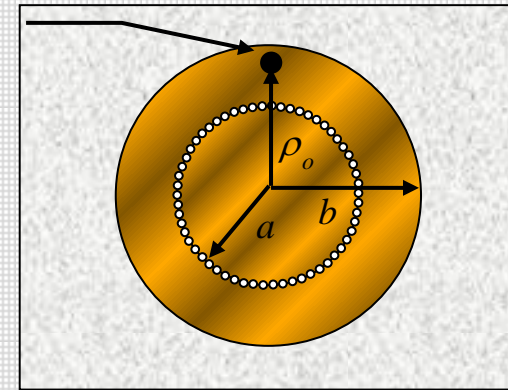
$$\beta_{TM_0} a = 1.842$$

Patch resonance: $k_1 a = 1.842$

Note: $\beta_{TM_0} < k_1$ (The RSW patch is too big to be resonant.)



SIDE VIEW



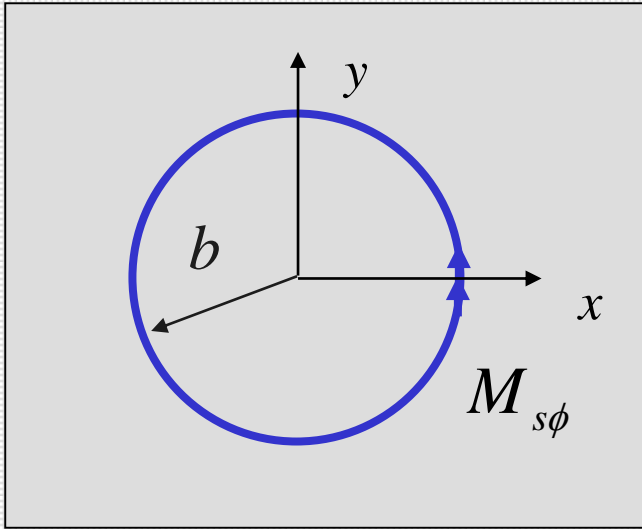
TOP VIEW

$$\beta_{TM_0} b = 1.842$$

The radius a is chosen to make the patch resonant:

$$\frac{J_1(k_1 a)}{Y_1(k_1 a)} = \frac{J_1' \left(\frac{k_1 x'_{11}}{k_{TM_0}} \right)}{Y_1' \left(\frac{k_1 x'_{11}}{k_{TM_0}} \right)}$$

Reducing Lateral Wave



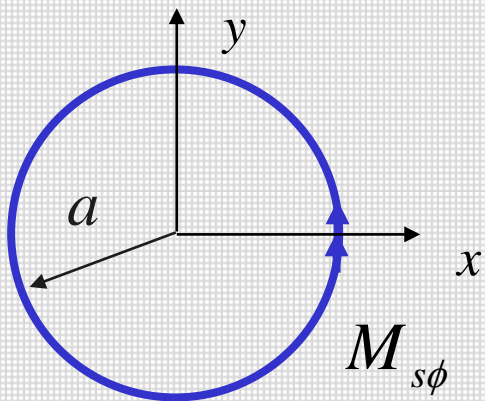
$$M_{s\phi} = -\frac{V_0}{h} \cos \phi$$

Lateral-Wave Field: $E_z^{LW} = A_{LW} \cos \phi \left(\frac{1}{\rho^2} \right) e^{-jk_0\rho}$ ($z = h$)

$$A_{LW} = BJ'_1(k_0b)$$

Set $J'_1(k_0b) = 0$

Reducing Space Wave



$$M_{s\phi} = -\frac{V_0}{h} \cos \phi$$

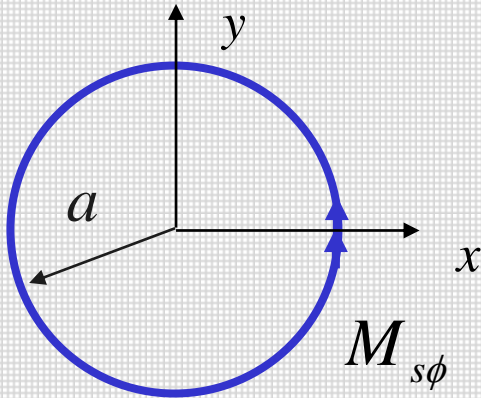
Assume no substrate outside of patch:

Space-Wave Field: $E_z^{SP} = A_{SP} \cos \phi \left(\frac{1}{\rho} \right) e^{-jk_0 \rho}$ ($z = h$)

$$A_{SP} = C J_1'(k_0 b)$$

Set $J_1'(k_0 b) = 0$

Thin Substrate Result



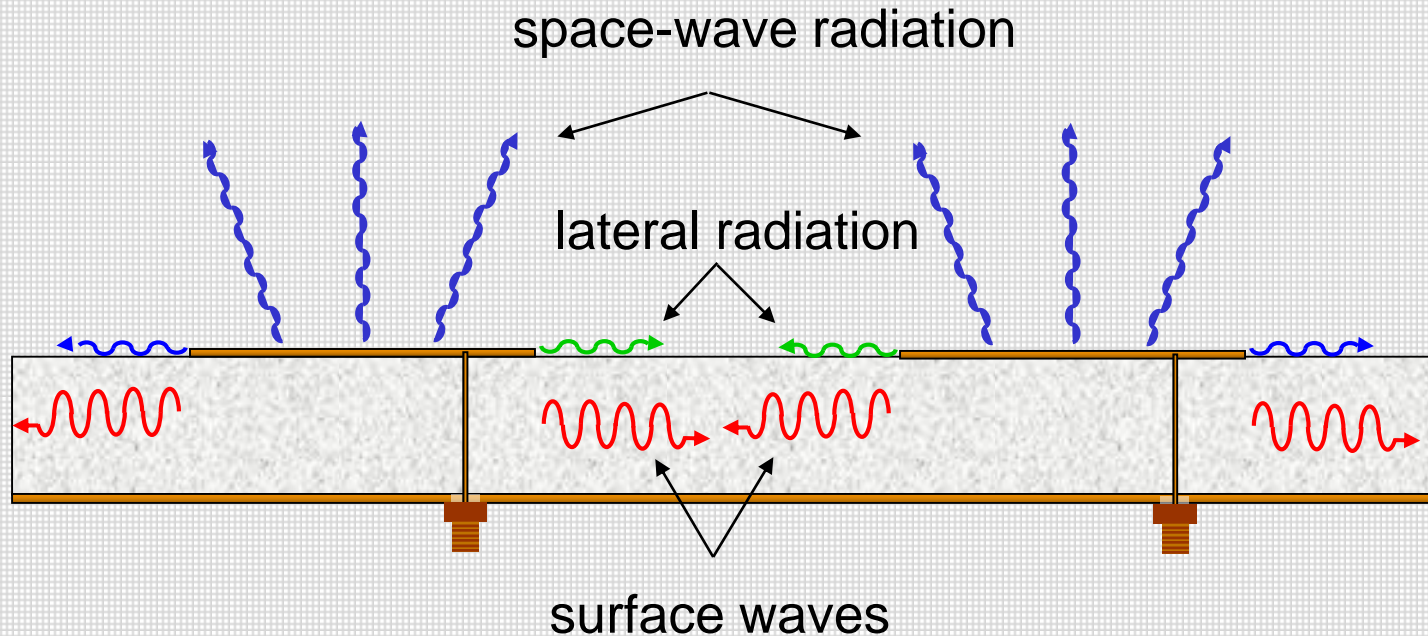
For a thin substrate:

$$\beta_{TM_0} \approx k_0$$

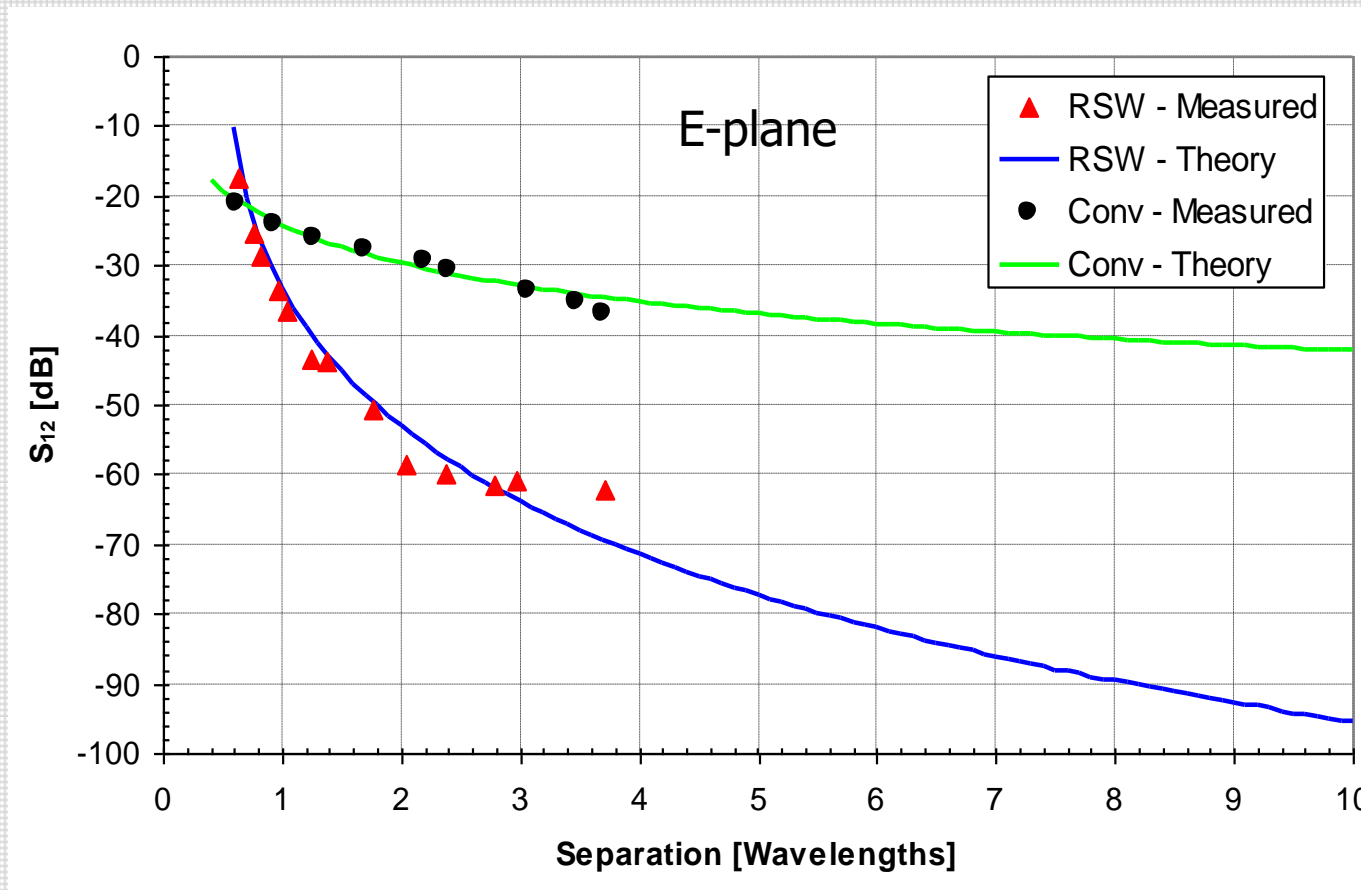
The same design reduces both surface-wave and lateral-wave fields (or space-wave field if there is no substrate outside of the patch).

Mutual Coupling

Reducing surface-wave excitation and lateral radiation reduces **mutual coupling**.



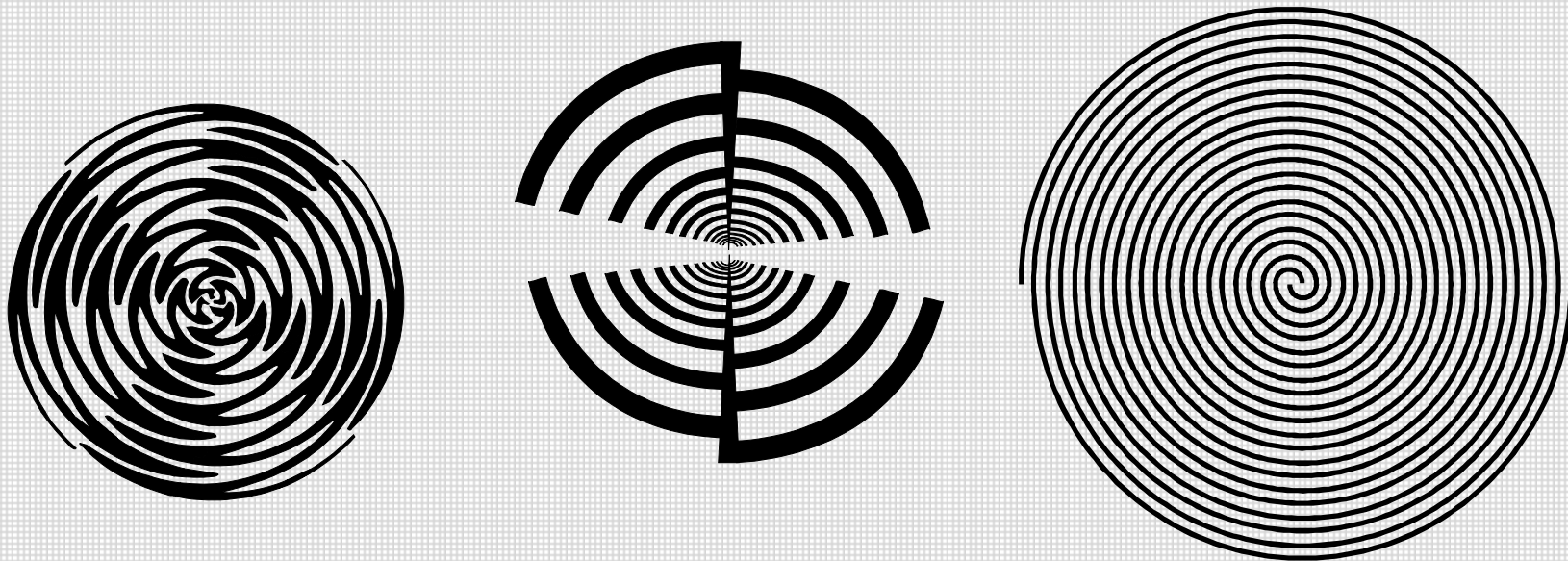
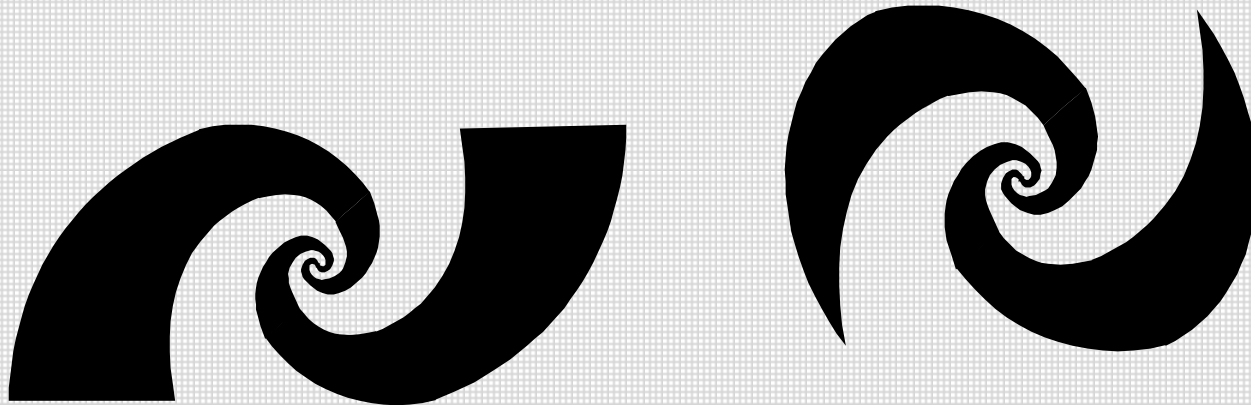
Reducing surface-wave excitation and lateral radiation reduces mutual coupling.



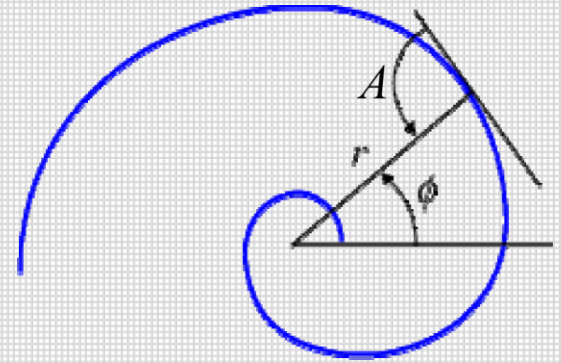
“Mutual Coupling Between Reduced Surface-Wave Microstrip Antennas,” M. A. Khayat, J. T. Williams, D. R. Jackson, and S. A. Long, IEEE Trans. Antennas and Propagation, Vol. 48, pp. 1581-1593, Oct. 2000.

Spiral antennas

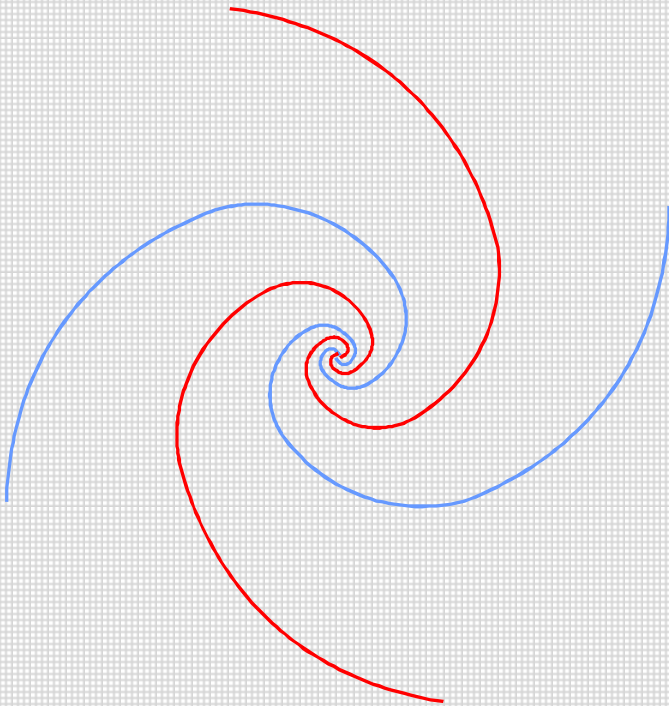
Frequency independent antennas



$$r(\phi) = ke^{\alpha\phi} \quad L = \int_{r_0}^r \sqrt{r^2 \left(\frac{d\phi}{dr} \right)^2 + 1} \, dr$$



$$A = \frac{1}{\operatorname{tg} \alpha}$$

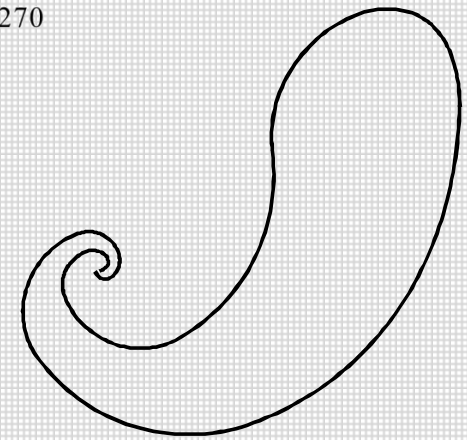
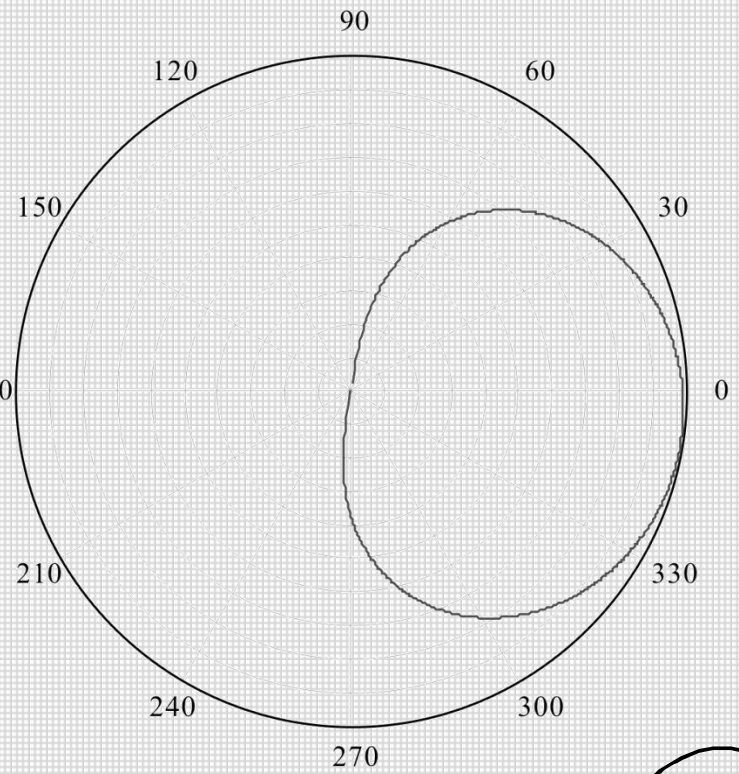
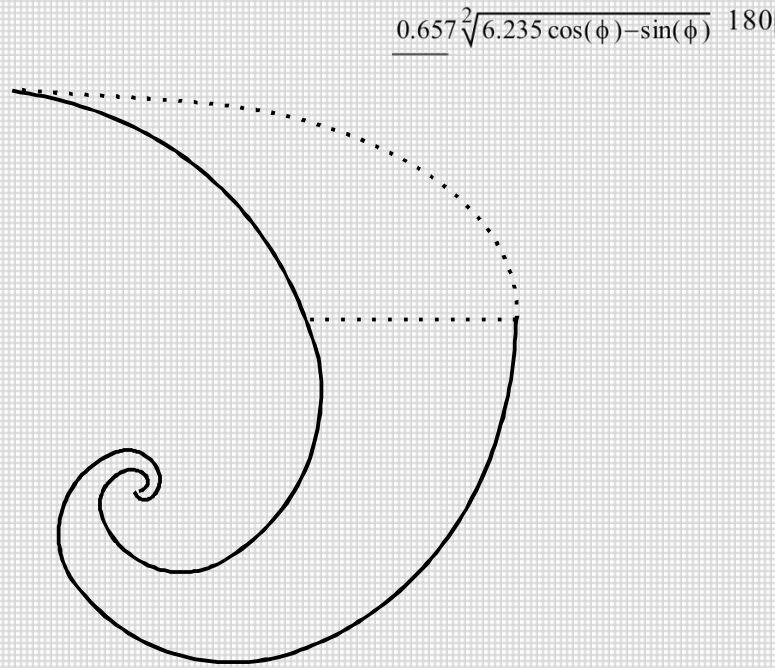


$$r_1(\phi) = ke^{\alpha\phi} \quad r_2(\phi) = ke^{\alpha(\phi-\delta)}$$

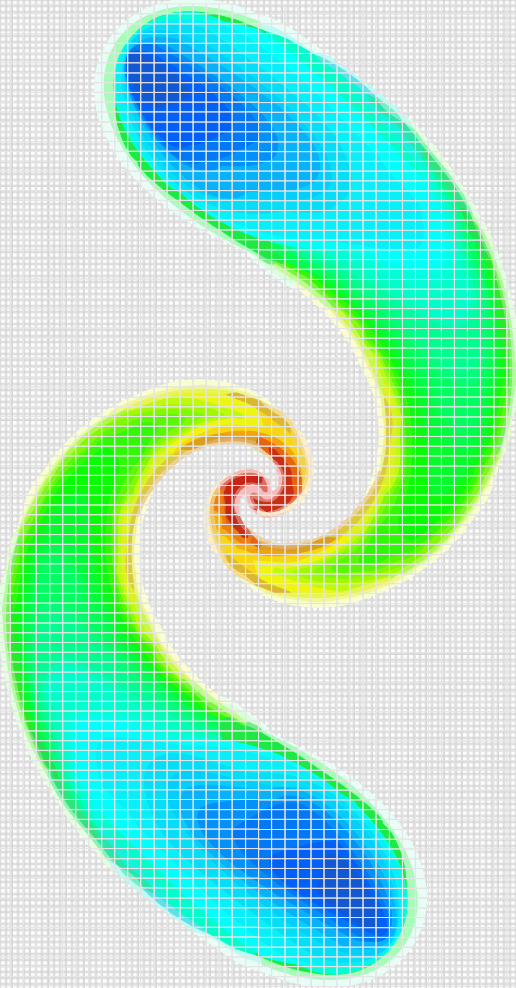
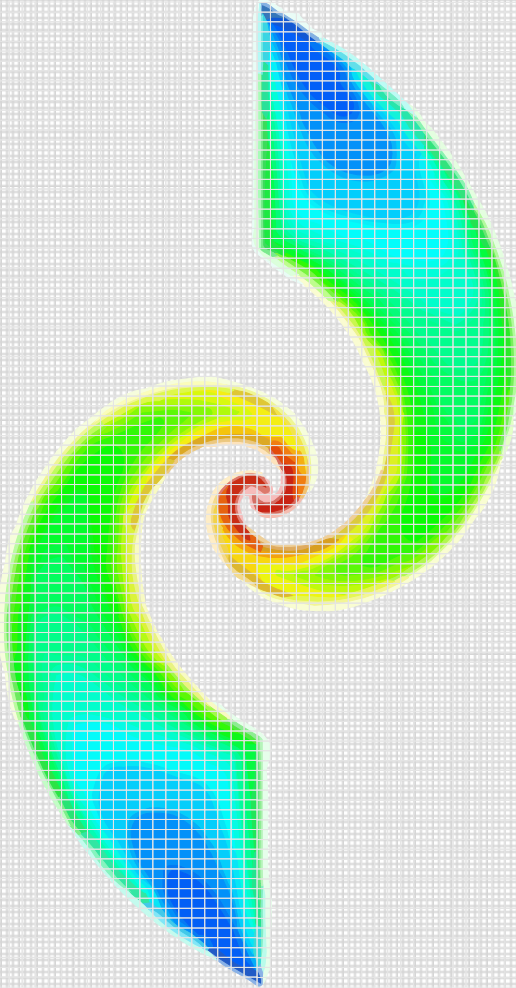
$$r_3(\phi) = ke^{\alpha(\phi-\pi)} \quad r_4(\phi) = ke^{\alpha(\phi-\pi-\delta)}$$

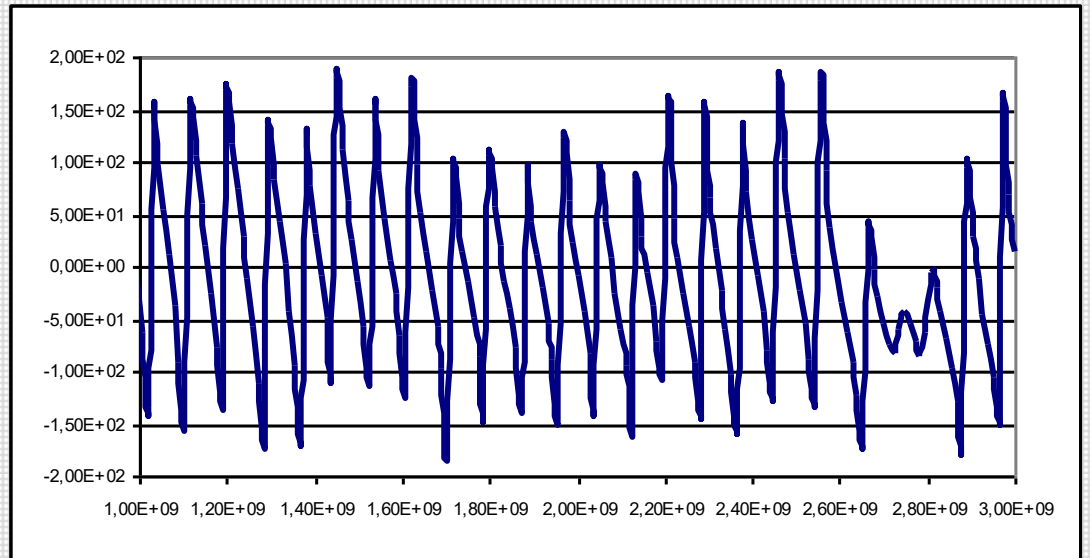
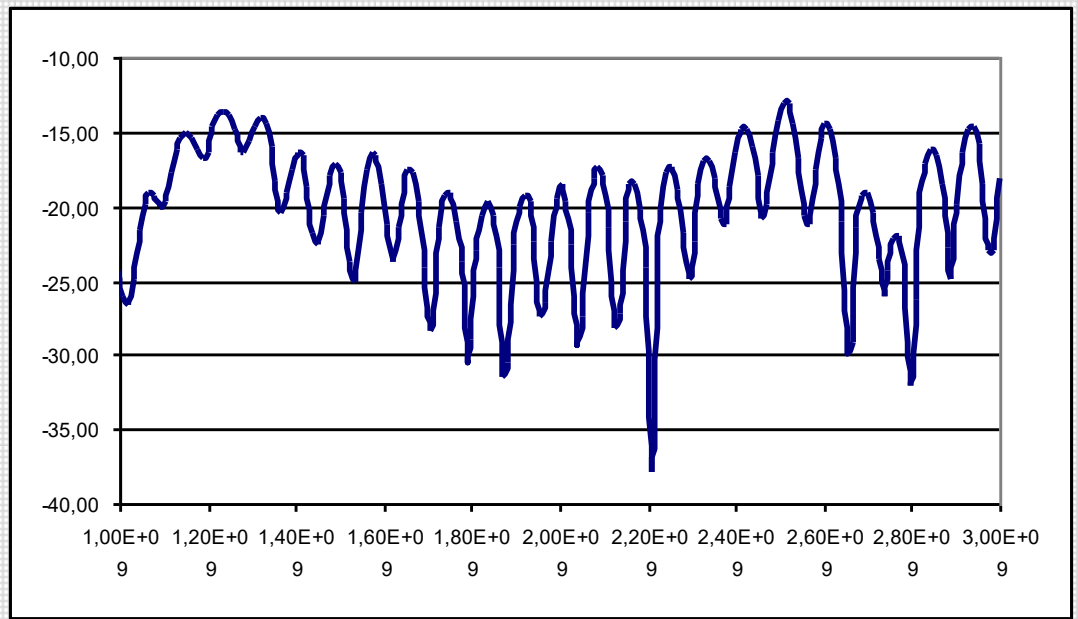
$$\frac{r_2}{r_1} < 1 \quad \frac{r_4}{r_3} < 1 \quad \langle 0,37;0,97 \rangle$$

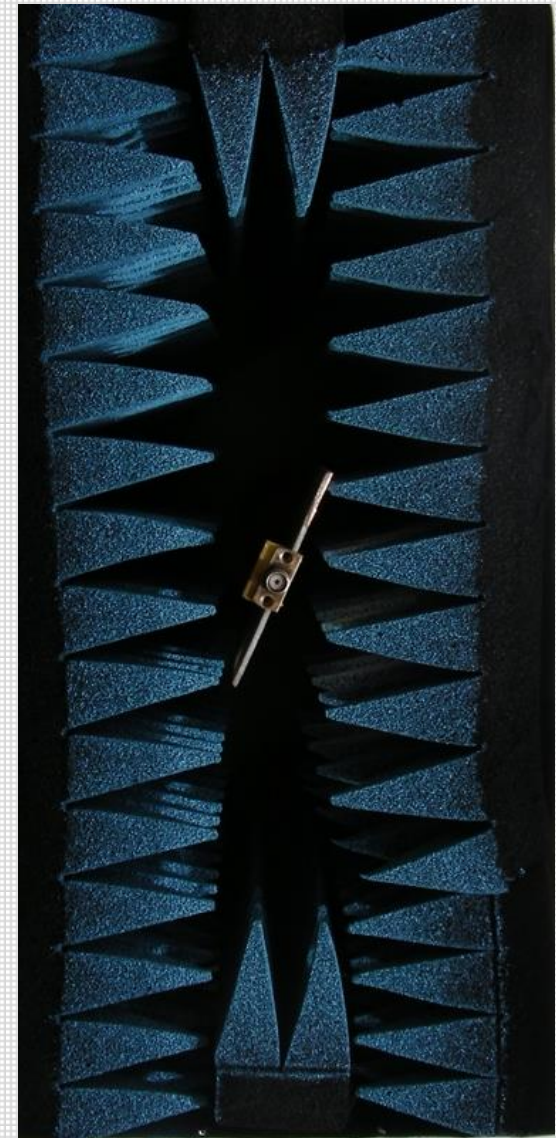
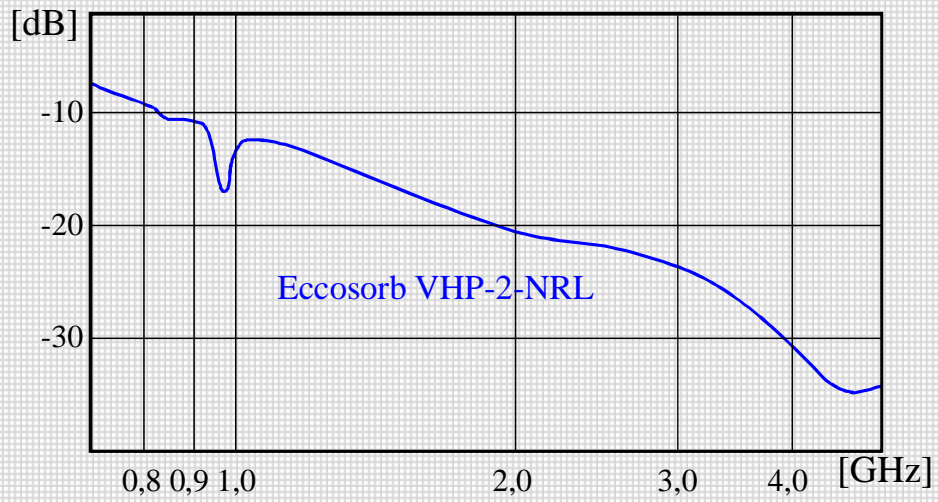
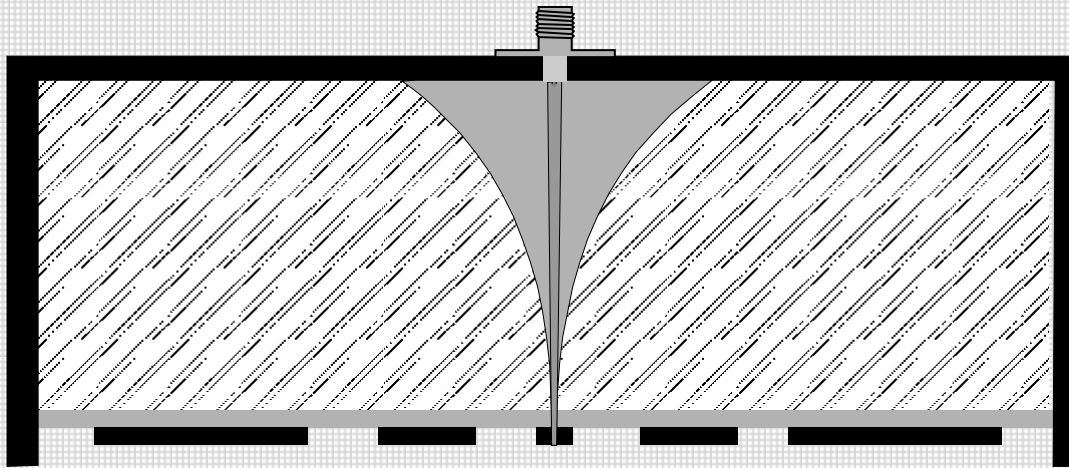
$$\alpha \in \langle 0,2;1,2 \rangle$$

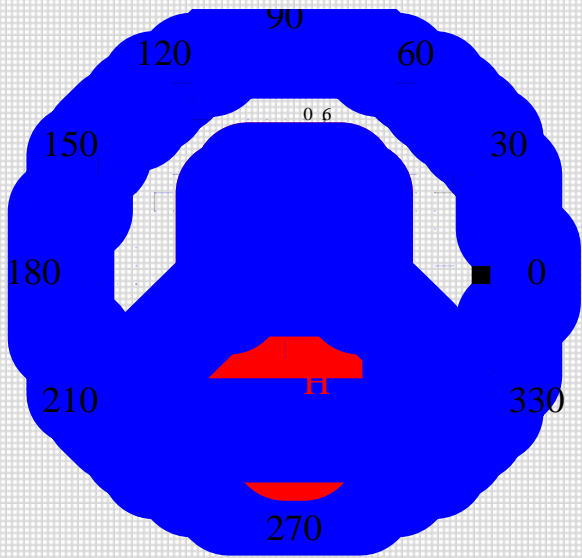


FDTD

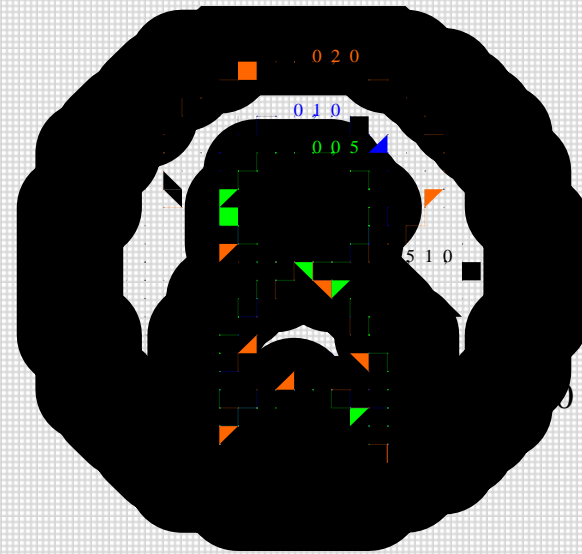








Charakterystyki promieniowania dipola półfalowego leżącego na suchym piasku



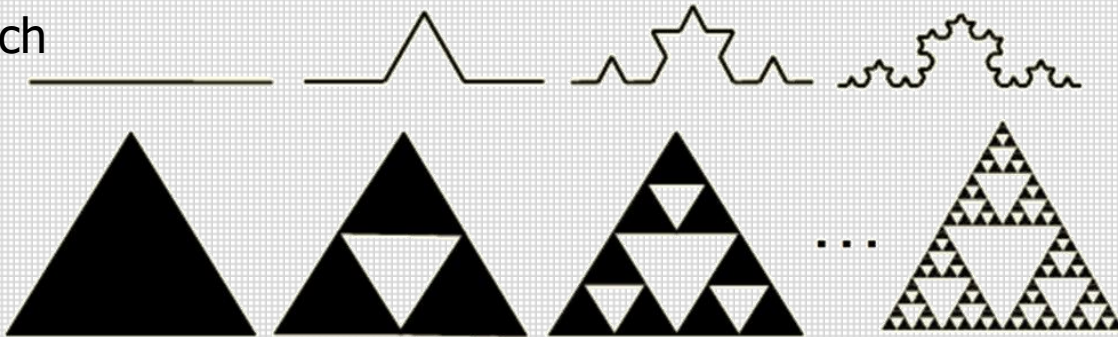
Zależność wertykalnej charakterystyki promieniowania od wysokości zawieszenia dipola półfalowego (wyr. w długościach fali)

Fractal antennas

Fractal is the self-similar structure

deterministic fractals

Koch

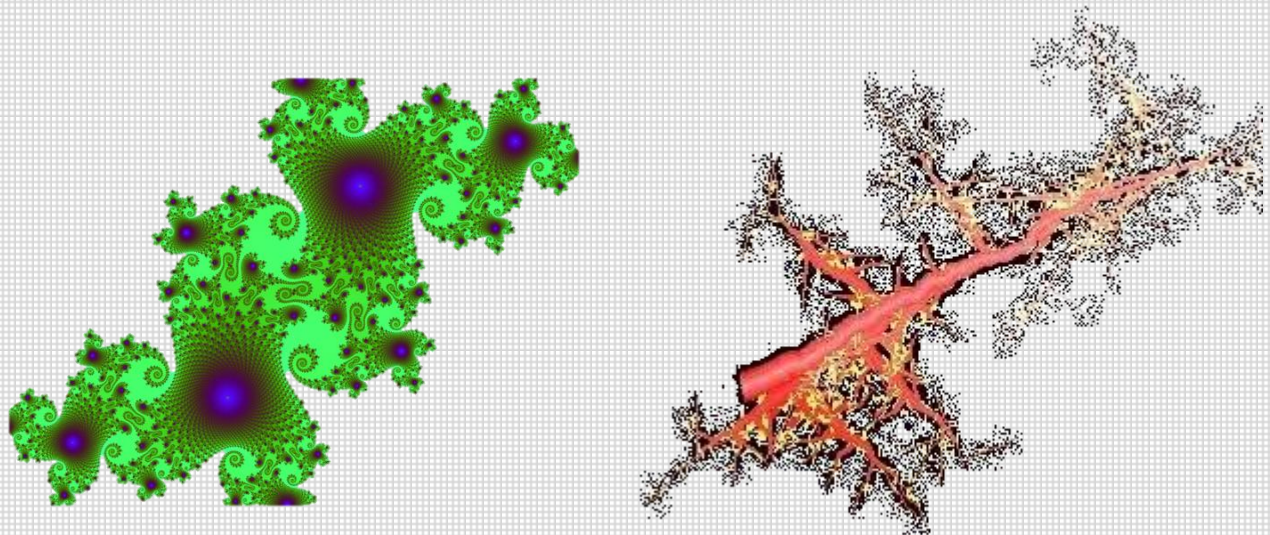


Fractal object of infinite length in a finite area: $D > 1$

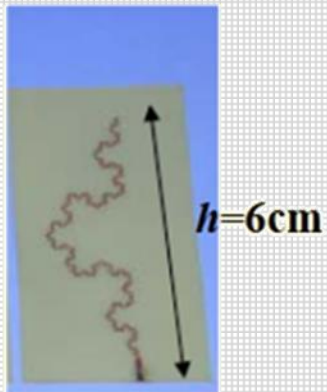
Fractal object of zero area but infinite length: $D < 2$

Sierpiński

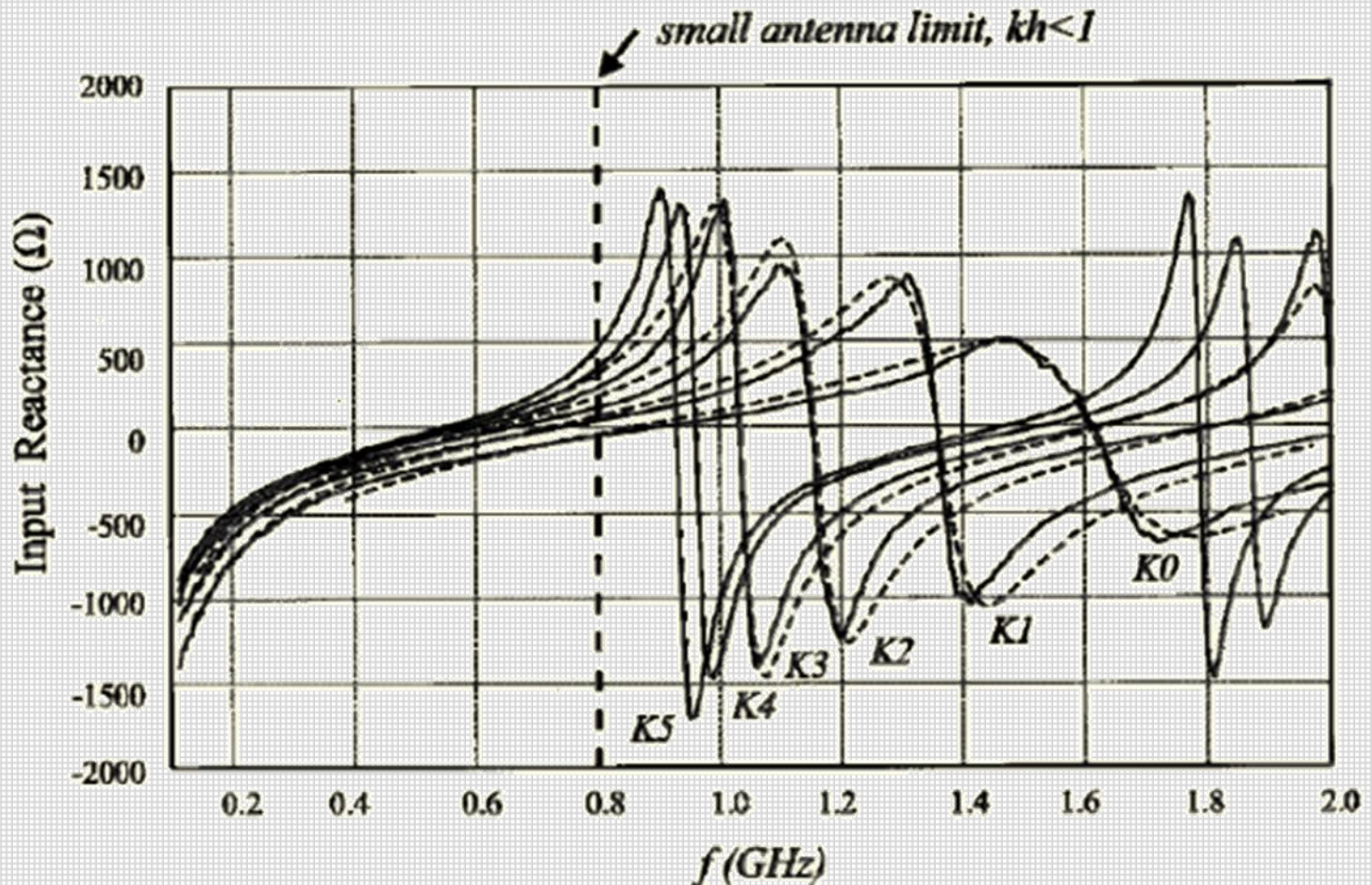
stochastic fractals



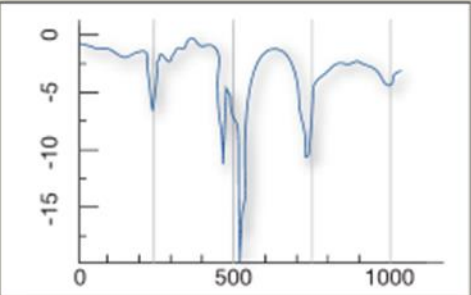
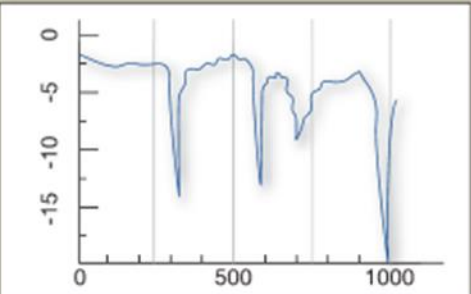
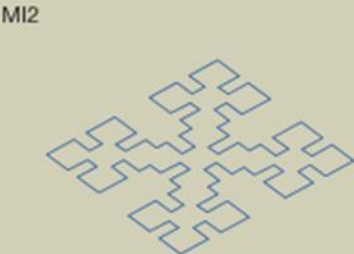
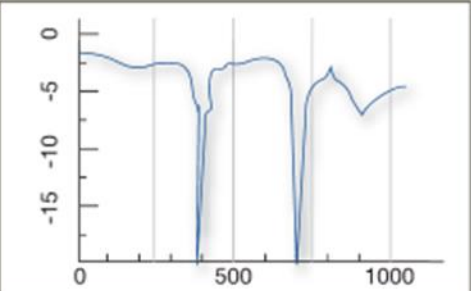
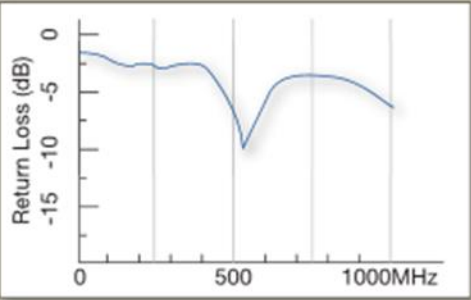
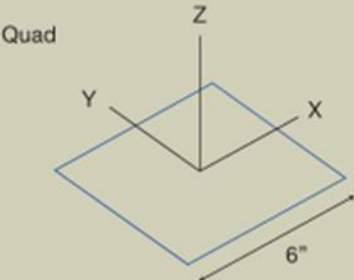
Preliminary studies by Puente et al. showed that the resonant frequency decreases as the iteration number increases (longer wire packed into the same area).



Koch monopoles

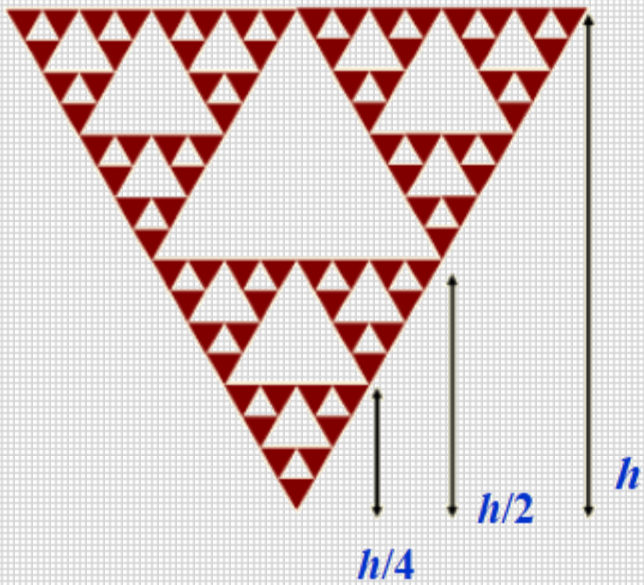


Hilbert curve antennas

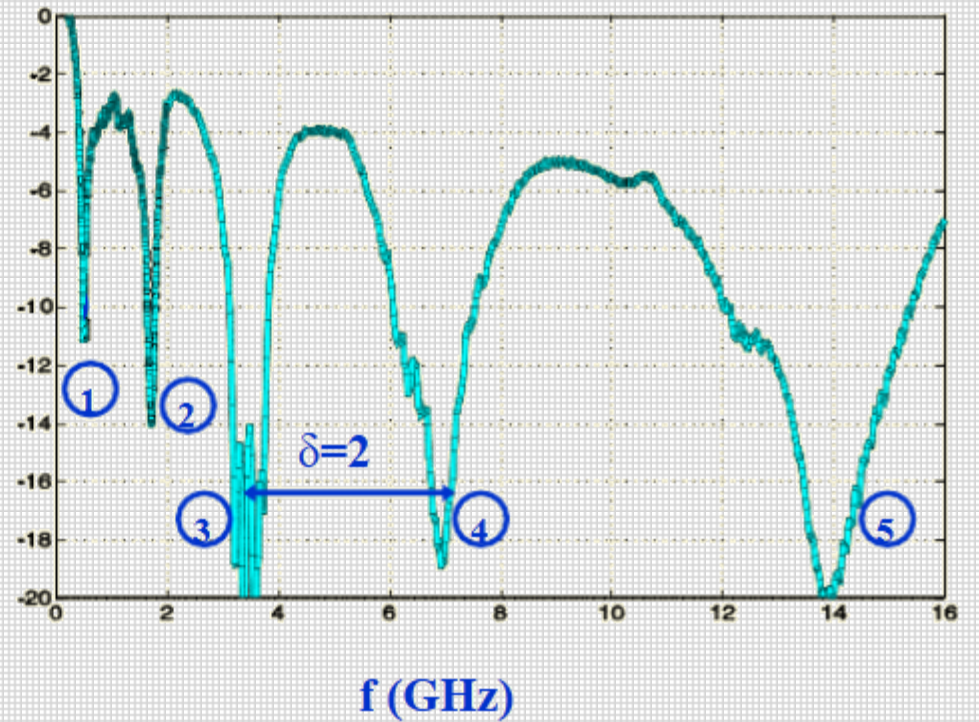


Sierpinski Antenna

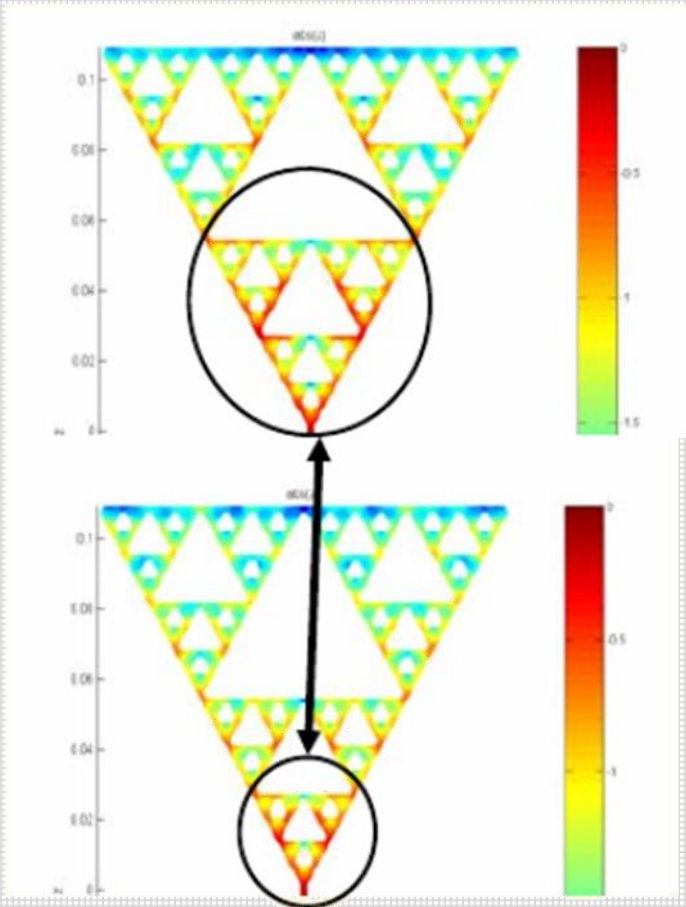
of 5 iterations (S-5)



Reflection Coefficient



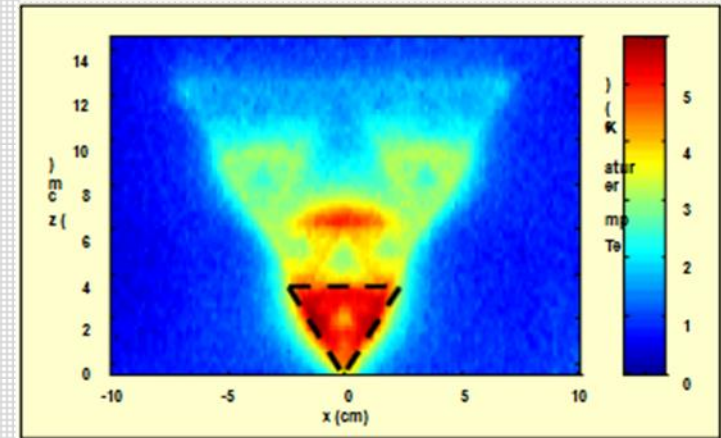
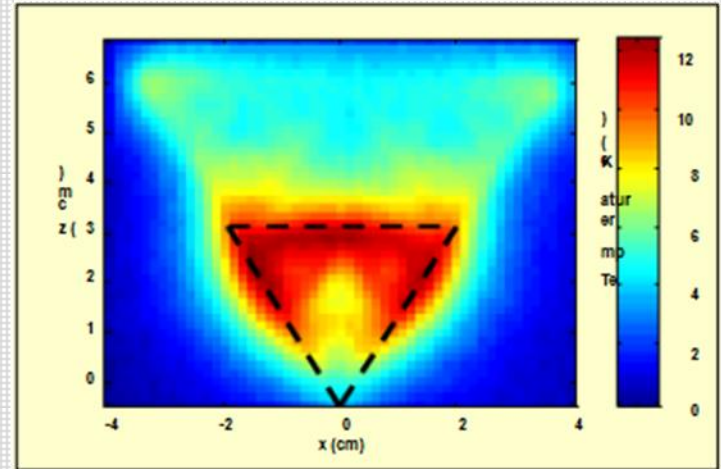
Numerical simulation at UPC



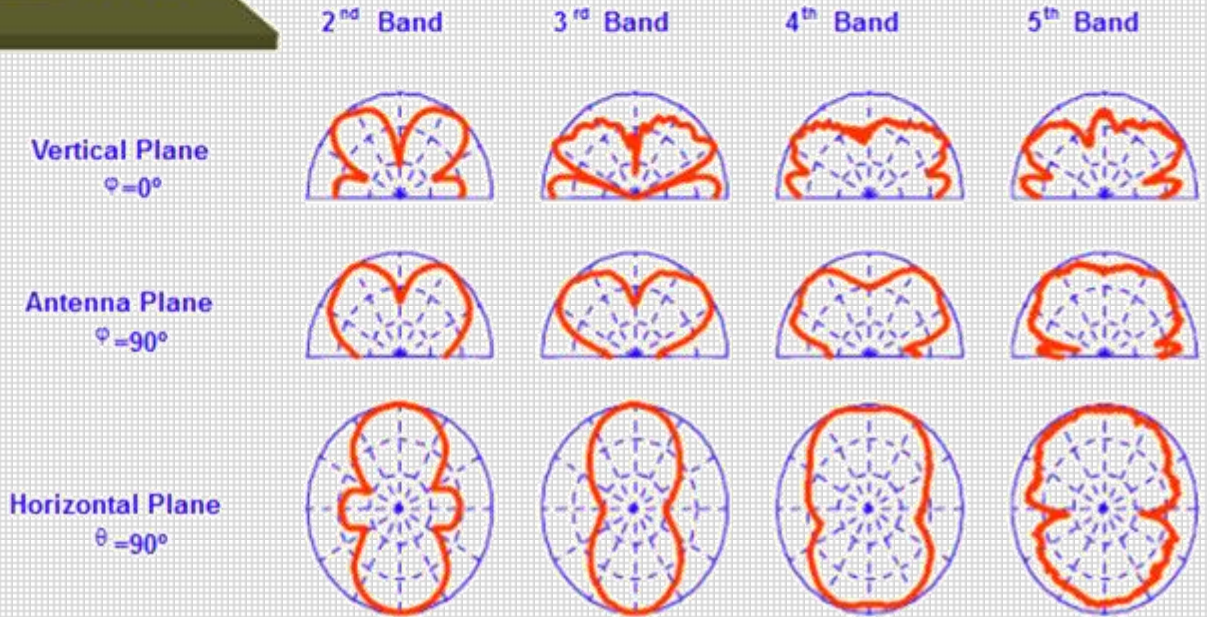
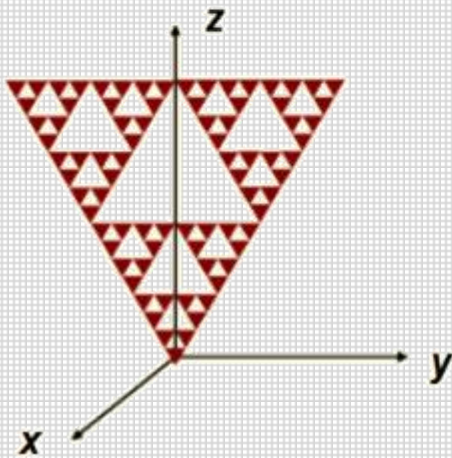
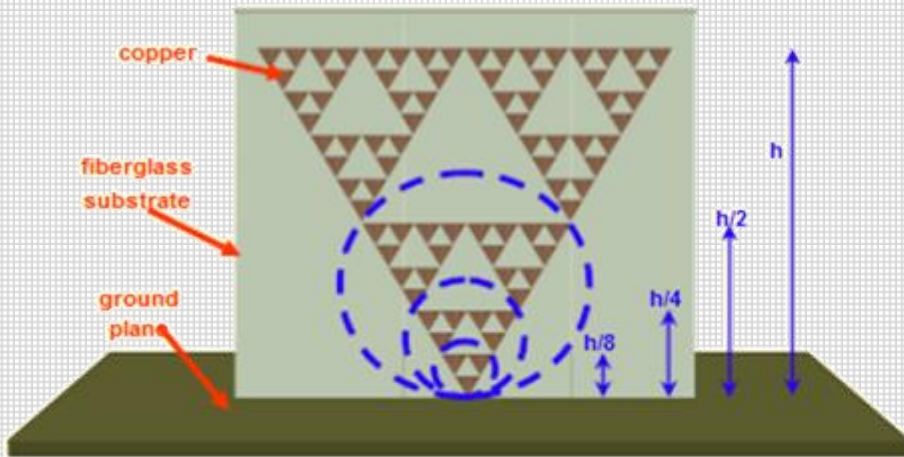
2rd band

3th band

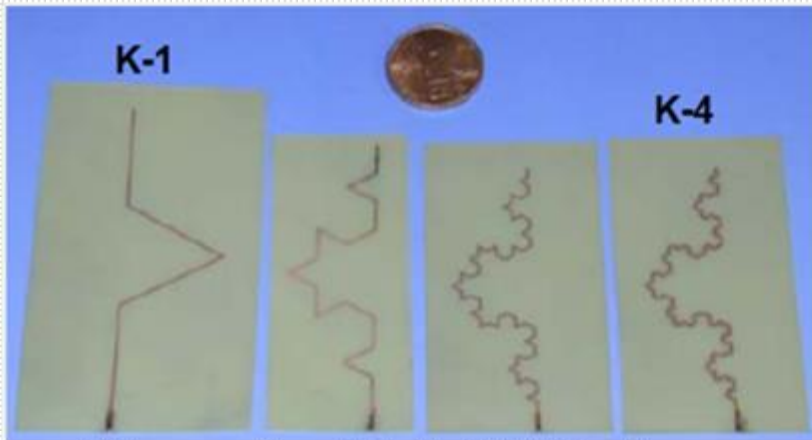
Measurement at UPC (IR technique)



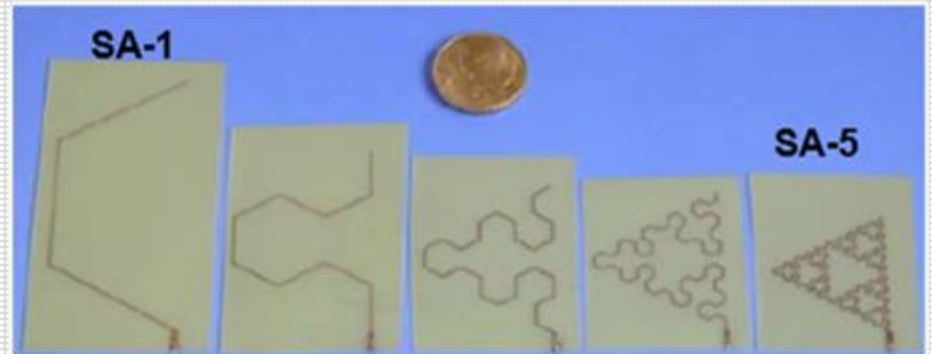
Radiation pattern measured at different bands



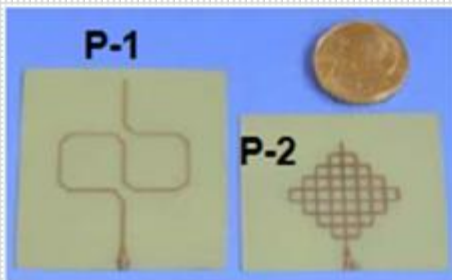
Fabricated planar pre-fractal monopoles



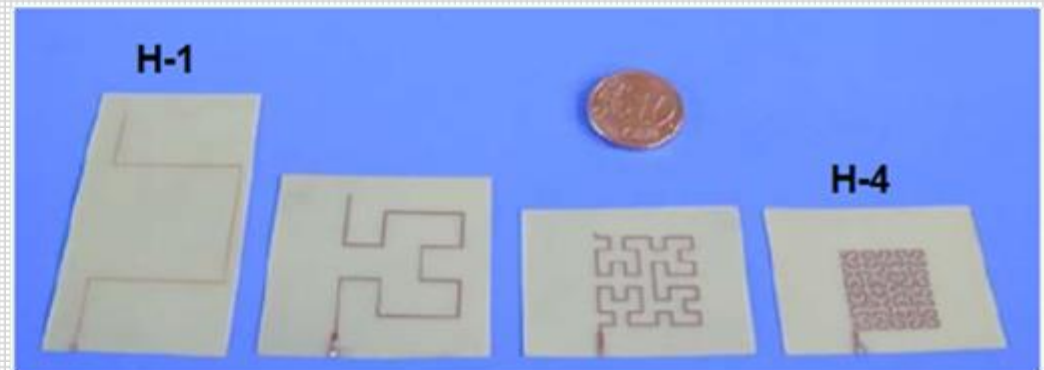
Koch monopoles $D=1.26$



Sierpinski Arrowhead monopoles $D=1.58$



Peano monopoles $D=2$



Hilbert monopoles $D=2$

References

Microstrip Patch Antennas, K. F. Fong Lee and K. M. Luk, Imperial College Press, 2011.

Microstrip and Patch Antennas Design, 2nd Ed., R. Bancroft, Scitech Publishing, 2009.

Microstrip Patch Antennas: A Designer's Guide, R. B. Waterhouse, Kluwer Academic Publishers, 2003.

Microstrip Antenna Design Handbook, R. Garg, P. Bhartia, I. J. Bahl, and A. Ittipiboon, Editors, Artech House, 2001.

Advances in Microstrip and Printed Antennas, K. F. Lee, Editor, John Wiley, 1997.

CAD of Microstrip Antennas for Wireless Applications, R. A. Sainati, Artech House, 1996.

Microstrip Antennas: The Analysis and Design of Microstrip Antennas and Arrays, D. M. Pozar and D. H. Schaubert, Editors, Wiley/IEEE Press, 1995.

Millimeter-Wave Microstrip and Printed Circuit Antennas, P. Bhartia, Artech House, 1991.

The Handbook of Microstrip Antennas (two volume set), J. R. James and P. S. Hall, INSPEC, 1989.

Microstrip Antenna Theory and Design, J. R. James, P. S. Hall, and C. Wood, INSPEC/IEE, 1981.